

## Use Authorization

In presenting this thesis in partial fulfillment of the requirements for an advanced degree at Idaho State University, I agree that the Library shall make it freely available for inspection. I further state that permission to download and/or print my thesis for scholarly purposes may be granted by the Dean of the Graduate School, Dean of my academic division, or by the University Librarian. It is understood that any copying or publication of this thesis for financial gain shall not be allowed without my written permission.

Signature \_\_\_\_\_

Date \_\_\_\_\_

**MULTI-HAZARD ANALYSIS OF WIND TURBINE CONCRETE  
FOUNDATIONS UNDER WIND FATIGUE AND EARTHQUAKE LOADINGS**

by

Ikwulono David Unobe

A thesis

submitted in partial fulfillment

of the requirements for the degree of

Master of Science in the Department of Civil Engineering

Idaho State University

May, 2014

## Committee Approval

To the Graduate Faculty:

The members of the committee appointed to examine the thesis of IKWULONO DAVID UNOBE find it satisfactory and recommend that it be accepted.

---

Major Advisor:

**Dr. Andrew Sorensen**

---

Committee Member:

**Dr. Arya Ebrahimpour**

---

Graduate Faculty Representative:

**Dr. Leonid Hanin**

## **Acknowledgements**

I acknowledge my maker, the Supreme Being and ultimate structural engineer, whose mysterious designs obey no known laws but withstand the eternal test of time for giving me the strength and wisdom to carry out this seemingly arduous task with relative ease and without whom my efforts would have been a farce.

I must also thank without reservation from the bottom of my heart my advisor Dr. Andrew Sorensen for guiding me through this project. My immense gratitude and appreciation goes to my thesis committee as well as the entire faculty of the department of Civil Engineering for their unalloyed support, training, encouragement, and cheerful willingness to impart priceless knowledge to me.

My deepest gratitude goes to my parents Prof. and Mrs. E. Unobe for their love, encouragement and support, morally, financially and otherwise and my siblings Ejakuwa, Egboche and Adah for all the love.

To all my friends, colleagues and peers, who made this ostensibly difficult transition easier for me, you forever have my gratitude.

## TABLE OF CONTENT

List of Figures.....	ix
List of Tables.....	x
Abstract.....	xi
CHAPTER ONE – INTRODUCTION	
1.1 Background and Motivation.....	1
1.2 Problem Definition and Scope.....	5
1.3 Objectives.....	6
1.4 Methodology.....	6
1.4.1 System Identification.....	6
1.4.2 Fatigue Analysis.....	7
1.4.3 Seismic Analysis.....	7
1.4.4 Multi-Hazard Analysis.....	8
1.5 Limitations.....	9
1.6 Thesis Overview.....	9
CHAPTER TWO – LITERATURE REVIEW	
2.1 Design of Wind Turbine Foundations.....	11
2.2 Natural Hazards.....	18
2.2.1 Natural Hazards.....	18
2.2.2 Seismic Analysis of Wind Turbines.....	21
2.2.2.1 Monte Carlo Procedure for Seismic Analysis.....	25
2.2.3 Fatigue Analysis of Wind Turbines.....	26
2.2.3.1 Fatigue Model for Concrete.....	32
2.3 Multi-Hazards.....	33
2.4 Reliability Analysis.....	38
2.5 Sensitivity Analysis.....	40
2.6 Finite Element Analysis.....	40
2.6.1 ANSYS Finite Element Model.....	42

2.7 Summary.....	43
<b>CHAPTER THREE – METHODOLOGY</b>	
3.1 Methodology Overview.....	45
3.2 Monte Carlo Simulations.....	46
3.2.1 Fatigue Analysis.....	46
3.2.2 Seismic Analysis.....	47
3.2.3 Multi-Hazard Analysis.....	48
3.3 Finite Element Analysis.....	48
3.4 Fatigue Analysis in MATLAB.....	49
3.5 Seismic Analysis in MATLAB.....	53
3.6 Multi-Hazard Analysis in MATLAB.....	55
3.7 Finite Element Analysis.....	56
3.7.1 ANSYS Finite Element Model.....	56
3.7.1.1 Modeling the Concrete Foundation.....	56
3.7.1.2 Element Types.....	57
3.7.1.3 Real Constants.....	59
3.7.1.4 Material Properties.....	60
3.7.2 Model Geometry.....	66
3.7.2.1 Meshing.....	67
3.7.2.2 Loads and Boundary Conditions.....	68
3.8 Fatigue Analysis.....	68
3.8.1 Fatigue Analysis.....	68
3.8.2 Seismic Analysis.....	70
3.9 Sensitivity Analysis.....	71

## CHAPTER FOUR – MONTE CARLO SIMULATIONS

4.1 Seismic Analysis.....	72
4.2 Wind Fatigue Analysis.....	75
4.3 Multi-Hazard Analysis.....	77
4.4 Sensitivity Analysis.....	79
4.4.1 Seismic Sensitivity Analysis.....	79
4.4.2 Wind Fatigue Sensitivity Analysis.....	82
4.4.3 Multi-Hazard Sensitivity Analysis.....	85
4.5 Conclusions.....	88

## CHAPTER FIVE – FINITE ELEMENT ANALYSIS RESULTS

5.1 Model Validation.....	89
5.2 ANSYS Wind Fatigue Analysis.....	91
5.3 ANSYS Seismic Analysis.....	95
5.4 ANSYS Multi-Hazard Analysis.....	97
5.5 Conclusions.....	100

## CHAPTER SIX – DISCUSSION AND CONCLUSION

6.1 Discussion of Results.....	102
6.2 Conclusions.....	103
6.3 Recommendation.....	105
6.4 Future Work.....	105
Bibliography.....	106
Appendix A – Time History Plots.....	111
Appendix B – Wind Rose Diagram.....	114

## List of Figures

Figure 1.1 – Wind turbine concrete foundation.....	4
Figure 2.1 – Loading mechanism of wind turbine foundations.....	14
Figure 2.2 – Possible failure mechanism of tower to foundation connection.....	14
Figure 2.3 – S-N curve for concrete model.....	33
Figure 3.1 – Outline of methodology used.....	46
Figure 3.2 – Solid 65 element.....	58
Figure 3.3 – Solid 187 element.....	59
Figure 3.4 – Real constant set for reinforcement in ANSYS.....	60
Figure 3.5 – Uniaxial stress-strain curve for reinforced concrete.....	63
Figure 3.6 – Meshed model.....	67
Figure 3.7 – ANSYS model with fatigue loads.....	70
Figure 4.1 - Graph of earthquake magnitude against probability of failure.....	74
Figure 4.2 – Graph of probability of failure against time.....	76
Figure 4.3 – Graph of probability of failure against earthquake magnitude.....	78
Figure 4.4 – Graph of probability of failure against footing depth for magnitude 7.0 earthquake.....	80
Figure 4.5 – Graph of probability of failure against area for magnitude 7.0 earthquake..	81
Figure 4.6 – Graph of probability of failure against height of tower at year 20.....	83
Figure 4.7 – Graph of probability of failure against modulus of rupture.....	84
Figure 4.8 – Graph of multi-hazard probability of failure against foundation depth.....	85
Figure 4.9 – Graph of multi-hazard probability of failure against foundation area.....	86
Figure 4.10 – Graph of multi-hazard probability of failure against tower height.....	86
Figure 4.11 – Graph of multi-hazard probability of failure against modulus of rupture..	86
Figure 5.1 – Cracking of concrete under pullout load.....	90

Figure 5.2 – Cumulative fatigue analysis in ANSYS postprocessor.....	91
Figure 5.3 – Cumulative distribution function for selected nodes.....	93
Figure 5.4 – Nodal stresses of footing under fatigue loading.....	93
Figure 5.5 – Nodal stresses through a cut section.....	94
Figure 5.6 – Nodal stresses of foundation under seismic excitation.....	96
Figure 5.7 – Nodal stresses through a cut section.....	97
Figure 5.8 – Nodal stresses of footing under combined loading.....	98
Figure 5.9 – Nodal stresses through a cut section.....	99

## List of Tables

Table 3.1 – Stress range cycles for mean wind speeds.....	51
Table 3.2 – Model and statistical uncertainties for fatigue limit state.....	52
Table 3.3 – Element types for working model.....	57
Table 3.4 – Material properties.....	61
Table 3.5 – Foundation dimensions on ANSYS.....	66
Table 3.6 – Anchor bolt dimensions on ANSYS.....	66
Table 3.7 – Commands used in the SOLN CTRL option in ANSYS.....	69
Table 4.1 – Relationship between earthquake magnitude and probability of failure.....	73
Table 4.2 – Time and probability of failure relationship under cyclic wind loading.....	75
Table 4.3 – Multi-hazard analysis results.....	77
Table 4.4 – Seismic reliability sensitivity to foundation depth.....	79
Table 4.5 – Seismic reliability sensitivity to foundation area.....	80
Table 4.6 – Wind fatigue sensitivity to tower height.....	82
Table 4.7 – Wind fatigue sensitivity to compressive strength of concrete.....	84
Table 5.1 – Comparison between hand calculations and ANSYS model.....	90
Table 5.2 – Wind fatigue reliability analysis results.....	92
Table 5.3 – Probability of failure over design lifetime for selected nodes.....	92
Table 5.4 – Seismic reliability analysis results.....	95
Table 5.5 – Stresses of selected nodes under combined loading.....	98

## **ABSTRACT**

Over time, and under varying cyclic loading from wind forces, there is a reduction in the structural integrity of structural systems due to fatigue, increasing their vulnerability to additional non-typical loads such as earthquakes. This results in a multi-hazard loading scenario not considered in current design load considerations. The present research aims to numerically predict the effect of a seismic load (earthquake) on a wind turbine foundation that has undergone fatigue over time due to constant exposure to wind forces. This work expands on the research of previous scholars who have successfully determined the reliability of wind turbines to different singular load types as encapsulated in design codes, by carrying out a multi-hazard reliability analysis using the computational tools MATLAB and Finite Element Analysis (using ANSYS) to understand the behavior of the structure under this specific combined load effect.

# CHAPTER ONE

## INTRODUCTION

### 1.1.BACKGROUND AND MOTIVATION

Structures are designed to withstand the external forces acting on them using a series of standard load combinations. On the most basic level, structures are designed for strength and serviceability (performance). Adequate strength is obtained by designing structural members against buckling, yielding, instability and fracture in accordance with the applicable building code specifications. Serviceability issues include deflection, vibration and corrosion.

Presently, code standards require structural engineers to design structures for the controlling load case. While this practice is sufficient for single hazard design, it fails to consider the possibility of multiple hazard occurrence and the differences in structural response due to load application in multiple hazard scenarios (Chen, 2011). Events of recent history such as the September 11 attacks, hurricane Katrina, and the Fukushima nuclear plant meltdown due to the magnitude 9 Tohoku earthquake and subsequent tsunami, have brought to the fore the relative risk of previously unimagined multi-hazard scenarios. This has helped bring into the limelight the relatively nascent field of multi-hazard engineering. Dutinh and Simiu (2010) in conducting a study on the safety of structures in strong winds and earthquakes suggested that current prevalent design principles of basing final designs on the most demanding loading condition might be inadequate. Using a water tower design located in an area of high seismicity and winds to illustrate this claim, they showed that there exists a significant risk of limit state exceedance in situations where the two

loading conditions act simultaneously as opposed to them acting independently. They concluded that although the probability of simultaneous occurrence of the two loading conditions was low perhaps even notional, it does exist and poses a threat to the safety of structures deemed reliable under current standards. Multi-hazard engineering utilizes multiple levels of probabilistically defined design criteria to achieve more predictable structural response to simultaneously occurring hazards (Dutinh and Simiu, 2010; Ayyub and McCuen, 2011). This provides a greater structural reliability for a wider spectrum of loading as well as helps evaluate design decisions.

A wind turbine is a device that converts the kinetic energy of wind into electrical energy. It is made up primarily of three parts: the nacelle which carries the operational parts, the tower and the foundation. The foundation and the tower together make up the structural system of a wind turbine. The tower carries the nacelle and transfers all loads acting on the structure to the foundation via the anchor bolt connection.

One possible combination of multi-hazard loading that is likely to occur is that of wind related fatigue and earthquake. This is especially true in areas of high seismic activity that are also ideal locations for wind energy generation. With respect to wind and seismic forces, deflection, vibration, buckling and fatigue are of particular concern especially in the design of slender structures under which wind turbines are classified. The history of wind power shows a general evolution from the use of simple, light devices driven by aerodynamic drag forces, to heavy, material intensive

drag devices, to the use of light, material efficient aerodynamic lift devices of the modern era.

Until recently, wind powered mills were primarily used as a mechanical device for pumping water for domestic use and irrigation purposes on farms. In the late 19<sup>th</sup> century however, they began to be experimentally used in generating electricity. With further developments in available materials and structural systems, the wind turbine kept evolving in its architecture with the horizontal axis wind turbine (HAWT) consisting of either a slender tapering tower or a lattice tower combined with a foundation system carrying a nacelle and blades on top being the most commonly seen in practice today (Dodge, 2006). Figure 1.1 shows an example of a wind turbine foundation with the anchor bolt connections used to attach the tower to it.

With cutting edge technology and increasingly novel structural designs also comes a heightened risk of failure from external forces such as wind and earthquakes. One major area of concern from these loads is the anchor bolt to foundation connection. Failure in the anchor bolts can occur via a number of modes, including: yielding, shear, and bond weakening. Cyclic loading from regular winds to which the tower is exposed could weaken the bond between the anchor bolt and concrete footing making these connections very susceptible to one time seismic events. The failure of one anchor bolt would cause a redistribution of loads among the other bolts and thus an increase in their stresses. This could lead to a progressive failure of the other anchor bolts and result in collapse of the wind turbine. Although wind turbines' structural systems are generally designed to adequately resist such forces individually, the available codes and consequently actual designs do not take into account possible

multi-hazard scenarios of these loads acting in tandem on the structures. Furthermore, there does not currently exist a standard code for the design of wind turbine foundations in the United States. Current designs are based on the International Electromechanical Commission's design standards (IEC 61400) (Kuhn et al, 2010). This work aims at bridging this critical gap between current design methods and possible multi-hazard loading scenarios with a particular emphasis on wind fatigue and seismic effects on the foundation. Two analytical methods (finite element analysis and Monte Carlo simulations in MATLAB) are used in this study to achieve this aim. This is done because no field studies or physical testing is carried out in this research to validate the analysis, thus, utilizing two independent methods to validate the results obtained is necessary.



Figure 1.1: Wind Turbine concrete foundation with anchor bolts (Ceren, 2013)

## **1.2 PROBLEM DEFINITION AND SCOPE**

This work addresses the multi-hazard effect of wind fatigue and seismic forces on a wind turbine foundation with an aim to determining, through analytical techniques, the structural reliability of the concrete foundation of a wind turbine under the loading conditions in consideration at a probable site located in the Idaho Falls, Idaho as a case study. This location was chosen because Idaho Falls is located in a region of moderate to high seismicity and is also recognized as a good location for wind energy generation as proven by the recent emergence of several wind farms in the region.

A concise overview of research carried out to date on reliability analysis and its peculiar applicability to the engineering environment with regards to structural engineering is provided in Chapter 2 as well as a discussion of wind turbines analysis and design methodology as currently practiced. Although it is difficult to formulate a multi-hazard type analysis for a complete structural system, this thesis puts forward four questions that help to define a scope within which the analysis can be made for a subsystem of the support:

1. What is the direct effect of cyclic wind loading on the capacity of a wind turbine's foundation to withstand impact loads?
2. What is the reliability index and consequently the probability of failure of a wind turbine foundation from an earthquake of a certain magnitude and/or distance?
3. What is the multi-hazard effect of cyclic wind fatigue and a one-time seismic event on a wind turbine's foundation?
4. How efficient is the current design of these structures to withstand multi-hazard loads as espoused above?

Resolving these pertinent questions enhances the understanding of structural response to multi-hazard scenarios and thus promotes the cause of multi-hazard engineering.

### **1.3 OBJECTIVES**

With the intention of proffering satisfactory answers to the questions posed above, the objectives of this work are set out as:

1. Determine the short term/long term effects of wind fatigue on structural capacity of a concrete foundation, specifically the bond between the anchor bolts and the concrete.
2. Determine structural response of wind turbines' foundations to seismic activities.
3. Ascertain the structural response of a wind turbine foundation exposed to fatigue conditions from wind forces over time and a singular seismic event.
4. Provide a better understanding of multi-hazard analyses especially its applicability to structural engineering design codes.

### **1.4 METHODOLOGY**

In order to accomplish the objectives of this study as laid out above, a systematic methodology has been developed and is broken down into four areas: system identification, fatigue analysis, seismic analysis and multi-hazard analysis.

#### **1.4.1 System Identification**

- Structural design specifications for a typical wind turbine foundation are obtained.
- Wind speed data for the site is obtained.

- Seismic activities data for the site is also obtained.

#### 1.4.2 Fatigue Analysis

- A numerical model is built in MATLAB for the purpose of carrying out the fatigue reliability.
- The wind speed data is converted into wind forces and transferred to this model.
- Damage due to the wind forces is calculated using the ERES/COE field fatigue model for concrete as defined in chapter two.
- Damage accumulation on the model is calculated as per Miner's rule.
- The fatigue reliability analysis is then be carried out using first order second moment reliability method, defined as (Nowak & Collins, 2000);

$$\beta = \frac{a_0 + \sum_{i=1}^n a_i \mu_{xi}}{\sqrt{\sum_{i=1}^n (a_i \sigma_{xi})}} \quad (1.1)$$

- A finite element model of the concrete footing is developed in ANSYS and a transient fatigue analysis is carried out.
- Damage usage is then calculated in the ANSYS postprocessor.
- The damage usage values are utilized in analyzing the reliability of the footing under the fatigue loads.

#### 1.4.3 Seismic Analysis

- Monte Carlo simulations (Musson R.M.W., 1999) are utilized to determine appropriate ground motions for design earthquakes needed for the analysis.

- These ground motion data is used to carry out reliability analysis of the foundation considering displacement as a limit state.
- Fragility curves are then developed which serve to estimate the probability of reaching a defined damage state for a range of intensity values. This probability of failure at a certain damage state is determined by an exceedance of the limit state given by (Rao, 2011):

$$g(x) = r - 2.5 \quad (1.2)$$

- The acceleration time history data obtained for the seismic events of interest are integrated twice using the trapezoidal rule to obtain displacement time history.
- The finite element analysis model in ANSYS is then subjected to seismic time-history analysis by applying the displacement time history.
- Reliability analysis is then carried out using the resultant stresses from the seismic analysis to determine the effect of these earthquakes on the performance of the foundation.
- Fragility curves are then developed from the reliability analysis to estimate the probability of reaching a defined damage state for a range of seismic magnitudes.

#### 1.4.4 Multi-Hazard Analysis

- The probabilities of failure from both analyses are combined using the equation as defined by Ayyub and McCuen (2011):

$$P_f = P_{ffat} + P_{feq} - (P_{ffat} * P_{feq}) \quad (1.3)$$

A review of the literature shows that the foundation footing of a wind turbine is most susceptible to damage from earthquake induced ground motions. Fatigue failure as well is most likely to occur at the tower to foundation connection due to the concentration of stresses at that section (Dexter and Ricker, 2002). Hence, valuable insight into the behavior of wind turbines under multi-hazard loadings will be gained by studying the effects of these loading conditions on a wind turbine foundation system as is the basis of this thesis. Understanding the effects of multi-hazard loading patterns on structures will aid in refining design methodologies for these structures to better withstand the vagaries of nature.

## **1.5 LIMITATIONS**

This research is limited to the study of two hazards (earthquakes and wind fatigue) likely to occur simultaneously on wind turbine foundations. It does not take into considerations other loading scenarios that could probably occur as well. Also, the performance of the structure is determined from its inception up to the moment an earthquake occurs. This study therefore does not take into consideration the possible change in behavior of the foundation to fatigue stresses after the occurrence of a seismic event.

## **1.6 THESIS OVERVIEW**

The scope of this thesis includes the strategies and methodologies used in the problem formulation, analyses and implementation portions of the research. It is broken down in a logical progression into six chapters. The first chapter (Introduction) gives a general outline of the problem definition, issues raised and a proposed methodology for formulating a framework to resolving the issues. This is followed by a review of

literature (Chapter 2) applicable to the study from whence suitable solution strategies are explored and assessed and the most appropriate to the problems defined decided upon. Chapter 3 presents a detailed methodology for carrying out the analyses identified. Chapter 4 presents distinct results for the fatigue and seismic analyses of a wind turbine structural system under cyclic wind loading using the MATLAB code developed for this purpose. The finite element analysis of the system under both loading scenarios, as well as under the combined multi-hazard loading is examined in Chapter 5. A brief summary of the work done as well as conclusions drawn and recommendations for future studies are outlined in the final chapter.

## **CHAPTER TWO**

### **LITERATURE REVIEW**

This chapter presents a review of literature necessary to the study of natural hazards especially as they affect the structural integrity of wind turbine foundations. The chapter is divided into five component sections. The first section defines the design of wind turbine foundations and the regulatory guidelines for fatigue and earthquake limit designs. The second section defines natural hazards and outlines the procedure for analysis of each hazard. The third section describes the theory of multi-hazards and the combination of different hazards into a single, multi-hazard scenario. The fourth section enunciates the background of numerical reliability analysis and how it can be used in multi hazards analysis and the fifth introduces the concept of finite element analysis and its relevance to this study.

The purpose of this literature review is to go through material related to natural hazards especially as they affect wind turbine foundation design and lifetime structural integrity. Covering the issues as espoused above helps to identify gaps in research that need to be filled. In effect, the literature review is conducted with the intention of advancing research towards suggesting and establishing reliability based methodology for multi-hazard analysis of wind turbine support structures.

#### **2.1 DESIGN OF WIND TURBINE FOUNDATIONS**

The interplay of forces from the external environment, primarily due to the wind and the motions of the various components of the wind turbine results not only in the desired energy production but also in stresses in the constituent materials. These stresses are of primary concern in the design of the wind turbines' structural systems

because they directly affect the workability of the turbines hence the design must not only be functional in terms of extracting energy, it must also be structurally sound so that it can withstand the loads it experiences, and the costs to make it structurally sound must be commensurate with the value of the energy it produces (Manwell et al, 2002).

Electricity generating wind turbines traditionally consist of a rotor, the blades, the nacelle which houses most of the electrical components, the tower which carries the other composing parts and the foundation (Lavassas et al, 2003). The structural support system is a key component of the turbine system. It is composed of the foundation and the steel or concrete tower. As well as housing the critical components of the turbine, the tower also places the wind turbine at an elevation where desirable wind characteristics can be found. It also carries the loads from the nacelle and rotor and transfers them to the foundation. Hence, the structural properties of the tower as well as of the foundation are of utmost importance in the structural design of wind turbines as their combined performance has a large influence on the overall performance and structural integrity of the entire structure (Gwon, 2011). The main objective of the support system design is to avoid compromising structural integrity (Meilan & Tsouroukdissian, 2010). The structural design of a wind turbine support system consists of its two main parts: its tower and its foundation. The tower design is based primarily on wind and ice loads, loads acting from the blades, nacelle and additional equipment at the top of the tower in addition to wind loads acting on the tower. The foundation is designed according to the moment and axial loads resulting from the tower design and properties of the surrounding soil (Kuhn et al, 2010). There are three types of wind turbine towers generally used namely; lattice tower, tubular tower and the hybrid tower which is a combination of the first two. However, the

tubular tower is more widely used than the other two because of obvious advantages it enjoys such as providing an enclosed area for the placement of critical components as well as its aesthetic qualities, and less obvious advantages such as ease of maintenance and maintenance costs (Gwon, 2011). The conical shape is efficient in simultaneously increasing the tower strength and saving materials as well as reducing the exposed profile for wind forces at higher elevations. The tower is constructed in sections from rolled steel at a desired thickness, and is transported on site and bolted and/or welded together to create the massive towers (Kuhn et al, 2010). Gwon (2011) held forth that the taller the tower, the more power the wind system can produce and thus ideally, the tower should be at least 24 metres (79 ft) tall because the wind speed is lower and more turbulent closer to the ground.

Wind turbine foundations are designed to withstand a plethora of loads resulting from the installation and operation of the tower and wind generating equipment. These include axial and shear gravity loads from the tower and nacelle, overturning moments and vibrations from the installed machinery (Kuhn et al, 2010). Cracking is a major concern in wind turbine foundation design. This occurs due to a number of loading mechanisms resulting from thermal expansion/contraction during hardening as well as stresses from various structural loadings especially around the connections (Ceren, 2013). This results in significant loss of load carrying capacity and an increased risk of pullout of the anchor bolts holding down the tower into the foundation. As shown in Figures 2.1 and 2.2, the tower to foundation connection is a convergence point for several loads acting upon the structure and thus is identified as a likely failure point.

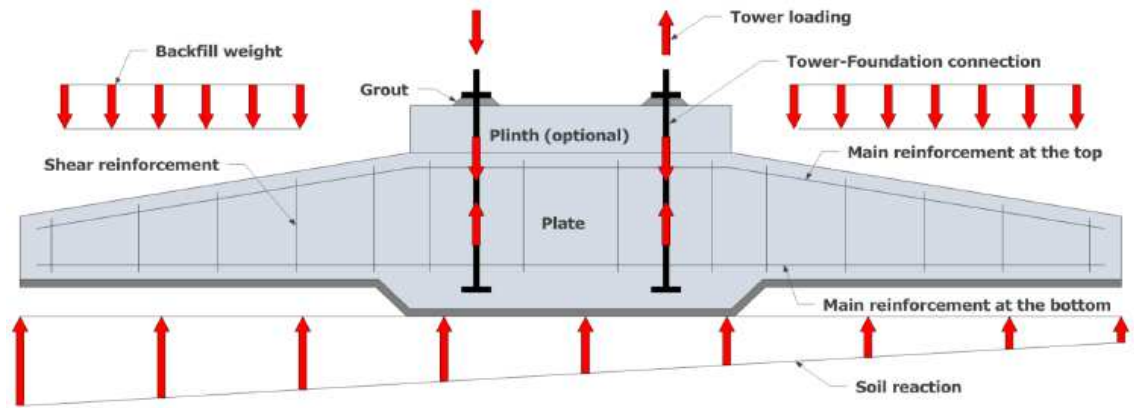


Figure 2.1: Loading mechanism of Wind turbine Foundation (Ceren, 2013)

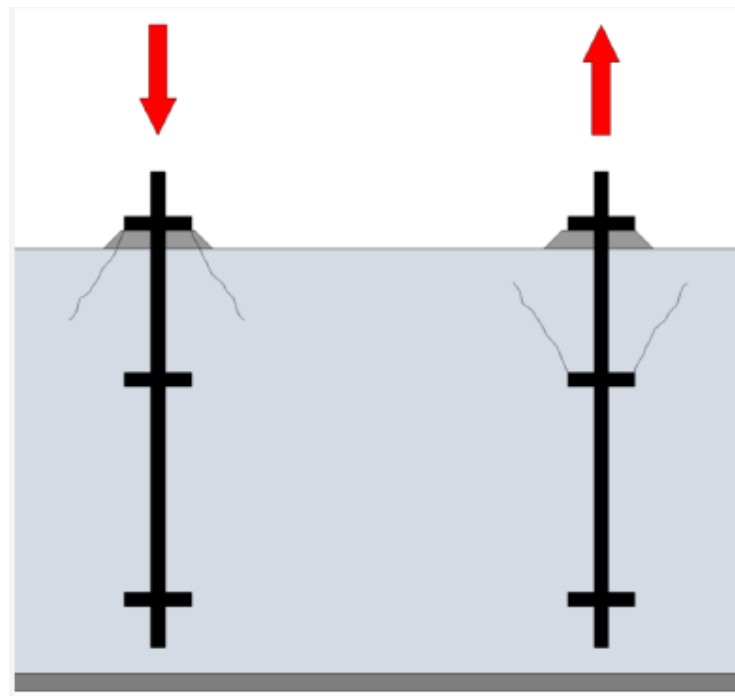


Figure 2.2 Possible failure mechanism of tower to foundation connection (Ceren, 2013)

A wind turbine support system is thus usually analysed for the various loads it will be subjected to during its design life including the dynamic behaviour of its mechanical components such as the control system and protection systems that is braking or pitch regulation. Hence as with the design of any structural system, the first step is to define the load cases. Design load cases are created by combining relevant design situations

(in this instance, turbine operating conditions) with various external conditions that influence the practical workability of the wind turbine. Usually design situations are classified into operating conditions and temporary conditions. Operating conditions are the normal working conditions of the wind turbine encompassing the power production, idling and standing still states. The temporary conditions include cases such as transportation, installation, fault checking and repairs. External conditions generally refers to the environmental conditions of the site the wind turbine is installed. Manwell and others (2002) deemed that the loads of primary concern in the design of a wind turbine could be classified into seven categories namely: static, steady (rotating), cyclic, transient, impulsive, stochastic, and resonance induced loads. Static loads are loads of reasonable constancy that act on a non-moving structure. Steady loads are also constant loads however; they act on the moving parts of the turbine. Cyclic loads are those which vary in a regular or periodic manner. Transient loads are time varying loads which occur due to some temporary external event. Impulsive loads are also time varying but of relatively short duration and with a significant peak magnitude. Resonance induced loads are cyclic loads that result from the dynamic response of some part of the wind turbine being excited at one of its natural frequencies (Manwell et al, 2002).

These loads experienced by the structural components of a wind turbine have a prevailing effect on both its ultimate strength and fatigue resistance. Manwell and others (2002) observed that wind turbines occasionally experience very high loads and must be able to withstand them. They however must also be designed to withstand the widely varying loads that accompany normal operation of the turbine due to starting and stopping, yawing and continuously changing wind speeds, loads

which can fatigue structural components such that they eventually fail at much lower loads than they would have when new.

After design conditions have been selected and load cases extrapolated, design load calculations are done and a prototype model is built. Load measurements are then done to check the wind turbine calculation model which is adjusted if necessary until some reasonable correlation between calculated and measured loads is obtained. A new load set is then produced for the design with the adjusted model. Veldkamp (2006) believes that although at present it seems impossible to calculate more accurately than this, there is some uncertainty in the design loads introduced by a limited number of load cases being evaluated at different wind speeds to model the artificial design wind load however more and longer calculation cycles will reduce this uncertainty to arbitrarily low levels.

Although wind energy production increased by over 109% in the last decade and is predicted to provide at least 20% of the United States' electricity by 2030 (Kuhn et al, 2010), the inherent lack of dedicated structural design codes for wind turbines in the United States means they are usually designed as per the building regulation codes for radio and television towers or in accordance with the IEC/European standards. This although not ideal, is the current industry trend as used in designing the Patrick Henderson Wind Turbine foundation model which has become a standard design model for a large number of wind farms across the United States including the Fossil Gulch wind farm in Henderson, Idaho (Stringer and Huo, 2007). Thus in defining a design methodology for a wind turbine to be built in Worcester Massachusetts, Kuhn and others (2010) adopted a design methodology based on the structural design regulations for radio towers and antennas contending that the shape of a tapered steel

radio or television tower is comparable to that of a wind turbine tower. Hence, they put forth a design methodology for the structural components as:

- Obtain the loads acting on the tower such as axial loads, moments and shear forces.
- Design for stresses using the LRFD approach to design for the tower diameter and thickness of the shell. To account for the taper along the tower height, the tower was broken into sections and an average diameter used for each.
- Design for the tower flange including its connections (anchor bolts) to the foundation.
- Design the tower foundation for a worst case scenario and thus make recommendations as to the proportions, materials and layout of the turbine.

Although they did succeed in designing a wind turbine as per industry standards, their work and outlined methodology did not account for the uncertainty in the loads acting on the wind turbine. These loads generally taken as consistent forces usually act in varying degrees of uniformity and thus are more probabilistic in nature than constant.

Lavassas and others (2003) espoused a probabilistic design methodology for the tower that involves designing the tower against four limit states namely plastic, buckling, fatigue and serviceability limit states. To illustrate this methodology, they designed a prototype wind turbine using detailed Finite Element Analysis (FEA) performed by applying appropriately chosen linearly or non-linearly elastic material and geometrical laws. To this end, the FEA software Strand7 was used along with equivalent simplified models computed by the STATIK-3 software. The reason for combining both detailed and simplified FEA models was the assessment of the reliability and accuracy of the numerical results. Their analyses determined that the

plastic limit state governed the design on the lower part of the structure and the buckling limit state the upper. Although the fatigue limit state did not govern the design, the authors did acknowledge that its effects are critical to determining the dynamic characteristics of the structure.

Cheng and others (2011) in analysing a foundation under the overturning moment limit state adopted a reliability approach based on the first order second moment reliability method (FORM) to determine the performance of the footing under gravity loads from the tower and nacelle. Their research produced results showing that the performance of the foundation is indeed influenced by the variability in the loadings and thus a probabilistic method of design is recommended. The work however, did not take into consideration the increased possibility of the footing exceeding the limit state as a result of additional loading from external sources such as high winds and seismic induced ground motions.

## **2.2 NATURAL HAZARDS**

This section reviews literature pertaining to natural hazards with emphasis on their destructive effects on structural integrity. It is broken into three parts. The first a broad definition and expose on natural hazards particularly earthquakes and winds and the second and third more detailed appraisals of literature on analysis the effects of these individual hazards on a structure.

### **2.2.1 NATURAL HAZARDS**

Natural hazards of geologic origins such as earthquakes and volcanic eruptions or of meteorological origin such as hurricanes, tornadoes, floods and droughts are known for their destructive impact on human life, economy and environment. Around the globe, the four principal natural disasters in terms of losses, earthquakes, windstorms,

floods and droughts, have claimed almost two million lives since 1990 with financial impact in excess of \$200 billion (Chen, 2012). Although it is not possible to completely avoid damage due to such disasters, mitigating their effects is possible by enhancing structural resilience. Engineering communities contribute to this by setting codes and standards for the design and rehabilitation of infrastructural systems a good example being the U.S., which propagates codes and standards for designs resilient to natural hazards as the Uniform Building Code, the International Building Code and the ATC-25 Report for seismic resilient designs as well as the ASCE-7 for the minimum design wind loads for buildings and other structures (Grigoriu & Kafali, 2007).

The sudden movement of the main tectonic plates relative to one another due to high frictional stresses is called an earthquake. The local shock generates waves in the ground which propagate over the earth's surface, creating movement at the bases (foundation) of structures. The magnitude of these waves reduces with distance from the epicentre hence different regions of the world are subject to varying levels of seismic activities (Archelor-Mittal, 2008). Estimation of seismic response of wind turbines is especially important with the rise of the development of wind farms in seismically active regions (Ishihara et al, 2011).

Earthquakes of varying magnitude are regularly experienced throughout the world. Most earthquakes are small and cannot be perceived without special instrumentation. Large earthquakes are rare, but can present a significant risk of damage to civil structures. The average time between large earthquakes (the return period) is often measured in hundreds or thousands of years. With a design life of approximately 20 years most turbines will not experience a strong earthquake, but as with all civil structures, the wind turbine is subjected to some level of seismic risk (Prowell &

Veers, 2009). The action applied by an earthquake to a structure is a ground movement with horizontal and vertical components with the horizontal being the most specific with regards to seismic design because of its strength and also because structures are better designed to withstand gravity (vertical loads) than horizontal forces (Archelor-Mittal, 2008).

Wind is air in motion. As the sun shines on the earth, different parts of the land and sea heat at different speeds. This results in high and low pressure areas and leads to the lift and fall of air masses across the entire globe. Structures deflect or stop the wind, converting the wind's kinetic energy into potential energy of pressure, thus creating wind loads. The intensity of the wind pressure depends on the shape of structure, angle of the induced wind, velocity of air, density of air and stiffness of the structure (Yang, 2006).

Natural wind gusts arise from naturally occurring variability in the velocity and direction of air flow. These gusts are assumed to constitute the fatigue inducing wind loads on turbine towers (Li et al, 2006; Repetto and Solari, 2001; Chen et al, 2003). Fatigue failures of structural components under the cyclic loading associated with these loads occurs in distinct phases- the crack initiation phase, followed by the crack growth phase and then rupture. The crack initiation phase is the life of the structural member until the formation of a surface crack under fatigue loading thus reducing the load carrying capacity of the member. The crack-propagation phase is the remaining part of the life until the crack length reaches a critical value at which point rupture occurs (Muhammed & Ristow, 2010).

Ability to adapt wind turbines for sites prone to extreme events like typhoons and earthquakes is a key point to reach a growth of wind energy worldwide. Wind turbines placed in sites prone to these extreme natural hazards require understanding

the phenomena to tailor specific designs that would guarantee its structural integrity (Meilan & Tsouroukdissian, 2010).

### **2.2.2 SEISMIC ANALYSIS OF WIND TURBINES**

Earthquakes are stochastic events that cannot be predicted but may be represented synthetically in order to design a structure. The main concerns for seismic loading; seismic risk, local soil properties and structural properties such as frequency, ductility and damping, are the same regardless of the type of structure being considered. Wind turbines suffer an extreme force at the base of the tower during an earthquake, induced by the direction of the earthquake. The earthquake may be near a fault, which can be represented by a large impulse in a short period of time; and/or a long period earthquake, which is a lower amplitude one but longer in time. Both can cause severe damage due to the nature of this cyclic loading (Meilan & Tsouroukdissian, 2010). Evaluation of wind turbine seismic loading is generally carried out using wind industry design standards which entail the calculation of a representative horizontal seismic load using local building code procedures and superimposing the load with the turbine emergency stop or normal operating loads. Ntambakwa and Rogers (2009) however deemed this approach as too simplistic especially given that building codes' seismic design provisions have a main goal of ensuring life safety in the event of an earthquake occurring, but as wind turbines are generally unoccupied structures, there exists a fundamental disconnect between the goals of the building codes and the practical requirements for wind turbine support systems.

Prowell and Veers (2009) in evaluating existing literature on seismic analysis of wind turbines advocated the use of full system models in analysing the seismic loading of wind turbines as against simplified models which remove the complexity of the rotor because the full models incorporate all possible factors to seismic risk and also has the

benefit of prediction of component loads instead of only tower loads. They however admit that the simplified model does adequately estimate the loads on the tower and foundation and can be used for design iterations. Probability based design methodology for seismic loading of buildings requires the proper matching of two quantities, the seismic capacity and the seismic demand. Demand is the description of the earthquake ground motion effects on the building while capacity is the ability of the building to resist the seismic effects. In estimating the seismic capacity, a sequence of inelastic static analyses is performed on the building when it is subjected to a set of increasing lateral loads. The building is thus pushed, hence the name pushover analysis, until its displacement reaches some predetermined limits. The displacement limit may be set on different criteria such as the maximum allowable storey drift or ductility limits. Appraising the seismic demand is done by determining a target displacement that is an estimation of the top displacement of the building when exposed to the specified level of ground shaking. To evaluate the damage potential of the building at the specified level of ground shaking, the target displacement should first be determined, and then a pushover analysis conducted in which the building is pushed until its top deflection matches the target displacement. The damage estimates from the pushover analysis at the target displacement level are considered to be representative of the structural damage to the building due to ground shaking (Tso & Moghadam, 1998). Kafali and Grigoriu (2007) in presenting a methodology for seismic intensity measure for fragility analysis defined seismic fragility of a structural system as the probability that a system response exceeds a critical value under seismic ground motions of specified intensities. Several studies have focused on comparing the frequency-domain and time-domain approaches to carrying out seismic analysis. Witcher (2005) concluded that although

both methods were adequate, the time domain method is advantageous and thus preferable because it is possible to correct a discrepancy in the system damping value at parked conditions unlike for the frequency-domain method for which this discrepancy cannot be corrected (Nuta et al, 2011).

Zhao and Maisser (2006) believe that although the wind turbine tower is the most important structural component when analysing dynamic response, the interaction between the structure, foundation and the surrounding soil is also significant as the inclusion of soil structure interaction resulted in reduced fundamental frequencies of the turbine, particularly in areas with flexible soil and thus this interaction should be included in dynamic analysis of wind turbines (Nuta et al, 2011). Although existing code provisions are few and current research has thus far established that seismic loads do not typically govern the design of the tower, Nuta and others (2011) opine that the seismic risk of wind turbine towers is still of importance to owners of wind turbine developments, especially farms, because as all towers are generally identical, a seismic event would affect them all in the same way and as such the failure of one tower could mean the failure of all, a situation having severe financial implications for developers and the economy alike. They thus postulated a methodology for determining the probability of damage for a wind turbine tower at various levels of damage using the finite element method (FEM).

By modelling a wind turbine and subjecting it to several dynamic analyses, Nuta and others (2011) examined the behavior under dynamic seismic loading and consequently put forth a methodology for seismic risk assessment. By carrying out a pushover analysis, they established that buckling failure most likely occurs close to the base of the tower. A time history analysis of the model indicated a different location for buckling to occur and this was explained as due to the effect of higher

modes in the dynamic seismic analysis using the time domain method. Fragility curves developed using the results obtained was then used to determine the probability of exceedance for a particular damage state.

Seismic hazard analysis is the estimation of the maximum amplitude of some ground motion parameter (e.g. peak ground acceleration, peak ground velocity, relative displacement, etc.) expected to occur once at a certain site or area within a particular time span (return period) (de Vos, 2010). There are two primary approaches to estimating the seismic hazard at a site. One is the deterministic approach in which the ground shaking at the site is estimated from one or more earthquakes of specified location and magnitude while the second method is the probabilistic method in which the contributions from all possible earthquakes around the site are integrated to find the ground motion that has a particular probability of not being exceeded at that place within some time period (Ebel & Kafka, 1999).

Ebel and Kafka (1999), Weatherill and Burton (2006) as well as de Vos (2010) although conceding that the deterministic analyses are less complicated than the probabilistic methods, opine that they are also too restrictive and fail to take several scenarios into account. The probabilistic methods however allow the use of several input values as well as continuous events and models, thus giving a more accurate depiction of the structure's response to stochastic loads.

However a standout drawback to probability seismic hazard analysis is that the predicted ground motion corresponding to some probability level is not related in a clear way to any single earthquake, since the ground motion in consideration corresponds to many different earthquakes around the site, each with a different probability of occurrence. Thus in proposing an alternative to the above methods, Ebel and Kafka (1999) utilize a Monte Carlo approach in generating a synthetic

earthquake catalogue by sampling with replacement a real earthquake catalogue and then calculating the seismic hazard using estimations of the ground motions at a given site or sets of sites due to the various earthquakes generated in the catalogue. Weatherill and Burton (2006), and Musson (2000) in highlighting the advantages of Monte Carlo simulations in probabilistic seismic hazard assessment determine it can be used to assess different seismic estimation approaches as well as used to calculate the possibility of earthquakes occurring away from areas of observed seismicity while also maintaining the existing patterns of low and high seismicity. It is also useful in identifying an encompassing design earthquake as well as being conceptually straightforward.

#### 2.2.2.1 Monte Carlo Procedure for Seismic Hazard Analysis

Ebel and Kafka (1999) developed a methodology for applying Monte Carlo methodology to seismic hazard analysis as follows;

- The seismic hazard is first quantified by a seismic hazard function  $P(a > a_0)$ , where P gives the probability that the ground motion  $a$  at a site will exceed the value  $a_0$  at least once in a given time period.
- The probability is then found using the function:

$$P(a > a_0) = 1 - e^{-\lambda_t(a_0)} \quad (2.1)$$

where:

$\lambda_t$  is the average rate of the number of times a particular ground motion

$a_0$  is exceeded in a time period T.

- For a stationary event process, the seismic hazard can simply then be estimated by counting the number of occurrences  $N_T$  with  $a > a_0$  at the site during a time period T giving;

$$\lambda_t(a_0) = N_T/T \quad (2.2)$$

- However, if the catalogue of past earthquakes is complete from the largest possible event near the site down to some small magnitude (below the level of significant ground shaking), then the seismic hazard for ground motion  $a_0$  is estimated using;

$$\lambda_t(a_0) = T/T_0 \sum H[a_k - a_0] \quad (2.3)$$

where:

H is the Heaveside step function which the cumulative distributive function of the random variable  $a$ ,

$T_0$  is the duration of the catalogue.

- Then again, as all available catalogues of historic earthquakes are much too short to represent the long term seismic activity in an unbiased manner, the incompleteness of the data is accounted for using the equation;

$$\lambda_t(a_0) = T/T_0 \sum Q_m P(a > a_0 | m_k, r_k) \quad (2.4)$$

where:

$Q_m$  is a factor that corrects for the underrepresentation of events with magnitude  $m$  in the catalogue,

$m_k$  represents the  $k_{th}$  earthquake in a catalogue occurring at a distance  $r_k$  from the site in question.

To utilize the above equations, synthetic earthquake catalogues need to be constructed by extending the known catalogues in time, as well as if necessary in magnitude and space (Ebel & Kafka, 1999).

### 2.2.3 FATIGUE ANALYSIS OF WIND TURBINES

Fatigue can be defined as the initiation and propagation of microscopic cracks into macroscopic cracks by the repeated application of stress (Li et al, 2006). The fluctuating nature of wind loading produces oscillating stresses with contributions

from resonant and background (sub-resonant) components thus inducing fatigue (Holmes, 2001). This causes a loss of lateral resistance of structures especially those with a high exposure to turbulent wind loads. This reduction in resistance may in turn help to amplify the effects of seismic activities on these structures (Banerjee & Prasad, 2011). Identification of particular structures that will exhibit fatigue is especially difficult because fatigue is a process with an unusually large amount of inherent variability (Dexter and Ricker, 2002).

Natural wind gusts arise from the naturally occurring variability in the velocity and direction of air flow. Changes in the velocity and direction of air flow produce fluctuating pressures on a structure, which can cause it to vibrate. The magnitude of the vibration is a random variable. The variable stress ranges in the structural components of the structure, which are caused by the random vibrations, will produce fatigue damage in the long term (Li et al, 2006).

Modern wind turbines are fatigue critical machines used to produce electrical power. Economic viability requires them to have both low initial cost and long term reliability. From their inception, wind turbines have experienced fatigue problems especially in “energetic” sites (sites with an average wind speed of 7 m/s (16mph) or more) however; turbines installed more recently have shown tremendous improvements (Sutherland & Veers, 1995).

Kacin (2009) asserts that every structure has an estimated length of time it can stand before failing due to fatigue damage. This she opined will be the point when a fatigue induced crack on the superstructure is allowed to grow to a point when it reduces a section’s capacity so much that it cannot carry the required loads. Accurately estimating fatigue life can help in mitigating these cracks and thus improving structural performance.

When performing the fatigue life assessment of structural elements, there are two basic methods that can be used. One considers an analysis of crack propagation at the point under consideration and is based on linear elastic fracture mechanics. The second approach, which is more commonly applied, uses a curve that shows the relation between cyclic stress range and number of cycles to fatigue failure in logarithmic scales. This is known as the Wohler curve or the S-N curve (Goransson and Nordenmark, 2011). These curves are derived from experimental data obtained from material fatigue tests.

Ariduru (2004) summarized a methodology for estimating fatigue life of a structure into five basic steps namely;

1. Conceiving a structural model
2. Developing a time history of the cyclic loads
3. Using the rainflow counting method, determine the stress history
4. Develop a stress range histogram, and
5. Using the Palmgren-Miner rule, draw up an estimate of the structure's fatigue life.

Fatigue evaluation procedures use cumulative damage at locations of critical stress to assess probability of cracking and failure (Rao & Roesler, 2004, Singh, 2006). This damage accumulation concept, postulated by Palmgren and Miner assumes that damage accumulates linearly and can be expressed as (Miner, 1954);

$$\text{Fatigue damage} = D = \sum_{i=1}^{\infty} \frac{n_i}{N_i} \quad (2.5)$$

where;

$n_i$  = number of load cycles at a particular stress level

$N_i$  = number of load cycles until failure at that stress level.

Thus the Miner rule was taken for the limit state of fatigue as;

$$g(x) = 1 - D \quad (2.6)$$

His results show that both the frequency domain method and the time domain method of carrying out rainflow counting are accurate. This result agreed with that of Ragan and Manuel (2007) who showed these methods to be more precise than the alternate Dirlik's spectral method (Ragan and Manuel, 2007).

Holmes (2001), developed a closed form solution for fatigue damage and fatigue life of structures under alongwind loading making some simplifying assumptions in the process but opining that the errors resulting from these assumptions were probably less than those resulting from the uncertainties in the input parameters in practical design considerations. He assumed that each cycle of a sinusoidal stress response inflicts incremental damage which depends on the amplitude of the stress and this accumulates in proportion to the number of cycles until failure occurs and thus developed a time dependent equation for narrow band fatigue loading i.e. wind loading situations produce resonant narrow- band vibrations such as the alongwind response of structures with low natural frequencies, and cross-wind vortex induced response of circular cylindrical structures with low damping eventually coming up with an equation of the form:

$$D = \frac{kV_0^+ T (\sqrt{2A})^m}{Kc^k} \Gamma\left(\frac{m}{2} + 1\right) \frac{c^{mn+k}}{k} \Gamma\left(\frac{mn+k}{k}\right)$$

$$= \frac{V_0^+ T (\sqrt{2A})^m c^{mn}}{K} \Gamma\left(\frac{m}{2} + 1\right) \Gamma\left(\frac{mn+k}{k}\right) \quad (2.7)$$

where:

D = Total expected fractional damage

$V_o^+$  = the rate of crossing of the mean stress

T = Time period

K = material dependent constant

$\sigma$  = standard deviation of the entire stress history

S = amplitude of cycles

$\Gamma$  = the Gamma function

However, to overcome some restrictions placed on the narrow band equation as shown above, he further developed a wide band equation as:

$$D = \frac{\lambda V_o^+ T (\sqrt{2A})^m c^{mn}}{K} \Gamma\left(\frac{m}{2} + 1\right) \Gamma\left(\frac{mn+k}{k}\right) \quad (2.8)$$

where:

A = a constant based on the longitudinal turbulence intensity

$\lambda$  = a parameter determined empirically

These equations did serve to estimate fatigue damage on a structure over time and also to determine its upper and lower fatigue lifetimes. However, his research only considered the alongwind loading condition on structures.

Veldkamp (2008) in a probabilistic evaluation of wind induced fatigue design identified a limit state function for wind fatigue taking into account important stochastic parameters influencing fatigue loads and their estimated distributions as:

$$Z'(x) = q_0 x_{dim} x_{\Delta\sigma A} SRF \gamma_f \gamma_m - \prod_j \frac{S(x_j; \forall i \neq j: x_i = x_{char,i})}{S(x_{char})} \quad (2.9)$$

where:

$Z'(x)$  = fatigue limit state function

$q_0$  = parameter for variation in fatigue strength due to load sequence effects;

$X_{dim}$  = parameter for variation in material dimensions;

$X_{\Delta\sigma A}$  = parameter for variation in constant amplitude fatigue strength.

$\gamma_f$  = load factor

$\gamma_m$  = material factor

SRF = stress reserve factor = 1.05

Using the above equation and by inputting the necessary parameters, he was able to determine the probability of failure for various components of a wind turbine due to fatigue and thus enhance optimisation of the said component.

Li and others (2006) in carrying out a fatigue analysis of sign structures employed a methodology as:

1. They simulated natural wind loadings numerically by obtaining a wind spectrum from prevailing wind pressures and then applying a Weibull distribution for a representative period of time in this case 10 minutes after which the simulated values were used in transient dynamic Finite Element Analyses. Representative wind loading histograms were generated at critical locations.
2. Dynamic stress analyses of prototype sign structures were conducted for critical details to obtain stress time histories for specific details.
3. They then performed fatigue analyses to estimate the fatigue life expectation of fatigue susceptible details under different wind environments.
4. The fatigue life expectations of the critical details were then compared so as to determine the fatigue prone areas of the support structure.

Fatigue cracking in concrete footing is a key failure mechanism and is the result of repeated applications of load at stress levels less than the flexural strength of the concrete (Rao and Roesler, 2004). This results in a stress field developing in the

concrete that depends on climatic conditions, footing dimensions, load transfer etc. After repeated cyclic load application, damage (cracks) develop, accumulate and propagate in the concrete.

### **2.2.3.1 Fatigue Model for Concrete**

Several fatigue models have been developed to determine fatigue damage in concrete. For this study, the ERES/COE field fatigue model was adopted. Developed using Corps of Engineers field aircraft data, failure is defined in this model as 50 percent cracking and the number of cycles to failure  $N$  is presented as (Rao and Roeler, 2006):

$$\log N = 2.13 SR^{-1.2} \quad (2.10)$$

where:

$SR$  = stress ratio experienced by a concrete slab and is computed by;

$$SR = \frac{\sigma}{MR} \quad (2.11)$$

$\sigma$  = total tensile stress applied at the location

$MR$  = modulus of rupture of the concrete.

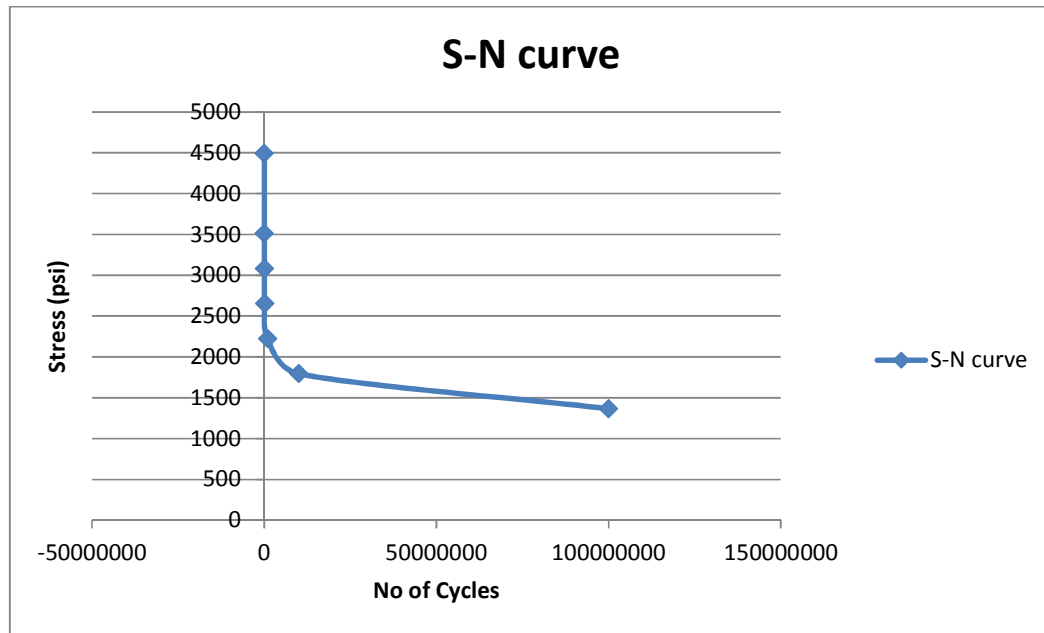


Figure 2.3: S-N curve for concrete model (Rao and Roeler, 2006)

### 2.3 MULTI- HAZARDS

Multi-hazard risk analysis of a system deals with the assessment of the system performance under multiple random loads caused by natural and/or manmade hazards, some of which may occur simultaneously (Grigoriu & Kafali, 2007). There is a growing interest in the development of procedures for the design of structures exposed to multiple hazards. The goal is to achieve safer and/or more economical designs than would be the case if the structures were designed independently for each hazard and an envelope of the demands induced by each hazard were used for member sizing (Potra & Simiu, 2009). The importance of consideration of possible multi-hazard events for the reliable performance evaluation of structures is well understood albeit poorly documented (Banerjee & Prasad, 2001).

In recent times, useful, if mostly ad hoc approaches to multi-hazard design have been proposed but a broad, multidisciplinary foundation for multi-hazard design still

remains to be developed. Potra & Simiu, (2009), hold forth that such a foundation should include a probabilistic component to account for the uncertainty of these hazards. In light of this, they proposed a nonlinear programming model for multi-hazard design involving optimization procedures as a means of integrating the design so that the greatest possible economy and efficiency is achieved while satisfying specified safety related and other constraints. This is done by considering a set of variables that characterize the structure and subjecting the variables to a set of constraints. A design that satisfies the set of constraints is then considered feasible. Optimization of the structure then involves selecting from the set of all feasible designs, the design that minimizes a specified objective function which may be representative of for example cost of the structure. While this procedure provides an integrative framework for optimization of a structure under constraints usually associated with hazards, it is quite involved and proves impracticable when considering more than two hazards or an extensive number of variables as is usually associated with natural hazards.

By outlining the multi-hazard analysis of an offshore platform, Grigoriu and Kafali (2007) defined some considerations for design and analysis under multi-hazards. The considerations are system fragility (system topology and hazard level) and multi hazards (consequences/safety levels and hazards concurrence). The delineation of these considerations led to their putting together a computational model showing temporal/spatial discretization and response levels for systems. They then came up with a probabilistic model of system reliability under multi hazards as

$$P_s(x) = \exp[-v_1\tau(1 - F_1(x)) - v_2\tau(1 - F_2(x)) - v_1v_2(\mu_1 + \mu_2)\tau(1 - F_{12}(x))] \quad (2.12)$$

where:

$v_k$  = mean arrival rate of hazard k

$F_k$  = cdf of hazard k intensity

$\mu_k$  = average duration of hazard k

$F_{12}$  = cdf of combined hazard intensity

From their findings, Grigoriu and Kafali (2007) then resolved that the effect of hazard concurrence is negligible and also that system failure under multiple hazards can be accurately estimated by an envelope of the failure probabilities under single hazards. Their conclusions however, failed to take into effect the different possible scenarios under which different hazards function and the possible long term effects some may have on structural systems.

McCullough and Kareem (2009) postulated that multi-hazard engineering strategies could be incorporated into design to enhance the inherent resilience and improve the robustness of structures by considering the design strategies for all hazards within a balanced all-inclusive design. They opined that a multi-hazard engineering approach has the potential to reduce the capacity for dynamic loads to inflict significant damage on structures by considering the multiple hazards with which a structure may be faced in all aspects of design and construction. In addition, they proposed the combination of multi-hazard engineering with performance based engineering which they believed will further increase the robustness of the system. They thus proposed a framework for performance based design in a multi-hazard environment as defining the individual and combined hazards, determining the structural responses associated with the range of hazards and intensities and developing fragility curves. System fragility

represents the conditional probability that the structural response exceeds a damage state given a hazard intensity. These damage states correspond to defined limit states which are related to performance levels. This proposed procedure is iterative and is performed until a performance level is achieved for the structure which is acceptable to all parties.

McCullough and Kareem (2009) also contended that probabilistic nature of the method is particularly important because of the many sources of uncertainty in multi hazard analysis.

This procedure does help to streamline the complex nature of multi-hazard analysis and offer an optimal framework for creating the best engineering design and analysis methodology for multi-hazard and performance based engineering. Duthinh and Simiu (2010) presented a study proving an increased risk of limit state exceedance for regions subjected to multiple hazards as compared to regions with risk of only one hazard. The premise upon which Duthinh and Simiu base their research on is that the American Society of Civil Engineers' design code (ASCE 7-05) treats regions affected by wind and earthquake separately, considering only the dominant loading in the design. Their research however revealed this principle to be inherently flawed as they showed that a structure within a region with overlapping hazards is at risk from both and thus will have an increased risk of limit state exceedance than when only one hazard scenario is considered. There have also been arguments that since the probability of both hazards occurring simultaneously is negligible, only the greater demand needs to be satisfied. This is invalid because while the physical stress on the structure does not increase for a multi-hazard region, limit states specified by the code are not solely dependent on the load demand, but also depend on the probability of the load occurrence. To resolve this problem of increased risk for multi-hazard regions,

Duthinh and Simiu (2010) proposed to modify ASCE 7-05 standards so that areas with both wind and earthquake hazards can be designed separately with corrected limit states so the risks in that region are similar to areas subjected to only one hazard. Using a case study of an overhead water tank structure, they showed that there was a significant increase in the design loads under multi-hazard consideration as compared to when the loads were computed using the greatest possible hazard scenario. They thus proposed a change to the modification factors recommended in ASCE 7-05 to correct this anomaly.

In exploring the structural response of mid to high rise buildings subjected to wind and earthquake loading, Chen (2012) found that these buildings are not often governed by gravity loads but by lateral loads from various natural hazards including high winds and earthquakes. She contends that while the current design practice for tall buildings requiring the consideration of only the controlling load case for structural design is adequate for areas where there is only the risk of one hazard, the method underestimates the increased risk for multiple hazards regions and does not consider the differences in structural response to different load types. These variations in structural requirements necessitate the consideration of a multi-hazard type loading scenario during design. Ragheb (2009) stated that because of the complex systems of variable loads and their slenderness, wind turbines are particularly susceptible to fatigue damage. The cyclic wind loading of wind turbines could cause failure if some critical level of damage is exceeded, this process once initiated, will cause damage which will grow with the load cycling hence reducing structural reliability until failure occurs. Hence, the occurrence of a seismic event in the area after this wind induced structural damage could thus increase the risk of failure of structural components.

## 2.4 RELIABILITY ANALYSIS

Probabilistic structural analysis may be defined as the art of formulating a mathematical model within which the behaviour of a structure can be determined under various loading and material property scenarios (Bomel, 2001). The direct use of probabilistic methods and structural reliability techniques in design is the latest step in the evolutionary process that is structural design. Although primarily used for very important structures or structures with high failure consequences, the use of probabilistic design is growing and is now incorporated into many codes of practice either in the calibration of partial factors of safety or proposed as an alternative design approach. Nowak and Collins (2000) defined a limit state as a boundary between the desired and undesired performance of a structure. These performance indices can be expressed mathematically in the form of probability of failure.

Bomel (2001) defined limit state as a state of the structure or part of the structure that no longer meets the requirements laid down for its performance or operation. They also opined that a 'Limit State' is a mathematical criterion that categorizes any set of values of the relevant structural variables (loads, material and geometrical variables) into one of two categories - the 'desirable' category and the 'adverse' category. The word 'failure' then means 'inability to satisfy the Limit State criterion', rather than a failure in the sense of some dramatic physical event.

Three types of limit states are considered in structural reliability analyses (Nowak and Collins, 2000):

1. Ultimate limit states which are mostly related to the loss of load carrying capacity.

2. Serviceability limit states which are generally related to the gradual deterioration, user's comfort or maintenance costs but however may not be directly related to structural integrity.
3. Fatigue limit states are defined under the loss of strength due to repeated loading. These limit states are related to the accumulation of damage and eventual failure under repeated loading. In any fatigue analysis, the critical factors are both the magnitude and frequency of load. For any of the above limit states, a component or system may fail in a number of failure modes including but not limited to buckling, yielding, bending fatigue, fracture etc., a situation which in the extreme leads to loss of structural integrity and can have consequences affecting the safety of lives and/or the environment.

The structural reliability analysis procedure as outlined by Bomel (2001) is as follows;

1. Identify all significant modes of failure of the structure or operation under consideration and define failure events.
2. Formulate a failure criterion or failure function for each failure event.
3. Identify the sources of uncertainty influencing the failure of the events, model the basic variables and parameters in the failure function and specify their probability distributions.
4. Calculate the probability of failure or reliability for each failure event, and combine their probabilities where necessary to evaluate the failure probability or reliability of the structural system.
5. Consider the sensitivity of the reliability results to the inputs and assess whether the design point values are physically feasible.

6. Assess whether the evaluated reliability is sufficient by comparison to a target value.

Toft and Sorensen (2008) in carrying out a reliability analysis for wind turbines concluded that wind turbines can fail due to a number of mechanisms and as such proper reliability analysis will need to include several failure mechanisms across different limit states especially the ultimate and fatigue limit states. Their calculations in subsequent example models showed wind turbines to have a higher annual probability of failure than other civil engineering structures. This they explained to be in line with code specifications and is so because the consequences of wind turbine failures are less severe than say for example buildings which have a higher occupancy rate. However this higher probability of failure is without taking into account non cyclic or permanent loads such as earthquake which could further raise the probability of failure a notch.

## **2.5 SENSITIVITY ANALYSIS**

Sensitivity analysis is carried out to determine the most important parameters affecting structural safety (Nowak and Collins, 2000). It is the study of how the uncertainty in reliability analysis can be allocated to different variables in the input. Sensitivity analysis is used to understand the relationship between the input variables and the resulting output in the reliability analysis. A study of the sensitivity analysis can be used to determine the extent to which uncertainty in a variable can affect the performance of the entire system.

## **2.6 FINITE ELEMENT ANALYSIS**

The finite element method (FEM) is a numerical technique for finding approximate solutions to partial differential equations (PDE) and their systems, as well as integral equations. In simple terms, FEM is a method for dividing up a very complicated

problem into small elements that can be solved in relation to each other. Its practical application is often known as finite element analysis (FEA). FEA uses a complex system of points called nodes which make a grid called a mesh to define the geometry of the model. Simply put, the finite element method involves modelling a structure using small interconnected elements called finite elements. A displacement function is associated with each finite element. This mesh is programmed to contain the material and structural properties which define how the structure will react to certain loading conditions. By using known stress/strain properties for the material making up the structure, one can determine the behaviour of a given node in terms of the properties of every other element in the structure. The total set of equations describing the behaviour of each node results in a series of algebraic equations best expressed in matrix notation. The response of mathematical models of a wide range of engineering designs from an engine block to an airplane wing to a building or parts of it can be discerned by discretization of the model into finite elements. This model can be discretized into a fine mesh of small components to give a good approximation of the behaviour of an actual built model or into a coarse mesh for faster computation. A wide range of analysis can be done using the finite element analysis including displacement, stress equivalent force and moments. The steps for carrying out a finite element analysis include (Logan, 2007);

1. Discretize and select element types.
2. Select a displacement function.
3. Define strain/displacement and stress-strain relationships.
4. Derive the element stiffness matrix and equations.
5. Assemble the element equations to obtain the global or total equations and introduce boundary conditions.

6. Solve for unknown degrees of freedom.
7. Solve for stresses and strains.
8. Interpret results.

With the development of the personal computer, several general purpose and special purpose programs have been developed for finite element analysis and thus with advances in solver programs, carrying out FEA for large complicated structures has become relatively easier.

The advantages of carrying out a finite element analysis include:

1. It makes modelling irregular shapes much easier.
2. It reduces the difficulty of managing general loading conditions.
3. It makes it possible to model bodies composed of different materials.
4. It can handle nonlinear behaviour arising from nonlinear materials as well as due to large deformations.

The general purpose program ANSYS is used in this work to carry out the ensuing analysis.

### **2.6.1 ANSYS Finite Element Model**

ANSYS is a general purpose finite element modelling package for numerically solving a wide variety of engineering problems. These problems include: static/dynamic structural analysis (both linear and non-linear), heat transfer and fluid problems, as well as acoustic and electromagnetic problems. Developed by ANSYS Inc., it is used in engineering research to carry out finite element analysis on a wide range of engineering structures. Carrying out a finite element analysis on ANSYS involves several steps including modelling the structure under investigation, meshing it, applying loads and boundary conditions and solving (ANSYS, 2010).

## 2.7 SUMMARY

With the field of multi-hazard engineering still in relative infancy, there are few completed studies upon which this research can draw from. However, from the ones conducted so far, it is evident that further research is required.

Grigoriu & Kafali (2007), Banerjee & Prasad (2011) and McCullough & Kareem (2009) all discussed the need for a multi-hazard platform for structural analyses. Using different hazards and scenarios, they all did come up with a guiding framework for multi-hazard design. Although their methodologies and results differed, they all generally agreed that for optimisation of structures, multi-hazard design is essential.

Dutinh & Simiu (2010) in continuing research showed using the reliability theory that there is an increased risk of limit state exceedance for regions subjected to multiple hazards thus further strengthening the argument for a multi-hazard analysis methodology. Other authors (Chen, 2001; Ragheb, 2009), in various studies helped to verify the claims of the above.

Much work has been carried out on both seismic and fatigue analyses of structures leading to standard design and analysis methodologies for both design scenarios. Authors such as Meilan & Tsourouldissian (2010), Ntambakwa & Rogers (2009), Prowell & Veers (2009), Holmes (2001) etc., have both initiated and verified procedures for the analyses.

All the studies and research carried out and presented above have consistently shown the increasing importance of reliability analysis in the structural design process especially in dealing with multiple possible failure scenarios. Toft & Sorensen (2008) specifically showed the need for continued research in using reliability analysis methods in wind turbine design given the huge uncertainty associated with analysing their performance thus turning previously assumed design constants into variables.

This thesis in drawing from the presented literature is set up to analyse the probable effects of seismic events on the fatigue capacity of wind turbine foundations especially as regards to their probability of failure under combined wind fatigue and earthquake loading. Review of the above presented material has helped to define a methodology based on FEM modelling and the reliability theory on which this research is based.

## **CHAPTER THREE**

### **METHODOLOGY**

The following is a description of the methods by which the multi-hazard risk to a wind turbine foundation is evaluated. This includes a description of the analysis for the individual hazards that together pose a multi-hazard risk as well as the multi-hazard risk assessment. These analyses are carried out by utilizing a MATLAB analytical code and the ANSYS finite element software.

#### **3.1 METHODOLOGY OVERVIEW**

This study is started by identifying a viable location for installation and implementation of wind turbines. Idaho Falls, Idaho is selected as a case study because of its proximity to several wind farms as well as its terrain and climatic suitability. It also lies in an area of high seismic activity. A wind turbine model design is selected for use in the study based on one designed by Kuhn and others (2010). Figure 3.1 gives an overview of the methodology used for this research.

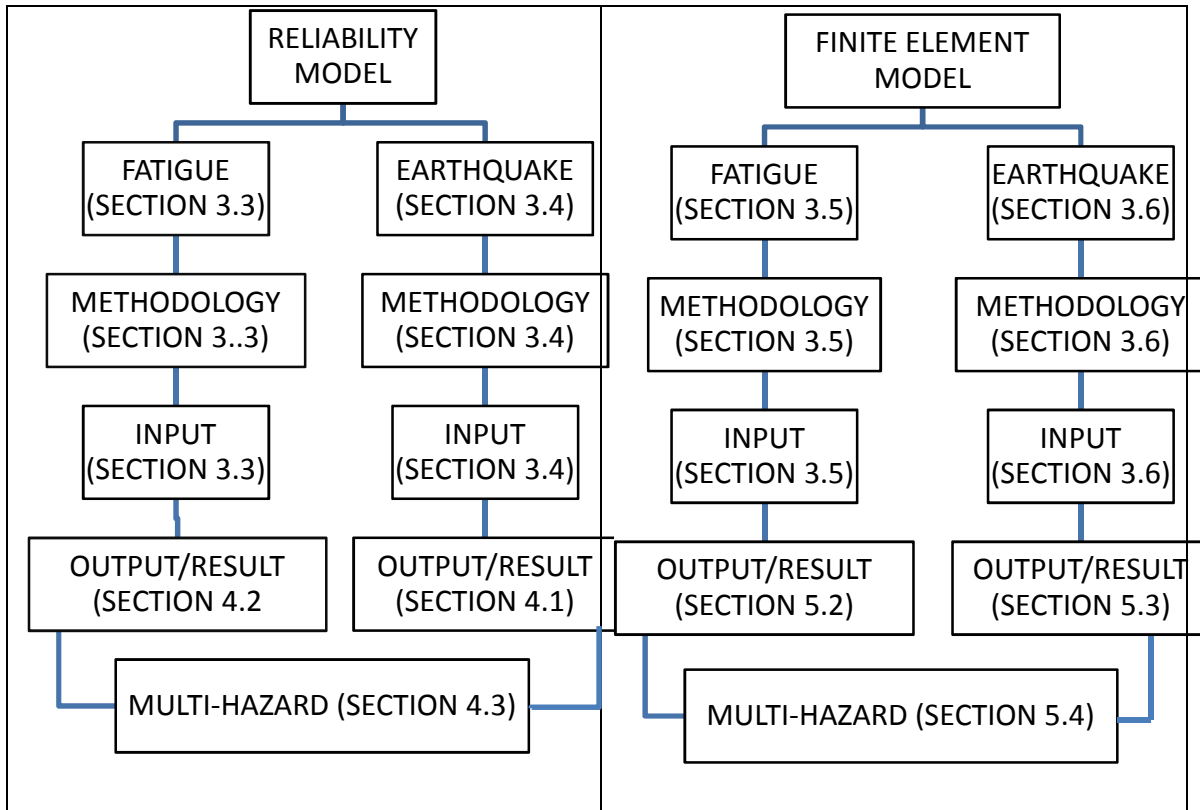


Figure 3.1: Outline of Methodology used

### 3.2 MONTE CARLO SIMULATIONS

In designing a methodology, the study is divided into three constituent parts for the Monte Carlo simulations: fatigue analysis, seismic analysis and multi-hazard analysis. Each of these analyses is further broken down into logical steps in MATLAB.

#### 3.2.1 Fatigue Analysis

The fatigue analysis is carried out using the following methodology:

1. Wind speed data is obtained for the Idaho Falls area. This is done in order to properly simulate environmental conditions expected to act on the turbine's foundation.

2. These wind speeds are converted into wind forces to properly gauge their effects on the concrete footing.
3. Stresses resulting from these wind forces acting on the concrete foundation are then calculated. This is necessary because the fatigue in a material is directly dependent on the stresses acting in it.
4. The number of cycles to failure at the computed stresses is then determined to estimate the fatigue life of the foundation at these stress ranges.
5. The actual frequency of the wind speeds is then computed. This is used to gauge the number of damage cycles the foundation undergoes at a particular wind speed.
6. The damage fraction from each wind speed is then calculated. This gives an estimate of just how much damage occurs at a particular wind speed.
7. The damage fractions are summed up as per Miner's rule to obtain the total damage sustained by the concrete foundation from cyclic winds.
8. The fatigue limit state is defined. This limit state equation is used to determine the fatigue reliability of the foundation.

### **3.2.2 Seismic Analysis**

1. The possible amplitudes of motion from a seismic event are computed using the surface wave formula and Monte Carlo simulations. This is done in order to obtain a wide range of possible ground motion data for a particular magnitude of earthquake.
2. The frequency ratio is determined for this range of data from the displacement transmissibility equation. The frequency ratio is used in vibration analysis to check for possible resonance in a structure at a particular frequency.

3. The seismic limit state is defined to determine the reliability of the foundation under seismic action.

### **3.2.3 Multi-Hazard Analysis**

1. The system is modeled in series. This is because both loading scenarios are independent events and their probabilities of occurrence are totally uncorrelated.
2. The multi-hazard reliability is determined by combining the probabilities of failure from both limit states.

### **3.3 Finite Element Analysis**

1. A reinforced concrete model with a steel anchor bolt imbedded in it is built in ANSYS. This is used for the finite element analysis to examine the bond interaction between the concrete and the steel bolt under the loadings in consideration.
2. The model is validated using a pullout analysis. By calculating the pullout force needed and applying it to the anchor bolt, the model shows a conical shaped crack which is in agreement with the pullout theory. This validates the behavior of the concrete.
3. Transient analysis is selected from the ANSYS solution options. This is used because both the loads are time dependent. Cyclic winds for the fatigue and displacement for the earthquake.
4. Each calculated wind load from the varying wind speeds are input as a time step. The displacement time history is also input as a time step.
5. The model is run and results obtained.

6. Stresses from both analyses are obtained from the ANSYS postprocessor.
7. Fatigue damage is calculated in the ANSYS post processor using the calculated number of cycles at each wind speed.
8. Fatigue reliability is determined using the fatigue damage values in the limit state equation.
9. Seismic reliability is calculated by checking for the possibility of cracking in the concrete due to the seismic stresses.
10. The multi-hazard stresses are obtained by carrying out a vector summation of the fatigue stresses and seismic stresses in the ANSYS post processor.
11. The multi-hazard reliability is computed by checking the possibility of cracking against the modulus of rupture using the first order second moment reliability method.

The necessary material properties as well as equations and loads for the analyses are obtained and used to define the research model as described in the ensuing sections.

### **3.4 FATIGUE ANALYSIS IN MATLAB**

The methodology for fatigue analysis is carried out using the following steps:

1. Obtain mean wind speeds. This is done using the wind rose diagrams published by the National Water and Climate Center resource library (NWCC, 2013) as seen in Appendix B.
2. Determine the wind pressures acting on the tower from the wind speeds by

$$P_{NW} = C_d * I_f * \left( \frac{V_m}{11.7} \right) \quad (3.1)$$

where:

$P_{NW}$  = Pressure from the wind

$C_d$  = drag coefficient for a cylindrical column

$I_f$  = Importance factor

$V_m$  = mean wind speed

3. Determine the stresses acting in the concrete due to these loads. This is calculated using the pressures acting on the tower as per IEC 61400-1(Li and others, 2005):

$$F = P_{NW} * A_{col} \quad (3.2)$$

$$M = F * (L/2) \quad (3.3)$$

$$S = \frac{M * c}{I} \quad (3.4)$$

where:

F = Force acting on the tower from the wind pressure

$A_{col}$  = Surface area of tower column

M = Overturning moment on base of column due to the wind load

L = height of tower

S = Stress range at base of column from the wind loads

c = centroid of column

I = moment of inertia

4. Using the fatigue model, estimate the number of cycles to failure (N) at the stresses calculated (Rao and Roeler, 2004):

$$\log N = 2.13SR^{-1.2} \quad (3.5)$$

$$SR = \frac{S}{MoR} \quad (3.6)$$

where:

N = number of cycles to failure at a particular stress range

SR = stress ratio

S = stress range acting on material

MoR = modulus of rupture of concrete

5. From the wind data of the NWCC, ascertain the appropriate frequency for varying wind speeds for each month by (NWCC, 2013):

$$T_i = t * f_i \quad (3.7)$$

where:

$T_i$  = time wind blows at a certain speed  $i$

$t$  = total time in the month under consideration in hours

$f_i$  = percentage of time wind blows at a certain speed  $i$ .

6. Compute the number of fatigue cycles ( $n$ ) arising from the wind speeds is then estimated using the time as calculated above and Table D—2 of the AASHTO Standard Specifications for Structural Supports for Highway Signs, Luminaires and Traffic Signals as reproduced in Table 3.1.

Table 3.1: Stress Range Cycles for mean wind speeds (NCHRP, 2012)

Mean Wind Speed $V_{\text{mean}}$ (mph)	Number of cycles $n$ (cycles/day)
$\leq 9$	9500
$9 < V_{\text{mean}} \leq 11$	15000
$> 11$	23000

7. Compute the damage fraction  $\frac{n}{N}$  for the monthly wind data.

where:

$n$  = number of wind cycles at a particular wind speed

$N$  = number of cycles to failure at the particular speed.

8. Sum up the damage fractions as per Miner's rule to obtain the cumulative damage

(D). Miner's rule is taken as (Miner,1945):

$$D = \sum \frac{n}{N} \quad (3.8)$$

9. Determine the fatigue limit state. In order to account for statistical uncertainty, certain uncertainty factors are taken into consideration in the fatigue limit state.

These alongside their distributions as well as their statistical descriptors are given in table 3.2 (Tarp-Johansen et al, 2002).

Table 3.2: Model and Statistical Uncertainties for Fatigue Limit state (Tarp-Johansen et al, 2002)

Uncertainty	Symbol	High		Low	
		Mean	St. Dev	Mean	St. Dev
Model Uncertainty	$X_R$	1	0.05	1.11	0.085
Miner's rule uncertainty	$\Delta$	1	0.3	1	-
Dynamic uncertainty	$X_{dyn}$	1	0.2	1	0.05
Exposure uncertainty	$X_{exp}$	1	0.2	1	0.05
Load/Stress uncertainty	$X_{str}$	1	0.05	1	0.03
Wind uncertainty	$X_{aero}$	1	0.2	1	0.1
Counting procedure uncertainty	$X_{RFC}$	1	0.02	1	0.02

The high values indicate the upper limits for the uncertainties and the low values the lower limits.

Thus, the fatigue limit state can be defined as;

$$g(x) = \Delta X_R - D\{X_R X_{dyn} X_{exp} X_{str} X_{aero} X_{RFC}\} \quad (3.9)$$

10. Compute the fatigue reliability index  $\beta_f$  and the corresponding probability of failure. This is carried out using first order second moment reliability method, defined as (Nowak & Collins, 2000);

$$\beta = \frac{a_0 + \sum_{i=1}^n a_i \mu_{xi}}{\sqrt{\sum_{i=1}^n (a_i \sigma_{xi})}} \quad (3.10)$$

where:

$\beta$  = reliability index (second moment measure of structural safety)

$a_i$  = constants

$\mu_{xi}$  = mean of random variable

$\sigma_{xi}$  = standard deviation of random variable.

### 3.5 SEISMIC ANALYSIS IN MATLAB

The reliability analysis of footings under seismic loads is carried to prevent exceedance of a resonance limit state, that is, to ensure that the natural frequency of the footing does not equal that of the seismic event. The procedure to analyze this is given as:

1. Compute the amplitude of ground motion. This is carried out using the standard surface wave formula (Spence et al, 1989) and Monte Carlo simulations:

$$M_s = \log A/T + 1.66 \log(D) + 3.30 \quad (3.11)$$

where:

$M_s$  = magnitude of earthquake on the Richter scale

A = amplitude of ground motion

T = period

D = distance from epicenter

The standard wave formula (Equation 3.4), relates the magnitude of an earthquake on the Richter scale with the amplitude of ground motion.

2. The frequency ratio r, is determined using the displacement transmissibility equation (Rao, 2011):

$$\frac{X}{A} = \sqrt{\frac{1 + (2\xi r)^2}{(1 - r^2)^2 + (2\xi r)^2}} \quad (3.12)$$

where:

X = amplitude of base motion

A = amplitude of ground motion

$\xi$  = damping ratio taken as 0.01

$$r = \frac{\omega_f}{\omega_n} \quad (3.13)$$

where:

$\omega_f$  = earthquake frequency

$\omega_n$  = natural frequency of the structure

3. To forestall resonance, a resonance limit state is used in this analysis. This is taken as;

$$r - 2.5 \geq 0 \quad (3.14)$$

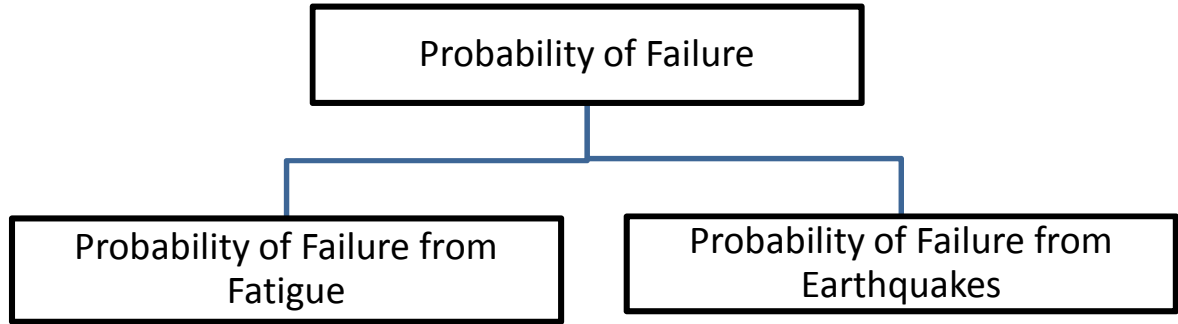
Thus the limit state is determined as:

$$g(x) = r - 2.5 \quad (3.15)$$

4. Compute the seismic reliability. Seismic reliability analysis is carried out using first order second moment reliability method. Using the limit state equation (Equation 3.15) developed; the reliability index and corresponding probability of failure are calculated from the FORM reliability index equation (equation 3.10).

### **3.6 MULTI-HAZARD ANALYSIS IN MATLAB**

For the multi-hazard analysis, the system is modeled as a system in series. This reasoning is substantiated by the fact that earthquakes and fatigue are totally independent hazards and have a probability of occurrence not related to the other in any way. Accordingly the system is modeled using event tree analysis as shown below (Ayyub and McCuen, 2011):



Thus, the system probability of failure is calculated as (Ayyub and McCuen, 2011):

$$P_f = P_{ffat} + P_{feq} - (P_{ffat} * P_{feq}) \quad (3.16)$$

Appendix C presents the MATLAB code developed for these analyses using the above methodology.

### **3.7 FINITE ELEMENT ANALYSIS**

A finite element analysis is also carried out in ANSYS using a methodology as described below.

#### **3.7.1 ANSYS Finite Element Model**

To create a finite element model in ANSYS, there are multiple tasks that have to be completed for the model to run properly. Models can be created using command prompt line input or the Graphical User Interface (GUI). For this model, the GUI is utilized. This section describes the different tasks and entries used to create the FE model.

##### **3.7.1.1 Modeling the Concrete Foundation**

Building the foundation model under investigation in this research in ANSYS involves a number of procedures. These include defining element types for the various components,

assigning material properties as obtainable in the foundation structure, building the volume with the right dimensions and assigning the material components to the various parts of the model.

### 3.7.1.2 Element Types

ANSYS has a wide range of elements from which to select. Each element can be used to model various types of structural units and thus has different properties. For this model Solid65 (concrete65) is used to model the foundation block and Solid187 is utilized for the anchor bolts. These element types were chosen because of their properties which closely align with the real world behavior of the structural unit under examination (Wolanski, 2004, Nguyen, 2010).

The element types for this model are shown in Table 3.3.

Table 3.3 – Element Types for Working Model

Material Type	ANSYS Element
Concrete	Solid 65
Steel Reinforcement	-
Anchor Bolts	Solid 187

Solid65 element is a specialized concrete element in ANSYS. Also known as the concret65 solid element, it is an eight node element with the built in option of having rebar in the concrete as well as nonlinear analysis option. Thus, it has an advantage over other solid element types in modeling reinforced concrete. It is also possible to specify a rebar material for use with this element for a more conventional reinforced concrete model (SAS, 2009).

The element has plasticity, creep, strain, stress and large deflection capabilities as well as special cracking and crushing capabilities which are essential in modeling the behavior of reinforced concrete elements. The rebar can be modeled in three directions and is capable of tension and compression but not shear. A schematic of this element is shown in Figure 3.2.

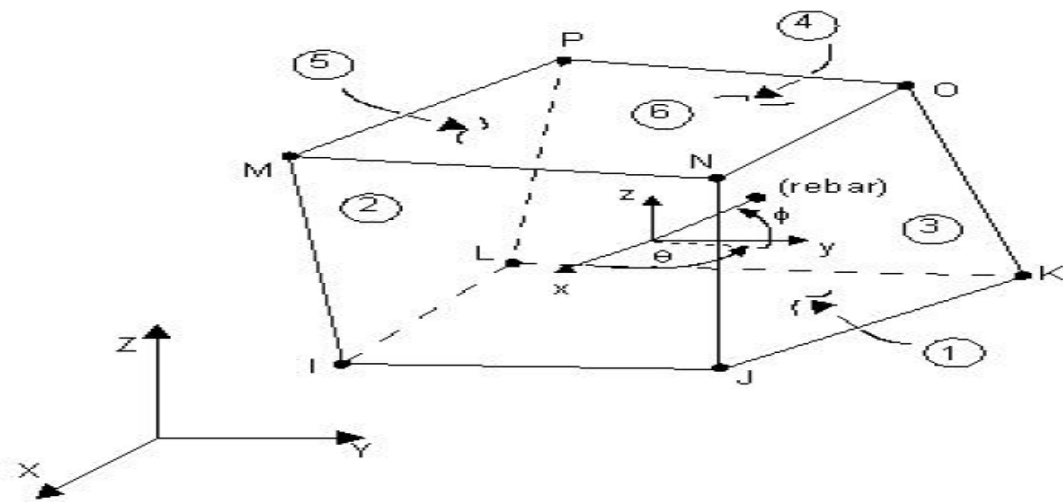


Fig: 3.2 Solid 65 Element (SAS, 2009)

Solid187 is used to model the anchor bolts and is a ten node solid element. It is used because its properties closely reflect the behavior of steel rods used in anchor bolts in actuality. It is also recommended by the ANSYS element manual for this very purpose of modeling anchor bolts. The element has plasticity, hyper elasticity, creep, stress stiffening, large deflections and large strain capabilities. It is defined by ten nodes with each having three degrees of freedom. A schematic of this element is shown below (SAS, 2009).

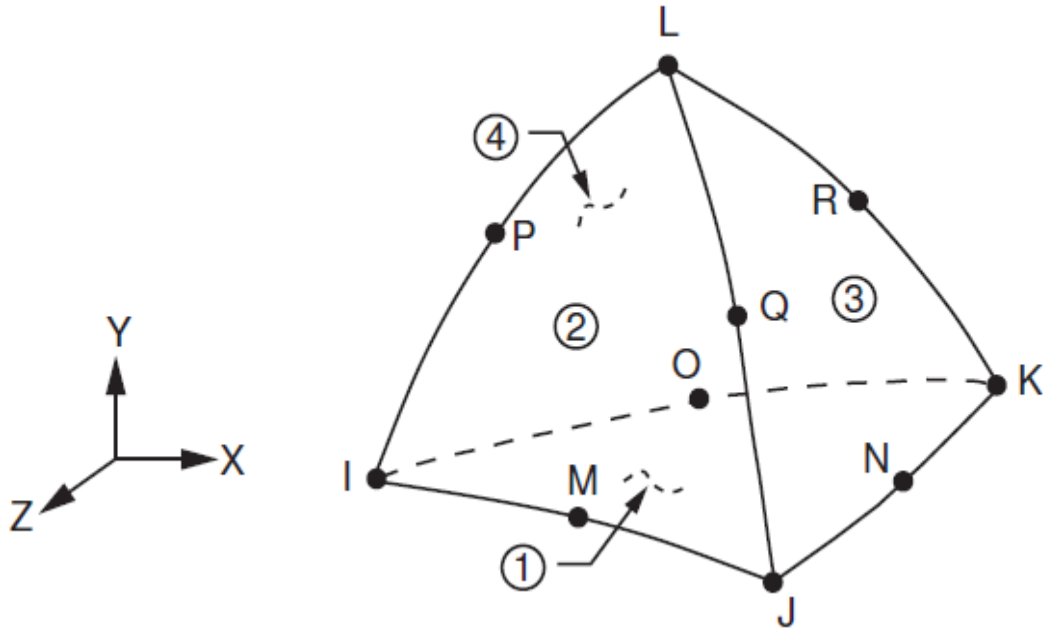


Fig. 3.3: Solid 187 Element (SAS, 2009)

### 3.7.1.3 Real Constants

Individual elements contain different real constants. No real constant set exists for the Solid187 element. Real Constant Set 1 is used for the Solid65 element. It requires real constants for rebar assuming a smeared model. Values can be entered for Material Number, Volume Ratio, and Orientation Angles. The material number refers to the type of material for the reinforcement as defined in the material properties. The volume ratio refers to the ratio of steel to concrete in the element. The orientation angles refer to the orientation of the reinforcement in the smeared model. ANSYS allows the user to enter three rebar materials in the concrete. Each material corresponds to x, y, and z directions in the element. The inbuilt reinforcement has uniaxial stiffness and the directional orientation is defined by the user as orientation angles. Figure 3.4 shows the real constant set values as used for this analysis.

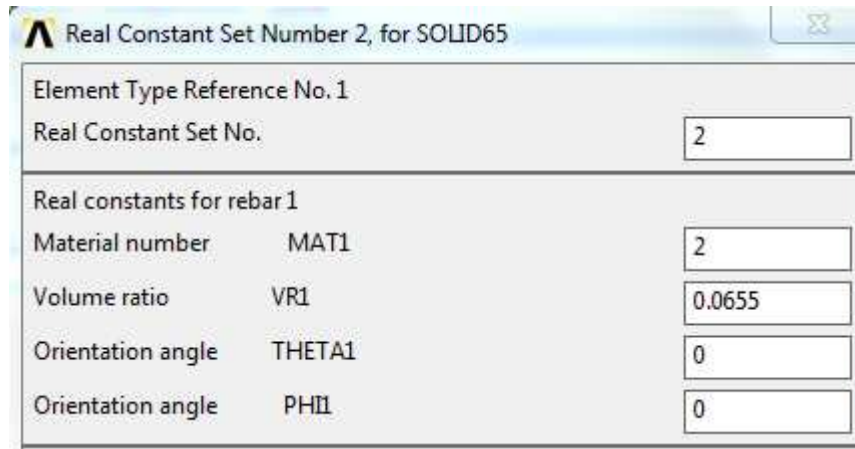


Fig 3.4: Real Constant set for reinforcement in ANSYS

### 3.7.1.4 Material Properties

Parameters needed to define the material models can be found in Table 3.4. As can be seen in the table, there are multiple parts of the material model for each element. Material Model Number 1 refers to the Solid65 element. The Solid65 element requires linear isotropic and multilinear isotropic material properties to properly model concrete. The multilinear isotropic material uses the von Mises failure criterion along with the William and Warnke (1974) model to define the failure of the concrete (Wolanski, 2004).  $E_c$  is the modulus of elasticity of the concrete ( $E_c$ ), and PRXY is the Poisson's ratio ( $\nu$ ). The modulus of elasticity is calculated using the relationship:

$$E_c = 57,000\sqrt{f'_c} \quad (3.17)$$

where  $f'_c$  = compressive strength of concrete and has a value of 4,800 psi. Poisson's ratio is assigned to be 0.3 (Wolanski, 2004).

Table 3.4: Material Properties (Wolanski, 2004, McGregor, 1993)

Material Model number	Element Type	Material Properties																			
1	Solid65	<table border="1"> <thead> <tr> <th colspan="2">Linear Isotropic</th> </tr> </thead> <tbody> <tr> <td>E<sub>x</sub></td> <td>3949076</td> </tr> <tr> <td>PRXY</td> <td>0.3</td> </tr> </tbody> </table>	Linear Isotropic		E <sub>x</sub>	3949076	PRXY	0.3													
		Linear Isotropic																			
		E <sub>x</sub>	3949076																		
PRXY	0.3																				
<table border="1"> <thead> <tr> <th colspan="3">Multilinear Isotropic</th> </tr> <tr> <th></th> <th>Strain</th> <th>Stress</th> </tr> </thead> <tbody> <tr> <td>Point 1</td> <td>0.00036</td> <td>1421.7</td> </tr> <tr> <td>Point 2</td> <td>0.0006</td> <td>2233</td> </tr> <tr> <td>Point 3</td> <td>0.0013</td> <td>3991</td> </tr> <tr> <td>Point 4</td> <td>0.0019</td> <td>4656</td> </tr> <tr> <td>Point 5</td> <td>0.00243</td> <td>4800</td> </tr> </tbody> </table>	Multilinear Isotropic				Strain	Stress	Point 1	0.00036	1421.7	Point 2	0.0006	2233	Point 3	0.0013	3991	Point 4	0.0019	4656	Point 5	0.00243	4800
Multilinear Isotropic																					
	Strain	Stress																			
Point 1	0.00036	1421.7																			
Point 2	0.0006	2233																			
Point 3	0.0013	3991																			
Point 4	0.0019	4656																			
Point 5	0.00243	4800																			
<table border="1"> <thead> <tr> <th colspan="2">Concrete</th> </tr> </thead> <tbody> <tr> <td>ShrCf-Op</td> <td>0.3</td> </tr> <tr> <td>ShCf-Cl</td> <td>1</td> </tr> <tr> <td>UnTensSt</td> <td>520</td> </tr> <tr> <td>UnCompSt</td> <td>-1</td> </tr> <tr> <td>BiCompSt</td> <td>0</td> </tr> <tr> <td>HydroPrs</td> <td>0</td> </tr> <tr> <td>BiCompSt</td> <td>0</td> </tr> <tr> <td>UnTensSt</td> <td>0</td> </tr> <tr> <td>TensCrFac</td> <td>0</td> </tr> </tbody> </table>	Concrete		ShrCf-Op	0.3	ShCf-Cl	1	UnTensSt	520	UnCompSt	-1	BiCompSt	0	HydroPrs	0	BiCompSt	0	UnTensSt	0	TensCrFac	0	
Concrete																					
ShrCf-Op	0.3																				
ShCf-Cl	1																				
UnTensSt	520																				
UnCompSt	-1																				
BiCompSt	0																				
HydroPrs	0																				
BiCompSt	0																				
UnTensSt	0																				
TensCrFac	0																				
2	Solid187	<table border="1"> <thead> <tr> <th colspan="2">Linear Isotropic</th> </tr> </thead> <tbody> <tr> <td>EX</td> <td>30,000,000 psi</td> </tr> <tr> <td>PRXY</td> <td>0.3</td> </tr> </tbody> </table>	Linear Isotropic		EX	30,000,000 psi	PRXY	0.3													
Linear Isotropic																					
EX	30,000,000 psi																				
PRXY	0.3																				
3	Reinforcement	<table border="1"> <thead> <tr> <th colspan="2">Linear Isotropic</th> </tr> </thead> <tbody> <tr> <td>EX</td> <td>30,000,000 psi</td> </tr> <tr> <td>PRXY</td> <td>0.3</td> </tr> </tbody> </table>	Linear Isotropic		EX	30,000,000 psi	PRXY	0.3													
		Linear Isotropic																			
		EX	30,000,000 psi																		
PRXY	0.3																				
<table border="1"> <thead> <tr> <th colspan="2">Bilinear Isotropic</th> </tr> </thead> <tbody> <tr> <td>Yang Stress</td> <td>60,000 psi</td> </tr> <tr> <td>Tang Mod</td> <td>2,900 psi</td> </tr> </tbody> </table>	Bilinear Isotropic		Yang Stress	60,000 psi	Tang Mod	2,900 psi															
Bilinear Isotropic																					
Yang Stress	60,000 psi																				
Tang Mod	2,900 psi																				

The compressive uniaxial stress-strain relationship for the concrete model is obtained using the following equations to compute the multilinear isotropic stress-strain curve for the concrete (MacGregor 1992):

$$f = \frac{E_c \varepsilon}{1 + \left(\frac{\varepsilon}{\varepsilon_o}\right)^2} \quad (3.18)$$

$$\varepsilon_o = \frac{2f'_c}{E_c} \quad (3.19)$$

$$E_c = \frac{f}{\varepsilon} \quad (3.20)$$

where:

$f$  = stress at any strain, psi

$\varepsilon$  = strain at stress  $f$

$\varepsilon_o$  = strain at the ultimate compressive strength

The multilinear isotropic stress-strain implemented requires the first point of the curve to be defined by the user. It must satisfy Hooke's Law;

$$E = \frac{\sigma}{\varepsilon} \quad (3.21)$$

where:

$E$  = modulus of elasticity

$\sigma$  = stress in material

$\varepsilon$  = strain in the material

The multilinear curve is used to help with convergence of the nonlinear solution algorithm.

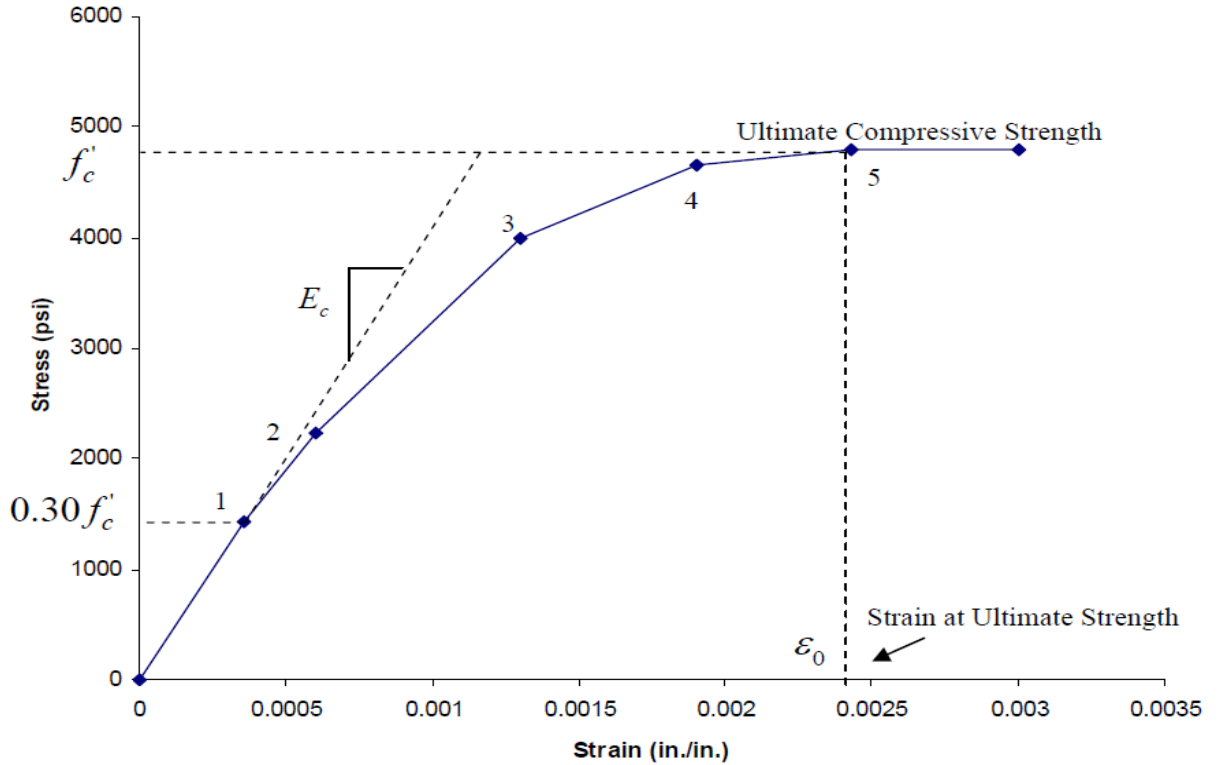


Figure 3.5 – Uniaxial Stress-Strain Curve for Reinforced Concrete (Wolanski, 2004)

Figure 3.5 shows the stress-strain relationship used for this study and is based on work done by Wolanski (2004). Point 1, defined as  $0.30f'_c$ , is calculated in the linear range (Equation 3.20). Points 2, 3, and 4 are calculated from Equation 3.18 with  $\epsilon_o$  obtained from Equation 3.19. Strains were selected and the stress is calculated for each strain. Point 5 is defined at  $f'_c$  and  $\epsilon_o = 0.0003 \text{ in./in.}$  indicating traditional crushing strain for unconfined concrete.

Implementation of this material model in ANSYS requires that certain constants be defined. These 9 constants are (SAS, 2009):

1. Shear transfer coefficients for an open crack;
2. Shear transfer coefficients for a closed crack;
3. Uniaxial tensile cracking stress;

4. Uniaxial crushing stress (positive);
5. Biaxial crushing stress (positive);
6. Ambient hydrostatic stress state for use with constants 7 and 8;
7. Biaxial crushing stress (positive) under the ambient hydrostatic stress state (constant 6);
8. Uniaxial crushing stress (positive) under the ambient hydrostatic stress state (constant 6);
9. Stiffness multiplier for cracked tensile condition.

Typical shear transfer coefficients range from 0 to 1, with 0 representing a smooth crack with complete loss of shear transfer and 1 representing a rough crack (no loss of shear transfer). The shear transfer coefficients for open and closed cracks were determined using the work of Wolanski (2004) as a basis. Convergence problems occur when the shear transfer coefficient for the open crack is set below 0.2. No deviation of the response occurs with the change of the coefficient. Therefore, the coefficient for the open crack is set to 0.3 (Table 3.4). The uniaxial cracking stress value is based on the modulus of rupture for concrete. This value is determined using (McGregor, 1993),

$$f_r = 7.5\sqrt{f'_c} \quad (3.22)$$

The uniaxial crushing stress in this model is based on the uniaxial unconfined compressive strength ( $f'_c$ ) and is denoted as  $f_t$ . It is entered as -1 to turn off the crushing capability of the concrete element as suggested by past researchers (Wolanski, 2004, Nguyen, 2010). The biaxial crushing stress refers to the ultimate biaxial compressive strength ( $f'_{cb}$ ). The ambient hydrostatic stress state is denoted as  $\sigma_h$ . This stress state is defined as:

$$\sigma_h = \frac{1}{3}(\sigma_{xp} + \sigma_{yp} + \sigma_{zp}) \quad (3.23)$$

Where  $\sigma_{xp}$ ,  $\sigma_{yp}$  and  $\sigma_{zp}$  are the principal stresses in the principal directions. The biaxial crushing stress under the ambient hydrostatic stress state refers to the ultimate compressive strength for a state of biaxial compression superimposed on the hydrostatic stress state ( $f_1$ ). The uniaxial crushing stress under the ambient hydrostatic stress state refers to the ultimate compressive strength for a state of uniaxial compression superimposed on the hydrostatic stress state ( $f_2$ ).

The failure surface can be defined with a minimum of two constants,  $f_t$  and  $f'_c$ . The rest of the variables in the concrete model are left to default based on these equations as defined by the ANSYS code (SAS, 2009):

$$f'_{cb} = 1.2f'_c \quad (3.24)$$

$$f_1 = 1.45f'_c \quad (3.25)$$

$$f_2 = 1.725f'_c \quad (3.26)$$

These stress states however, are only valid for stress states satisfying the condition given by equation 3.27.

$$|\sigma_h| = \sqrt{3}f'_c \quad (3.27)$$

Material Model Number 2 refers to the Solid187 element. The Solid187 element is utilized to model the anchor bolts transferring the tower loads to the foundation. Therefore, this element is modeled as a linear isotropic element with a modulus of elasticity for the steel ( $E_s$ ) of  $3e^7$  psi and Poisson's ratio ( $\nu$ ) taken as 0.3.

Material Model Number 3 refers to the reinforcement element. It is assigned with material properties of steel and it is assumed to be bilinear isotropic. Bilinear isotropic

material is also based on the von Mises failure criteria. The bilinear model requires the yield stress ( $f_y$ ), as well as the hardening modulus of the steel to be defined. The yield stress is defined as 60,000 psi, and the hardening modulus as 3000 psi (Wolanski, 2004).

### 3.7.2 Model Geometry

The FEA model involved modeling a part of the foundation block with one anchor bolt embedded as volumes based on dimensions and specifications for a wind turbine footing suggested by Kuhn (2011). The dimensions for the concrete volume are as defined in Table 3.5, while the anchor bolts are modeled as cylinders with dimensions as shown in Table 3.6

Table 3.5: Foundation Dimensions on ANSYS

Coordinates	Values (in)	
$X_1, X_2$	-5	5
$Y_1, Y_2$	-5	5
$Z_1, Z_2$	0	10

Table 3.6: Anchor Bolt dimensions on ANSYS

Component	Radius (in)	Coordinates $Z_1, Z_2$ (in)	
Head	1.5	4	5
Rod	0.75	5	11

The connection between the concrete block and the anchor bolts are presumed to be a perfect bond and as such modeled using the GLUE command. This modeling approach is validated by the works of Nguyen (2010) and Wolanski (2004) who show that the bond between concrete and steel is adequately represented in ANSYS using the GLUE command.

### 3.7.2.1 Meshing

To obtain good results from the Solid65 element, the ANSYS manual recommends the use of a mesh small enough to adequately characterize the behavior of individual elements in the model. Thus, the mesh is set up so as to create smaller elements. The mesh command used to create the necessary finite elements is also used to designate material attributes to each aspect of the model. A tetrahedral mesh is utilized for this model. This is used because it allows for meshing of irregular shapes and models with discontinuities (SAS, 2009).

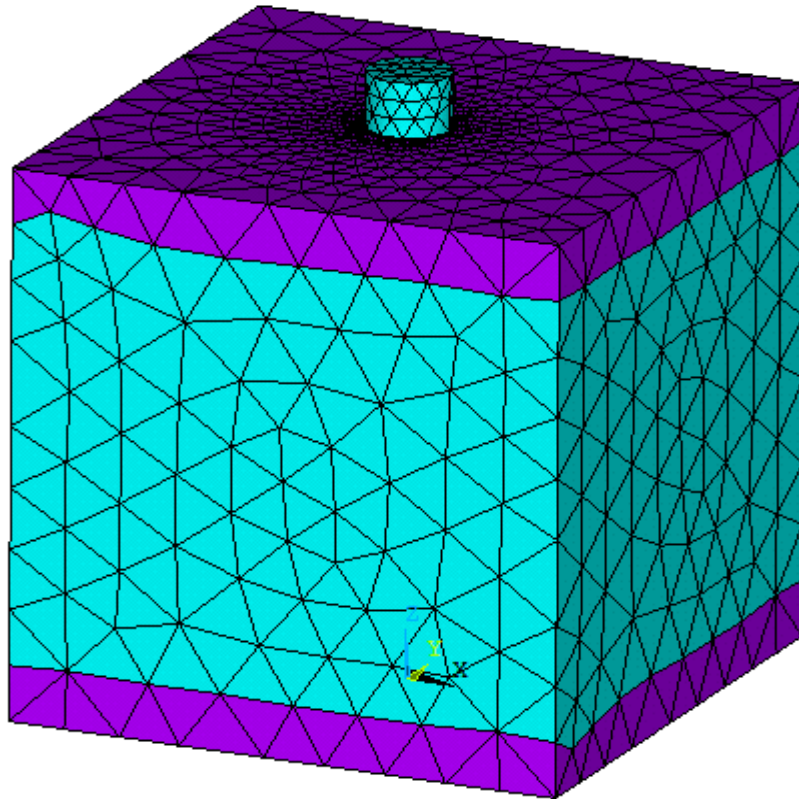


Fig. 3.6: Meshed model

### **3.7.2.2 Loads and Boundary Conditions**

Displacement boundary conditions are needed to constrain the model and to get a unique solution. To ensure the model replicates the real life behavior of a foundation block, boundary conditions are applied at surfaces identified as those acting in contact with the soil as support for the structure. The supports are modeled in such a way as to be fixed and thus resist movement in all directions.

The forces acting on the foundation from the superstructure are modeled as tensile and compressive pressures acting symmetrically on the anchor bolts. This is a combination of the gravity loads from the tower and the nacelle as well as the varying cyclic loads from wind forces converted into lateral pressures acting on the anchor bolts. The seismic loads are modeled as displacements owing to the time history accelerations acting on the foundation block's vertical sides.

The transient analysis option is used in this study as the solver of choice. This is because it allows for the use of time varying loads and displacements to determine the dynamic response of a structure.

### **3.8.1 Fatigue Analysis**

A procedure for executing fatigue analysis in ANSYS is determined as;

1. Obtain the wind pressures acting on the tower from the mean wind speeds (as in section 3.3).
2. Select the transient analysis option in ANSYS. This is used because the footing is under cyclic time dependent loading from the varying wind loads.
3. Input an appropriate time step size and other iteration control values. This is done in the GUI by Main Menu – Solution – SOLN CTRL. The SOLN CTRL

command dictates the use of linear or non-linear solution for the finite element model. In this analysis, the non-linear option is utilized. The commands used for this nonlinear analysis are as shown in Table 3.7

4. Define the boundary conditions and loads. The loads are input as obtained from the wind speed data (as described in Section 3.3). The boundary conditions are fixed in all directions to simulate a static ground condition.
5. Write the load step.

Table 3.7: Commands Used in the SOLN CTRL option in ANSYS

Basic Options	
Analysis Options	Small Displacement
Calc Prestress Effects	Yes
Time @ end of loadstep	10
Auto Time Step	ON
Time Increment	ON
Time Step Size	1
Transient Option	Ramped Loading
Nonlinear Options	
Line Search	ON
DOF Soln Predictor	ON for all substeps

6. Repeat the steps above for all necessary wind data, in this case, the mean monthly values, increasing the time at the end of the load case by 10 each time.
7. Solve for all load steps.
8. Using the calculated stress cycles (n), the fatigue model and the stresses obtained from the above steps, the fatigue command is used in the ANSYS post processor to determine fatigue damage (D) for selected nodes.
9. The fatigue damage values are then used alongside the statistical uncertainty values in the limit state equation (Equation 3.9) to determine the reliability index

and probability of failure. Figure 3.7 shows the model, in ANSYS, loaded for fatigue analysis.

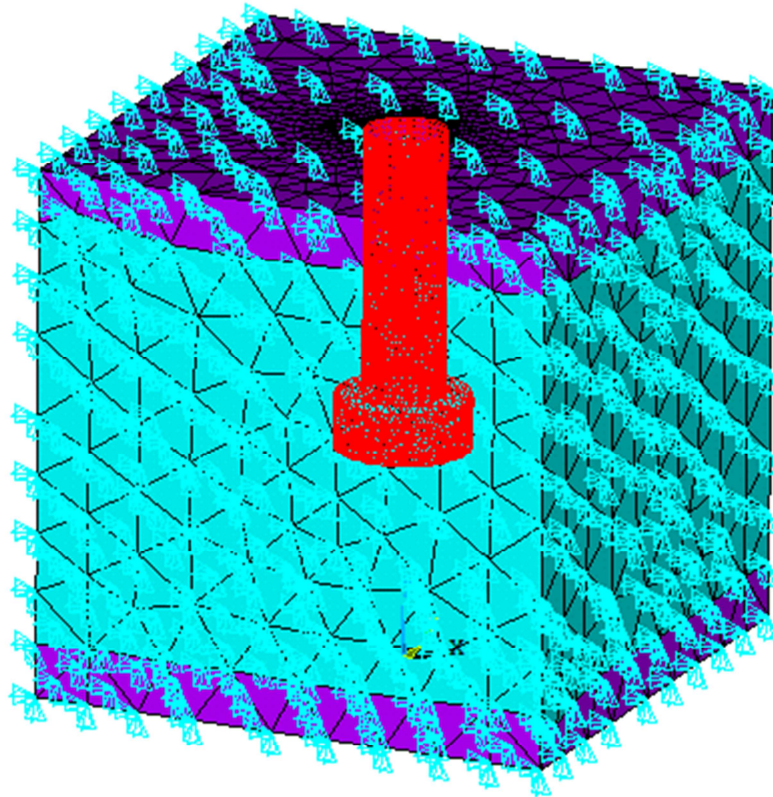


Figure 3.7: ANSYS model with Fatigue loads

### 3.8.2 Seismic Analysis

The seismic analysis in ANSYS is also carried out using the transient analysis option as follows;

1. Integrate the acceleration time history data twice over time to obtain displacement time history data.
2. Save the displacement time history data as a .txt file
3. Select the transient analysis option in the ANSYS solution menu.

4. Input an appropriate time step size and complete applicable options in the SOLN CTRLS option using Main Menu – Solution – SOLN CTRLS.
5. From the utility menu, select parameters and load in the text file with the table of displacement data. This is done in the GUI by Utility Menu – Parameters – Array Parameters – Read/Input data
6. Input the necessary loads and boundary conditions. In this case, the gravity loads acting on the footing. The initial boundary conditions are also defined as fixed in all directions before ground motion is applied.
7. Input the defined ground motion data table as a time dependent boundary condition.
8. Solve the load step.

### **3.9 SENSITIVITY ANALYSIS**

Sensitivity analysis is carried out to obtain a measure of the foundation's reliability response to several design parameters identified as essential in the reliability analysis. This helps in determining the most important parameters affecting structural safety. The sensitivity analysis is done using the methodology espoused by Nowak and Collins (2000):

1. Identify possible failure scenarios and parameters vital to these scenarios.
2. Calculate the system reliability for each of these scenarios, altering the parameters identified.
3. Calculate the overall system reliability from the different failure scenarios.
4. Determine the most sensitive parameters from the results obtained.

## **CHAPTER FOUR**

### **MONTE CARLO SIMULATION RESULTS**

Using the hitherto identified concrete wind fatigue model from Section 3.2, as well as the derived limit state equation, a wind fatigue reliability analysis is carried out. Monte Carlo simulations along with the displacement transmissibility equation and derived resonance limit state equation are also used to perform the seismic reliability analysis. This is done by utilizing the computational capacity of MATLAB to develop a code tailored from the developed methodology discussed in Chapter 3 for these analyses. The code is used to carry out the reliability analyses. The results of these analyses are presented and discussed in the ensuing Sections of this chapter.

#### **4.1 SEISMIC ANALYSIS**

The first analysis performed is the seismic reliability analysis. For this analysis, Monte Carlo simulations are employed to develop a catalog of probable earthquake magnitudes and then first order second moment reliability method (FORM) is utilized as described in Section 3.2 to determine the reliability and subsequently the probability of failure of the foundation for the developed earthquake catalog. The results show a direct correlation between magnitude and probability of failure with an increase in the magnitude resulting in an increase in the probability of failure of the foundation. It is pertinent to note that failure from a reliability point of view does not necessarily mean a total collapse of the structure under review. It is defined as the inability of the structure to meet certain design criteria specified for it.

Table 4.1 shows the probabilities of failure for magnitudes of earthquakes ranging between 6 and 8 on the Richter scale. Idaho experienced its largest earthquake ( $M_s = 6.9$ ) in 1983. Known as the Borah Peak Earthquake, it had its epicenter in the Lost River Range at Borah Peak, a site with similar ground characteristics to the Goshen North Wind farm located just outside Idaho Falls. Thus, the earthquake magnitudes chosen for this study are within a range of possible damaging earthquakes for the Idaho Falls region (USGS, 2013).

Table 4.1: Relationship between Earthquake magnitude and probability of failure

$M_s$	Rel. Index	$P_{fe}$
6	3.654	1.29E-04
6.1	3.509	2.25E-04
6.2	3.341	4.17E-04
6.3	3.148	8.21E-04
6.4	2.929	0.0017
6.5	2.678	0.0037
6.6	2.400	0.0082
6.7	2.086	0.0185
6.8	1.731	0.0417
6.9	1.333	0.0912
7	0.885	0.1881
7.1	0.378	0.3527
7.2	-0.197	0.578
7.3	-0.852	0.8029
7.4	-1.603	0.9455
7.5	-2.473	0.9933
7.6	-3.432	0.9997
7.7	-3.540	0.9998
7.8	-3.719	0.9999
7.9	-5.199	1
8	-5.491	1

The cumulative density curve is plotted as shown in Figure 4.1. This figure shows the full range of a cumulative distribution curve, from the very low probabilities of failure to the extreme peaking at 1. It shows the direct relationship between seismic reliability and earthquake magnitude.

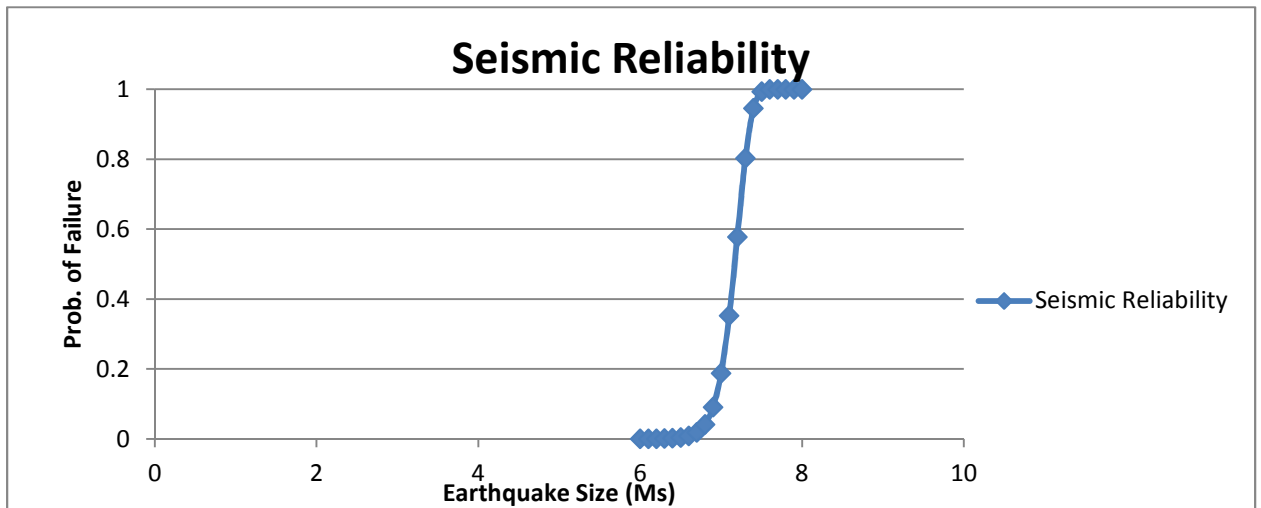


Figure 4.1: Graph of Earthquake magnitude against Probability of Failure

From Table 4.1, it can be established that the seismic reliability of the foundation is greatly affected by the magnitude of the earthquake under consideration. This is in line with the expected behavior as greater magnitudes result in higher range of ground frequencies leading to a greater probability of the ground motion frequency reaching resonance with the natural frequency of the footing. For earthquakes of magnitude 6 and below on the Richter scale, the seismic capacity of the footing is adequate to meet the resonance demand. However earthquakes of magnitude 6.9 and above show a definite rise in the probability of failure of the foundation culminating in a 100% probability of failure for magnitude 7.5 and above. Figure 4.1 shows the graphic description of this relationship. The cumulative distribution function shown in the figure is a complete

probability distribution curve of the probability of failure due to random variables of earthquake magnitude.

#### 4.2 WIND FATIGUE ANALYSIS

Wind fatigue reliability evaluation of the foundation is carried out using cumulative damage procedures to assess probability of concrete cracking and accordingly, failure. Using this Miner's damage accumulation concept as outlined in Section 3.3, as well as the first order reliability method (FORM) for the reliability analysis, the results obtained show a continuous increase in the probability of failure over the time frame the foundation is designed to be used. Table 4.2 presents the performance results for the years in view. Wind turbine foundations are usually designed for a 20 year life span and thus this time range is used in the wind fatigue reliability analysis.

Table 4.2: Time and Probability of Failure relationship under cyclic wind loading

Year	Rel. Index $\beta$	$P_{fr}$
1	3.220	6.40E-04
2	3.151	8.13E-04
3	3.090	0.001
4	3.011	0.0013
5	2.929	0.0017
6	2.863	0.0021
7	2.782	0.0027
8	2.707	0.0034
9	2.628	0.0043
10	2.556	0.0053
11	2.473	0.0067
12	2.395	0.0083
13	2.315	0.0103
14	2.238	0.0126
15	2.160	0.0154
16	2.081	0.0187
17	2.003	0.0226
18	1.925	0.0271
19	1.848	0.0323
20	1.771	0.0383

Figure 4.2 shows the cumulative distribution function for the wind fatigue reliability analysis. The CDF curve describing the wind fatigue reliability shows a ‘truncated’ S curve. This indicates that the time frame used for this analysis is less than the total anticipated wind fatigue life span of the footing.

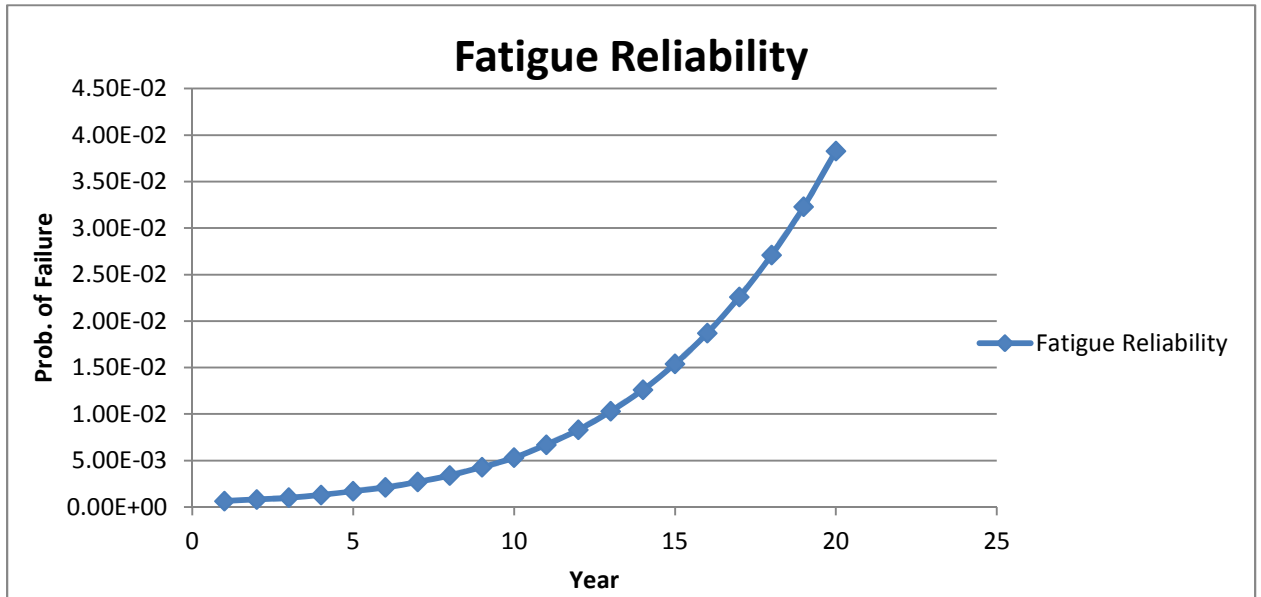


Figure 4.2: Graph of Time against Probability of Failure

From the wind fatigue analysis carried out, it can be seen that the wind fatigue capacity of the foundation meets the demand. This holds true for the entire 20 years design life span of the footing. Maximum wind fatigue damage after 20 years of operation is projected to result in a 3.4% chance of failure of the foundation keeping in mind wind fatigue failure refers to 50% cracking of the concrete for the model used. The cumulative distribution function of this probabilistic relationship depicted in Figure 4.2 shows a truncated CDF curve. This graphically portrays the same observation that the probability of failure from the wind load is low for the design life of the foundation.

### 4.3 MULTI-HAZARD ANALYSIS

For the multi-hazard analysis, the system is modeled as one in series. Thus the reliability is computed for each year of the wind turbine's design life of 20 years. The results are presented in Table 4.3 and Figure 4.3 respectively. The results show a progressive increase in the probability of failure and a concurrent decrease in its reliability.

Table 4.3: Multi-hazard Analysis Results

Earthquake Magnitude $M_s$	Probability of Failure/Year			
	1	5	10	20
6	7.69E-04	0.0018	0.0055	0.0384
6.1	8.64E-04	0.0019	0.0056	0.0385
6.2	0.0011	0.0021	0.0058	0.0387
6.3	0.0015	0.0025	0.0062	0.0391
6.4	0.0023	0.0034	0.007	0.0399
6.5	0.0043	0.0053	0.009	0.0418
6.6	0.0088	0.0098	0.0135	0.0462
6.7	0.0191	0.0201	0.0238	0.0561
6.8	0.0423	0.0433	0.0468	0.0784
6.9	0.0918	0.0927	0.0961	0.126
7	0.1886	0.1895	0.1925	0.2192
7.1	0.3531	0.3538	0.3562	0.3775
7.2	0.5783	0.5787	0.5803	0.5942
7.3	0.803	0.8032	0.8039	0.8104
7.4	0.9456	0.9456	0.9458	0.9476
7.5	0.9933	0.9933	0.9933	0.9935
7.6	0.9997	0.9997	0.9998	0.9998
7.7	1	1	1	1
7.8	1	1	1	1
7.9	1	1	1	1
8	1	1	1	1

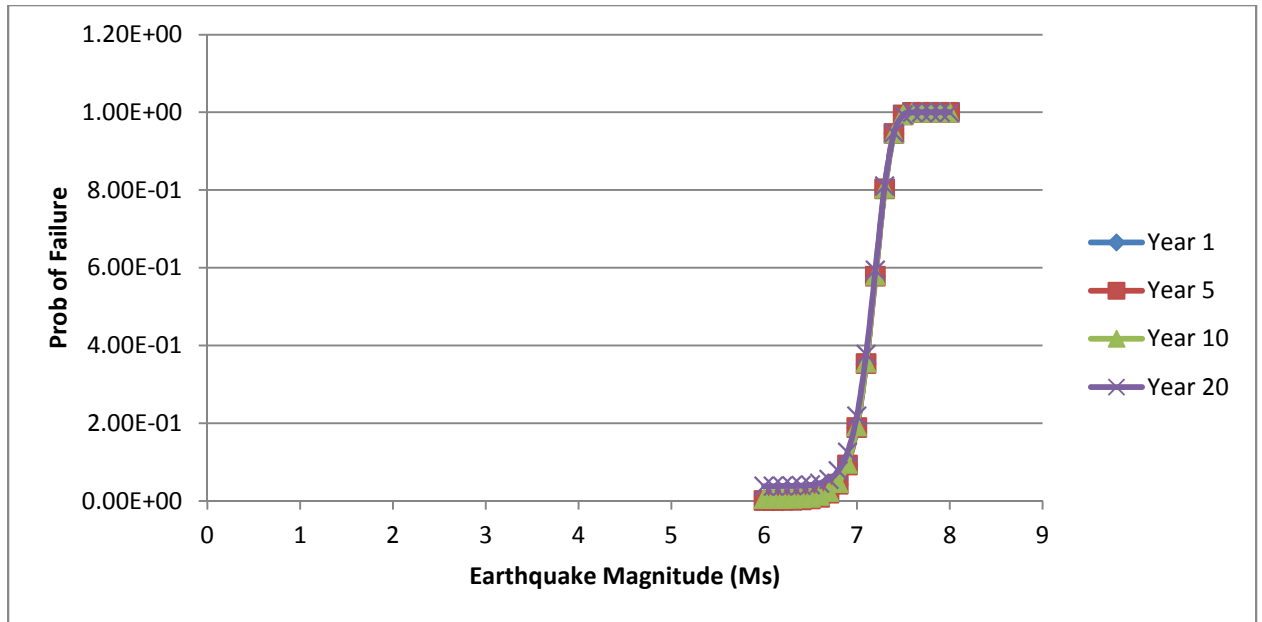


Figure 4.3: Graph of Probability of Failure against Earthquake Magnitude

From Table 4.3, it can be seen that there is an increase in the probability of failure of the foundation from the combination of both loading scenarios than from the individual loadings. This is in conformity with the theory of sequential multi-hazards constituting a higher risk of limit state exceedance than either hazard acting exclusively. For this study, it can also be seen from Table 4.3 that the hazard with a higher probability of failure will also have a controlling effect on the multi-hazard reliability as seen in this case with the seismic demand dominating wind fatigue in the multi-hazard reliability analysis. This is illustrated in Figure 4.3 which shows the cumulative distributive functions (CDF) for various years of operation. From the curves, it is feasible to draw the same conclusions as from Table 4.3. For a single magnitude of  $M_s = 6.9$ , there is a 37% change in the probability of failure over the 20 year design life under wind fatigue loads. However, a 10% change in the magnitude increases the probability of failure by 74%. The curves show very little variation from year to year lending credence to the observation that this

multi-hazard scenario is controlled more by the seismic reliability than by wind fatigue reliability.

#### 4.4 SENSITIVITY ANALYSIS

The sensitivity analysis is carried out to gauge the importance of identified design parameters to the reliability of the foundation. These design parameters include physical dimensions of footing, strength of concrete and the loading parameters. This analysis is carried out as discussed in Section 3.8.

##### 4.4.1 Seismic Sensitivity Analysis

The results of the simulations show that for the seismic reliability, the foundation is most sensitive to changes in its physical parameters as well as the earthquake size. This is as expected because the seismic capacity of the foundation is dependent on its natural frequency which in turn is inversely dependent on the mass. Table 4.4 shows the relationship between the foundation depth and probability of failure. Figure 4.4 shows the cumulative distributive function for a single earthquake.

Table 4.4: Seismic Reliability Sensitivity to Foundation Depth for magnitude 7.0 earthquake

$M_s = 7.0$		
Depth	Rel. Index $\beta$	$P_f$
1	0.97613	0.1645
2	1.010199	0.1562
3	1.022382	0.1533
4	1.1705	0.1209
5	1.225996	0.1101

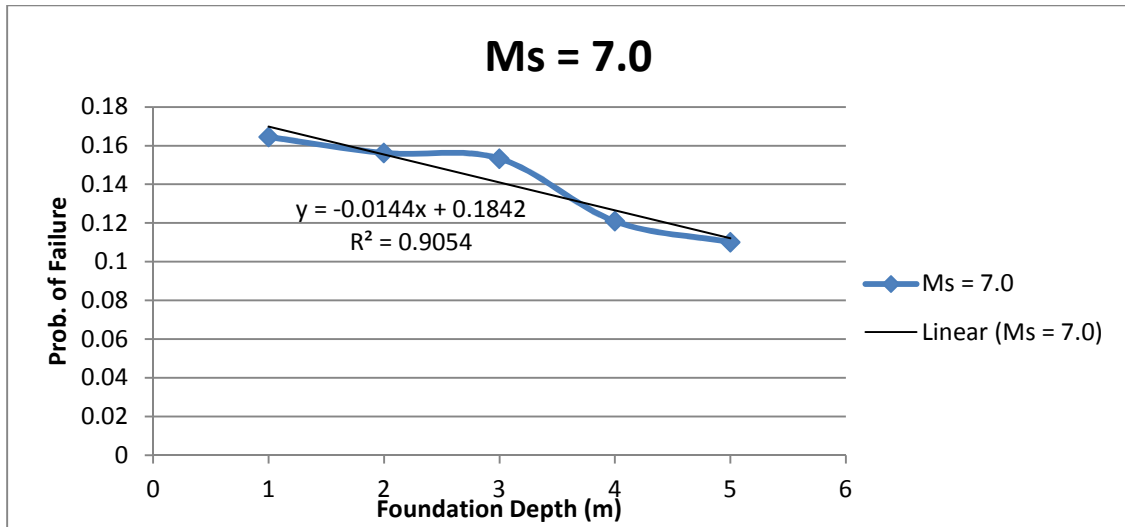


Figure 4.4: Graph of Probability of Failure against Footing Depth for magnitude 7.0 earthquake

Table 4.4 as well as Figure 4.4 shows an inverse linear relationship between the foundation depth and the probability of failure. An increase in the depth of the footing leads to a decrease in the probability of failure. However, the sensitivity of the seismic performance to changes in foundation depth is quite small with a 500% increase in the depth only resulting in a 49% decrease in the probability of failure.

Table 4.5 shows the progressive increase in the probability of failure with an increase in footing area. Figure 4.5 shows the cumulative distributive function of this probabilistic relationship.

Table 4.5: Seismic Sensitivity to Footing Area for magnitude 7.0 earthquake

$M_s = 7.0$		
Area	Rel. Index $\beta$	$P_f$
1	5.069282	2.00E-07
4	3.230958	6.17E-04
9	2.361524	0.0091
16	1.856376	0.0317
25	0.956539	0.1694

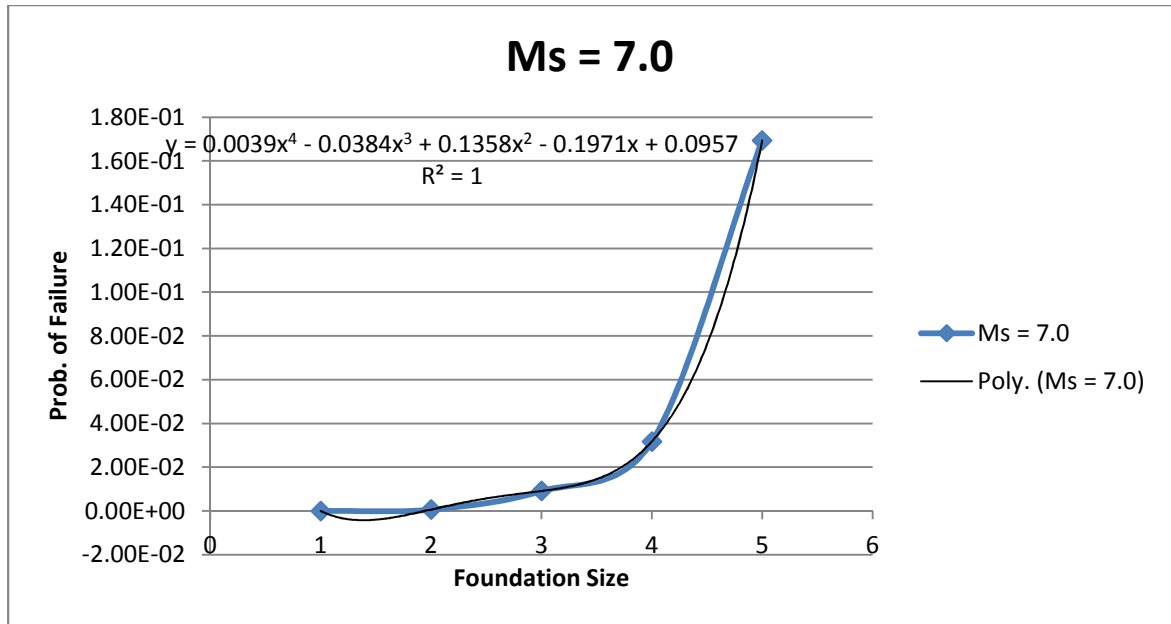


Figure 4.5: Graph of Probability of Failure against Footing Area for magnitude 7.0 earthquake

Table 4.5 and Figure 4.5 show that the foundation area is directly proportional to the probability of failure. An increase in the footing area will result in an increase in the probability of failure. The seismic reliability is quite sensitive to the foundation area as it is instrumental in the determination of the natural frequency of the footing. A 56% change in the area results in a 400% change in the probability of failure. The graph in Figure 4.5 is best represented by a polynomial function. This is because the relationship between the foundation area and its probability of failure is dependent on a number of equations, thus agreeing to the definition of a polynomial function as a subset of functions.

From the seismic sensitivity analyses carried out, it can be observed that the seismic reliability of the foundation is most sensitive to changes in the area of the footing and less sensitive to changes in the depth of the footing.

#### 4.4.2 Wind Fatigue Sensitivity Analysis

From the analyses carried out, it can be seen that in considering wind fatigue reliability, the concrete foundation is most sensitive to the height of the tower as well as the compressive strength of the concrete as exhibited by the modulus of rupture.

Table 4.6 shows a steady increase in the probability of failure from wind fatigue, of the foundation with an increase in the height of the tower. Figure 4.6 graphs the relationship between the height of the wind turbine tower and the probability of failure of the foundation from wind fatigue.

Table 4.6: Wind Fatigue Sensitivity to Tower Height

Year = 20	
Tower Ht (ft)	$P_f$
240	0.003542
250	0.033832
260	0.36964
270	0.867991
280	0.975605
290	0.991599
300	0.995324

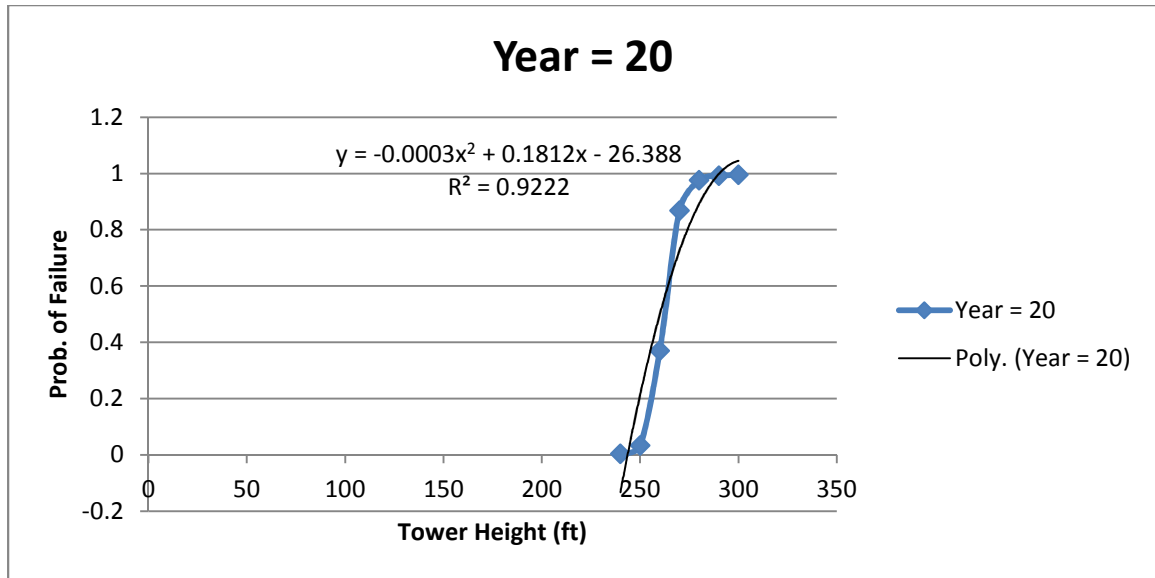


Figure 4.6: Graph of Probability of failure against Height of Tower at year 20

From Table 4.6, it can be deduced that the tower height shows a significant effect on the wind fatigue reliability of the footing. An increase in the tower height significantly decreases the wind fatigue capacity of the footing. This is as a result of some factors influenced by height of the tower including surface area under pressure, deflections from the fluctuating winds as well as weight of the tower. Figure 4.6 shows this relationship with a significant drop in the wind fatigue capacity to demand ratio between a tower of 240 ft and one of 250 ft on the same footing. This 4% change in the height of the tower results in a 700% increase in the probability of failure due to wind fatigue loading. This figure is best described by a polynomial function because the tower height is associated to the fatigue limit state using a number of derived functions.

The compressive strength of concrete is another variable considered in the wind fatigue sensitivity of the foundation. The modulus of rupture of the concrete is directly derived from the compressive strength and is used in the determination of the wind fatigue capacity of concrete.

Table 4.7 shows the relationship between the modulus of rupture of the concrete in the footing and the probability of failure from wind fatigue. Figure 4.7 shows an inverse relationship between the modulus of rupture of the concrete in the foundation and its probability of failure.

Table 4.7: Wind Fatigue Sensitivity to Compressive strength of concrete at year 20

Year = 20	
MOR (psi)	P <sub>f</sub>
520	0.033832
540	0.003761
560	0.00122
580	0.000739
600	0.000595
620	0.000542
640	0.00052

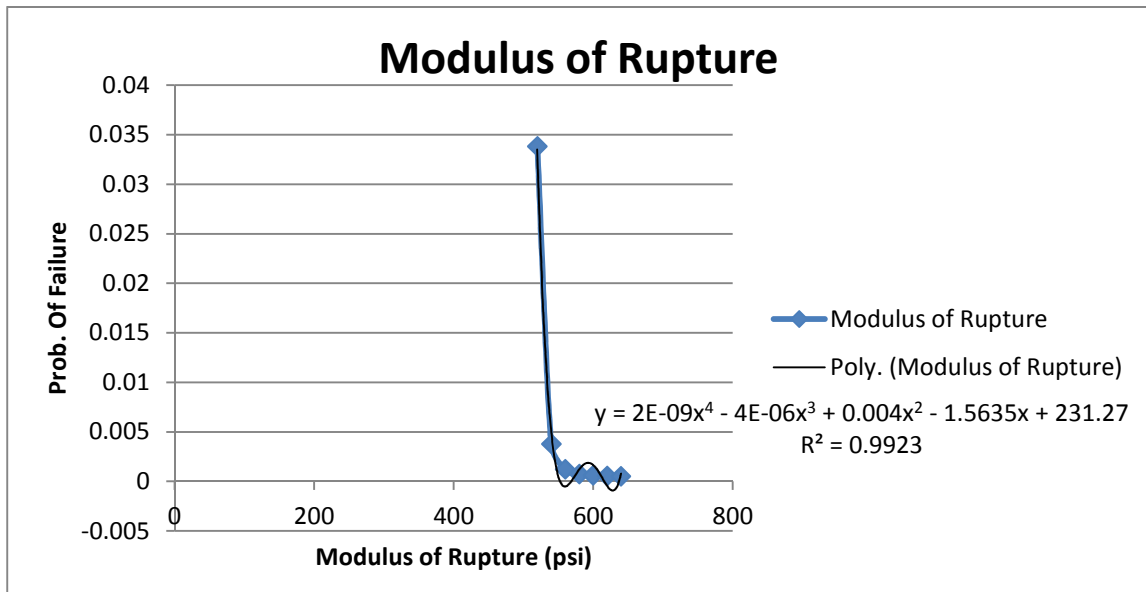


Figure 4.7: Graph of Probability of Failure against Modulus of Rupture

The change in probability of failure due to a change in the compressive strength is quite significant. As seen in Table 4.7, an increase in the compressive strength of the concrete

used in the foundation directly impacts on the wind fatigue capacity of the footing increasing it and thereby reducing its probability of failure from the fluctuating winds. This shows that the compressive strength is quite influential in the wind fatigue capacity of the foundation. A 4% increase in the modulus of rupture effects an 89% reduction in the probability of failure. Figure 4.5 graphs this relationship. It is best described by a polynomial function because the modulus of rupture is related to the fatigue limit state equation by a number of interconnected functions with few restrictions to their behavior.

#### 4.4.3 Multi-Hazard Sensitivity Analysis

The multi-hazard sensitivity analysis is carried out using the same variables as for the individual hazards. The results show a similar trend in the sensitivity of the foundation to the multi-hazard. This is in agreement with the theory of multi-hazards as the multi-hazard reliability is a mathematical combination of the reliabilities of the various hazards and thus dependent on their behavior. Figures 4.8 – 4.11 below, show the relationship between the multi-hazard probability of failure and the various parameters affecting its structural reliability.

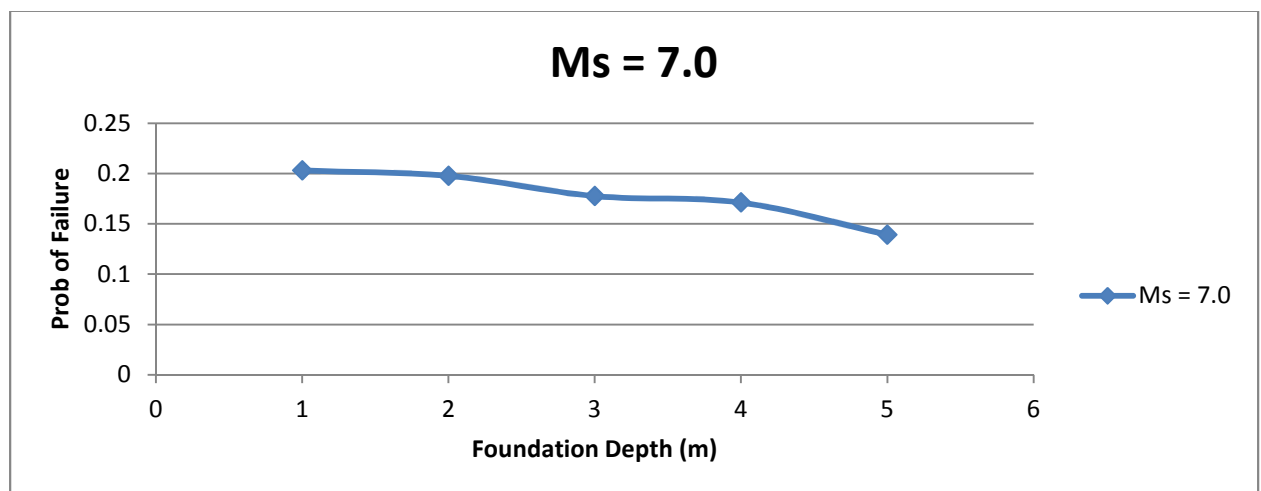


Figure 4.8: Graph of multi-hazard probability of failure against foundation depth

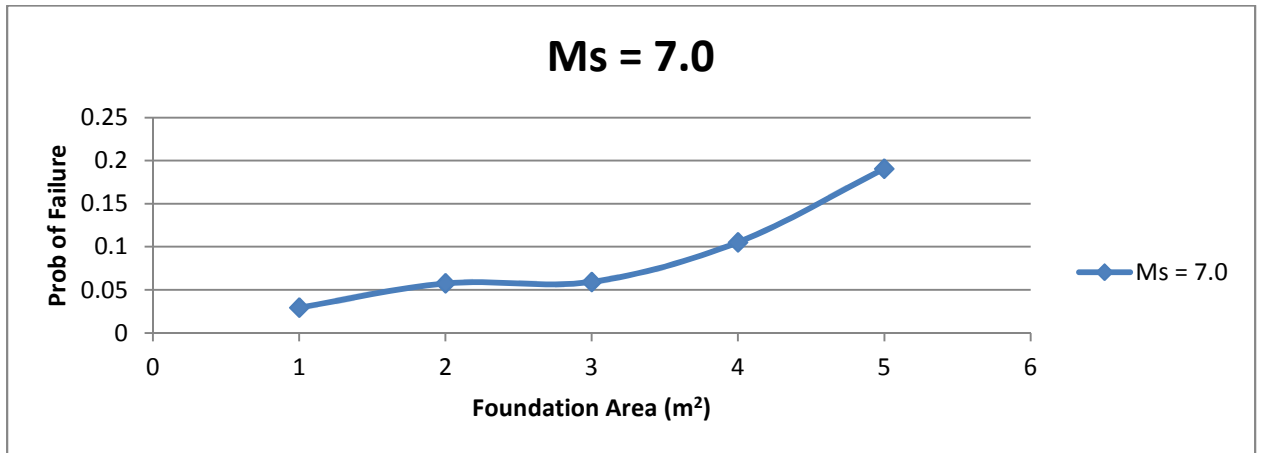


Figure 4.9: Graph of multi-hazard probability of failure against foundation area

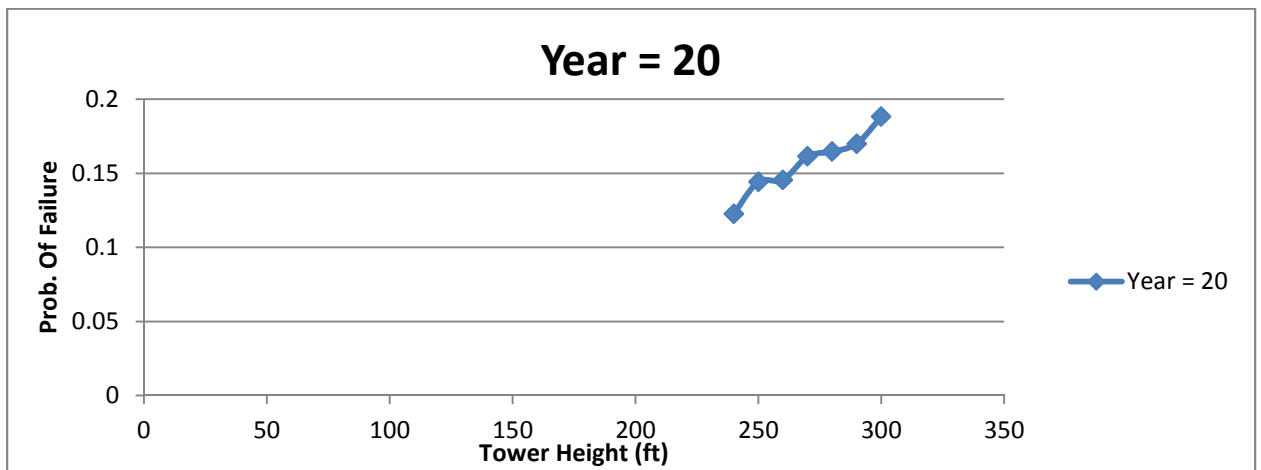


Figure 4.10: Graph of multi-hazard probability of failure against tower height

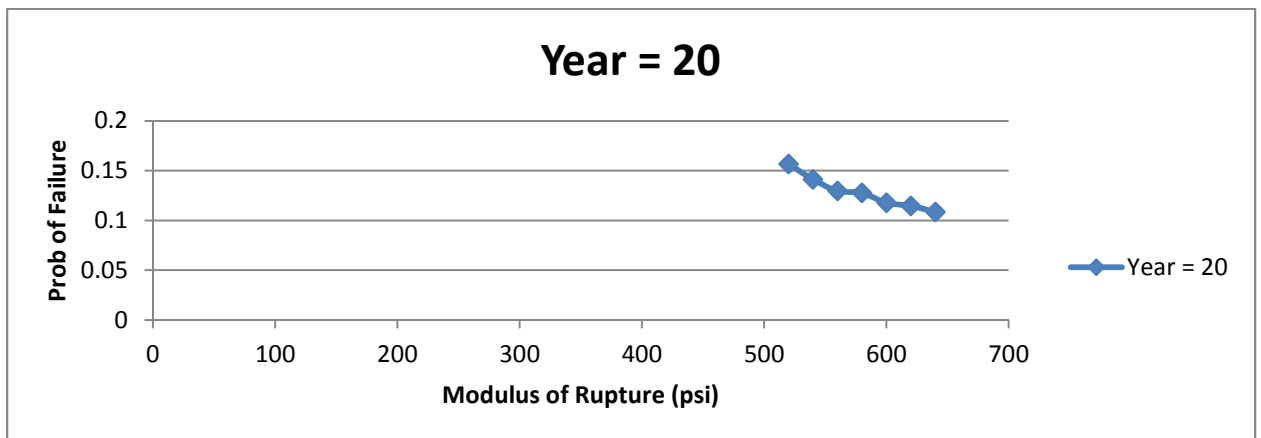


Figure 4.11: Graph of multi-hazard probability of failure against modulus of rupture

From the graphs, it can be seen that the foundation's response to multi-hazards is similar to its response to single hazards. However, there is a noticeable drop in the performance of the footing resulting from a unique loading scenario of having two different loading conditions acting on it at the same time.

The seismic analysis is most sensitive to the physical parameters of the footing as well as the earthquake size. Increasing the physical size of the footing leads to an increase in its seismic reliability. However, these changes are quite small and thus a change in size does not impact significantly on the seismic capacity of the foundation. Also, the wind fatigue reliability exhibits most dependence on the compressive strength of the concrete used and conversely the concrete mix. An increase in the compressive strength of the concrete and consequently the modulus of rupture, results in an increase in the wind fatigue reliability of the footing. The area of the foundation, compressive strength of the concrete and the height of the tower all demonstrate a polynomial relationship with the reliability of the foundation. This can be explained from the derivation of the limit state equations, from where it can be seen that the variables fulfill the conditions for a polynomial relationship including always being positive and real as well as not being in themselves exponents of any other variables. The resultant multi-hazard reliability studies in the sensitivity analysis indicate varying levels of sensitivity to the various parameters used. Whilst being very sensitive to the earthquake size, it shows less variation to changes in the physical parameters of the structural system.

## 4.5 CONCLUSIONS

1. The cyclic wind loads inducing wind fatigue in the foundation do not have a significant impact on its structural integrity over its design life. This is because the wind fatigue limit state is not the governing limit state in the foundation design and thus does not on its own pose a substantial threat to the foundation.
2. The earthquake magnitudes show a significant impact on the structural integrity of the foundation. This is especially true of seismic events of magnitudes 6.7 and above.
3. The multi-hazard analysis followed a similar trend. Although not very influential on its own, the fluctuating winds induced wind fatigue in combination with an earthquake event did show an increased possibility of foundation failure than either individual hazard acting alone.
4. The sensitivity analysis showed that that the foundation performance is sensitive to certain design parameters. The footing reliability showed sensitivity to the tower height, compressive strength of concrete, area of foundation and depth of the foundation in decreasing order of response.

## **CHAPTER FIVE**

### **FINITE ELEMENT RESULTS**

By employing the methodology defined for reinforced concrete models in ANSYS (Section 3.6), a finite element analysis model is constructed. A validation of the model is done by comparing the pullout crack shape with one from experimental work and also comparing the resultant fatigue stresses with those from hand calculations. Transient analysis is then used to carry out both the fatigue and seismic analysis with the fatigue damage usage analyzed in the ANSYS postprocessor. The results obtained and the analyses carried out using these stress results are encapsulated in the ensuing sections of this chapter.

#### **5.1 MODEL VALIDATION**

A model validation is carried out to ensure that the model designed with the input parameters would display similar behavior to a typically loaded reinforced concrete block. To validate the model thus, a pullout analysis is designed and run using the model. The resulting crack plot as shown in the figure below, shows a conical shape which is in line with the predicted behavior of concrete in a pullout analysis.

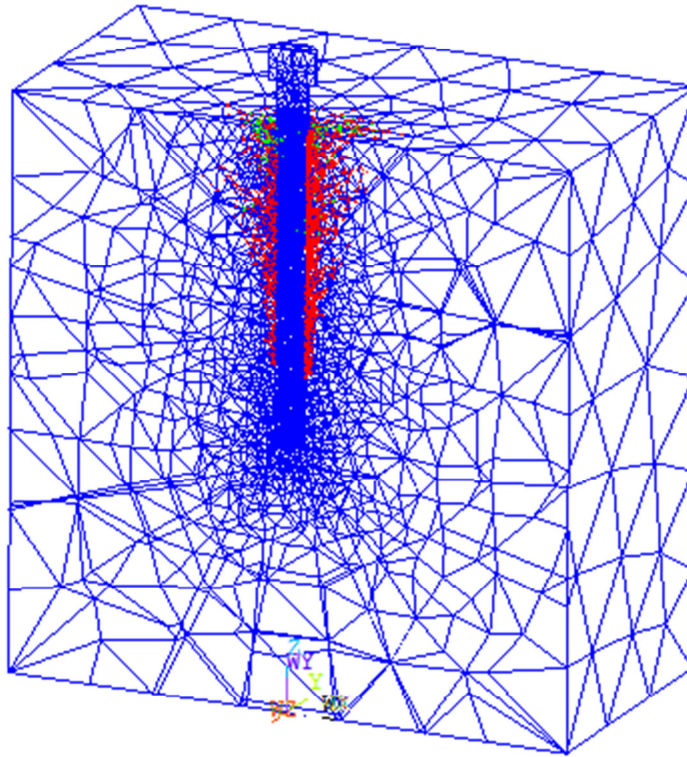


Figure 5.1: Cracking of Concrete under pullout load

Also, a comparison is made of the resulting stresses from the wind fatigue analysis of the model with those from hand calculations of a concrete block of equal dimensions. Table 5.1 shows the results of this comparison.

Table 5.1: Comparison between hand calculations and ANSYS model

	Average Stress (psi)	Percentage Difference
Hand Calculations	8.8	-
ANSYS	7.93	9.9

From table 5.1, there is a 10% variation between hand calculations of fatigue stress and the finite element analysis. Although a finer mesh would give more exact figures, these values were adjudged good enough as a finer mesh would also increase computational

time and exceed the number of elements allowed for ANSYS Educational license used in this research.

## 5.2 ANSYS Wind Fatigue Analysis

The results of the fatigue analysis computed in ANSYS were evaluated and the top ten stressed nodes were selected for analysis. The stresses obtained for the highly stressed nodes were used to determine reliability indices and probabilities of failure for each of the nodes. Figure 5.2 shows the fatigue cumulative usage as calculated in ANSYS from the cyclic wind loads. Tables 5.2 and 5.3 show the fatigue reliability results for selected nodes from the model. Figure 5.3 shows the cumulative distributive function (CDF) curve for these highly stressed nodes. Figures 5.4 and 5.5 show the nodal stress plots of the finite element analysis model in ANSYS.

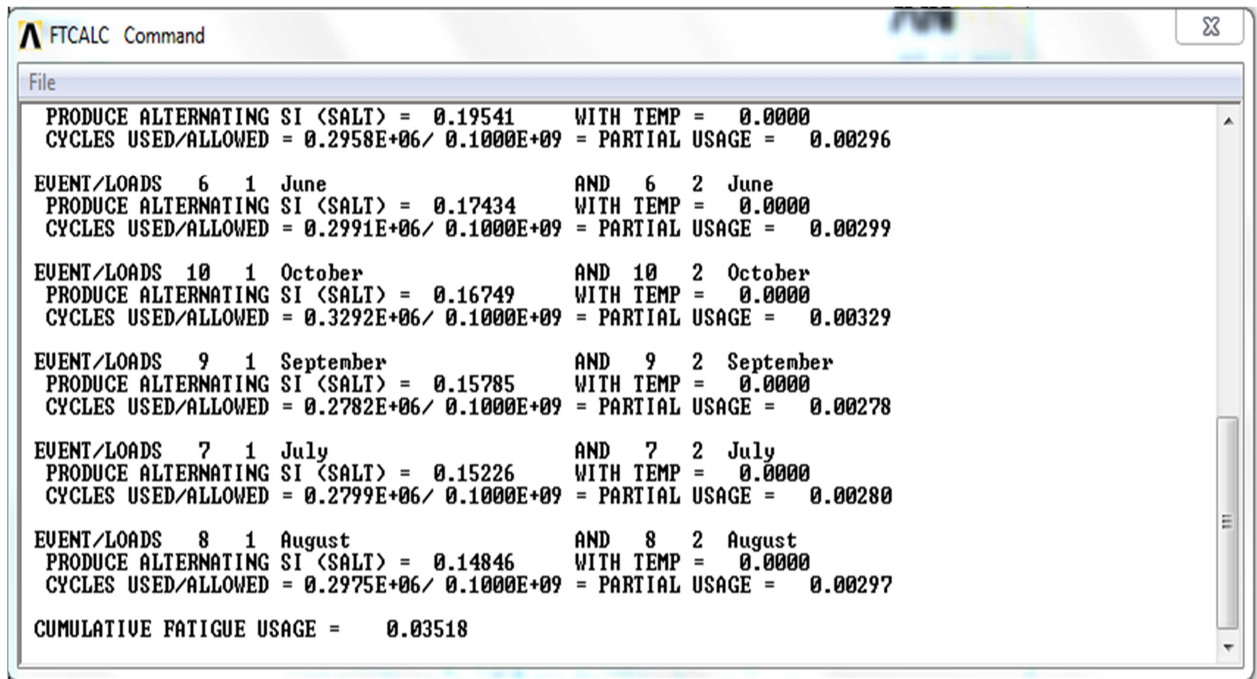


Figure 5.2: Cumulative Fatigue Analysis in ANSYS Post processor

Table 5.2: Wind Fatigue Reliability Analysis Results

S/No	Node	Stress (psi)	Cum. D	Rel. Index $\beta$	$P_f$
1	29	122.61	0.70	0.76	0.22
2	30	122.86	0.77	0.55	0.29
3	34	120.79	0.70	0.76	0.22
4	35	123.71	0.70	0.76	0.22
5	36	121.13	0.70	0.76	0.22
6	39	121.86	0.77	0.55	0.29
7	40	126.28	0.77	0.55	0.29
8	43	123.18	0.77	0.55	0.29
9	47	123.41	0.77	0.55	0.29
10	52	122.96	0.77	0.55	0.29

Table 5.3: Probability of Failure over the Design Lifetime for Selected Nodes

Year	$P_f$		
	Node 29	Node 30	Node 34
1	0.00076	0.00079	0.00076
2	0.00116	0.00126	0.00116
3	0.00175	0.00198	0.00175
4	0.00264	0.00311	0.00264
5	0.00396	0.00482	0.00395
6	0.00586	0.00737	0.00585
7	0.00856	0.01107	0.00855
8	0.01231	0.01627	0.01229
9	0.01740	0.02339	0.01737
10	0.02413	0.03286	0.02409
11	0.03282	0.04505	0.03277
12	0.04378	0.06031	0.04369
13	0.05724	0.07884	0.05713
14	0.07338	0.10074	0.07324
15	0.09229	0.12593	0.09212
16	0.11397	0.15419	0.11376
17	0.13827	0.18520	0.13803
18	0.16502	0.21849	0.16474
19	0.19389	0.25354	0.19358
20	0.22455	0.28981	0.22419

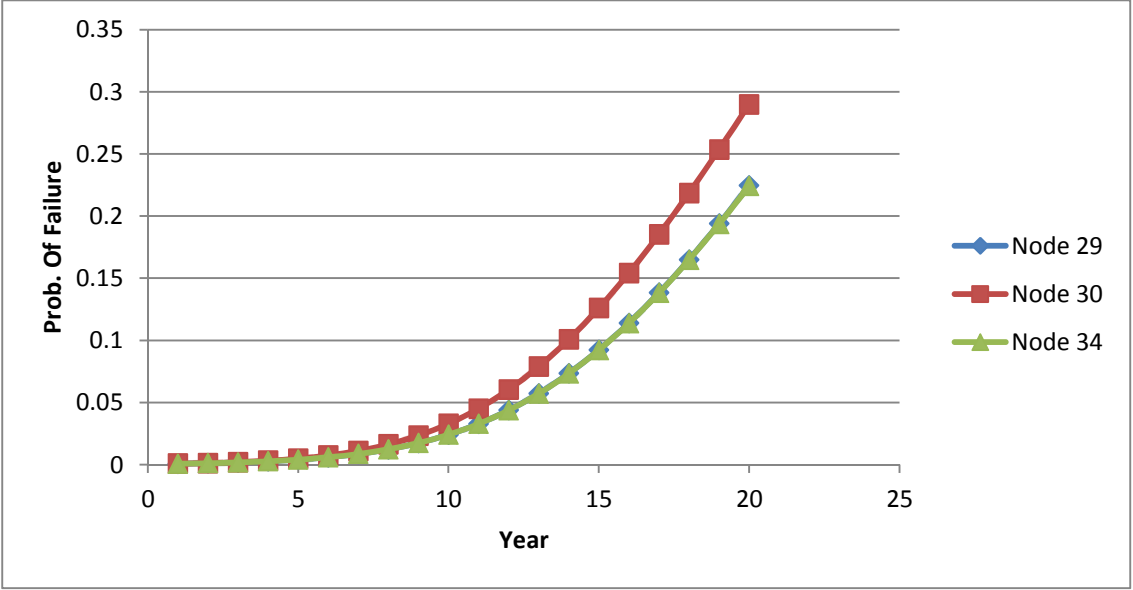


Figure 5.3: Cumulative Distribution Function for selected nodes

NODAL SOLUTION  
 STEP=9999  
 SEQV (AVG)  
 DMX =.224E-04  
 SMX =142.864

**ANSYS**  
 NOV 10 2013  
 22:07:18

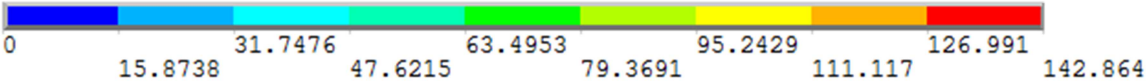
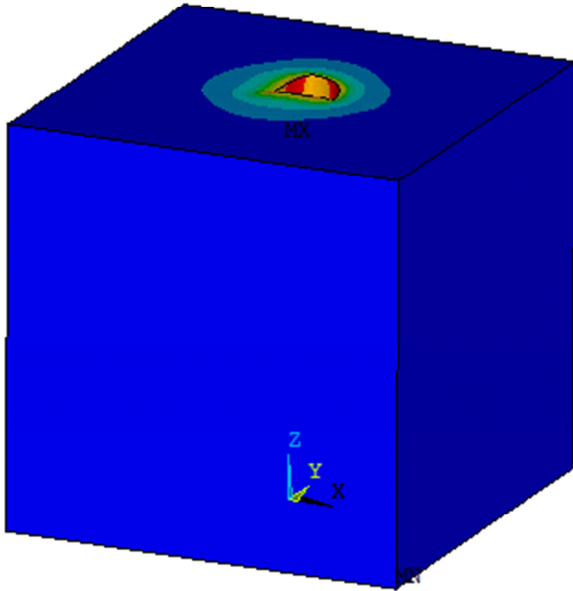


Figure 5.4: Nodal Stress of footing under fatigue loading

STEP=9999  
SEQV (AVG)  
DMX =.224E-04  
SMX =142.864

NOV 10 2013  
22:08:24

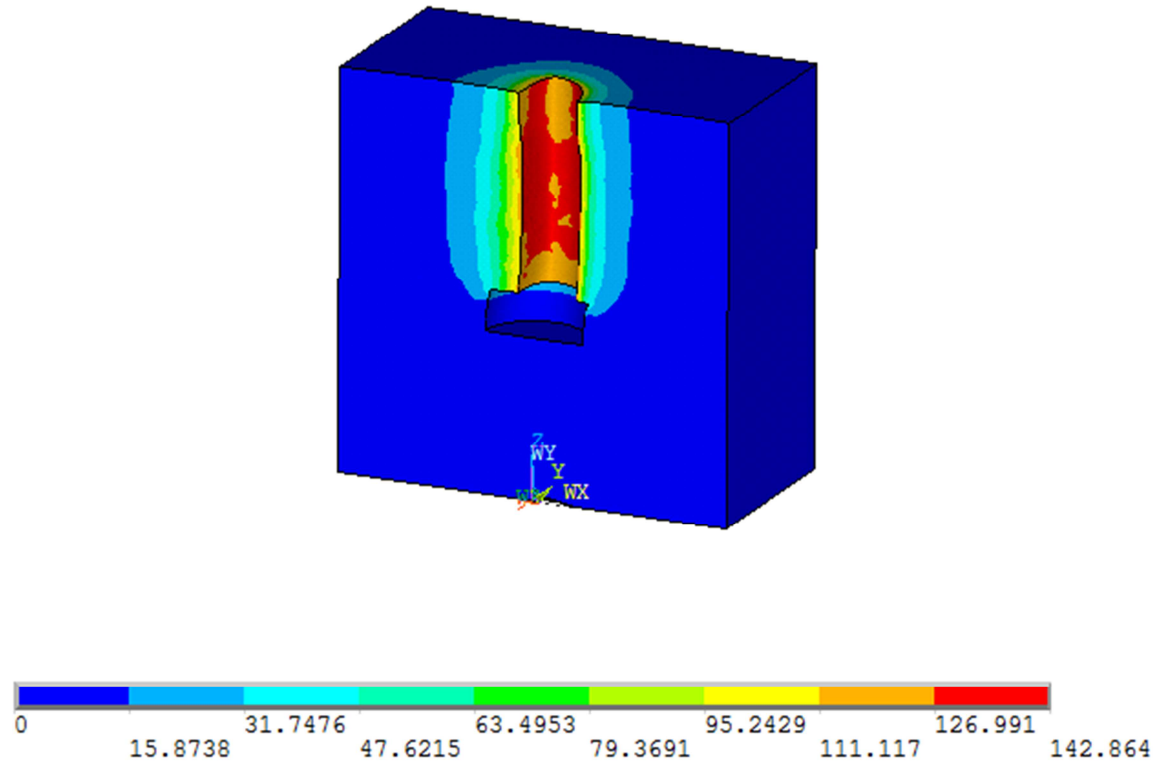


Figure 5.5: Nodal Stresses through a cut section

Table 5.2 gives the stress results obtained from the fatigue analysis carried out in ANSYS. It also gives the cumulative damage arising from the cyclic loading as per Miner's rule. The reliability index and probability of failure calculated using FORM (as defined in Section 3.1), show the performance indices for a footing after twenty years in operation being the design lifetime of wind turbines' structural systems.

The graph above shows the direct linear relationship between time and the probability of failure from wind loads. At the expected end of the turbine's life cycle of 20 years, there is a 28% chance of failure due to the cyclic winds.

### 5.3 ANSYS Seismic Analysis

Seismic analysis is carried out using the ground motion data obtained for the Borah Peak earthquake of 1983. Stress values obtained from the seismic analysis carried out in ANSYS are used to determine the reliability index and probability of failure of the same nodes examined in the fatigue limit state. These structural performance indices are obtained using a cracking limit state with the modulus of rupture of the concrete taken for the system capacity. Table 5.4, shows the results of this assessment.

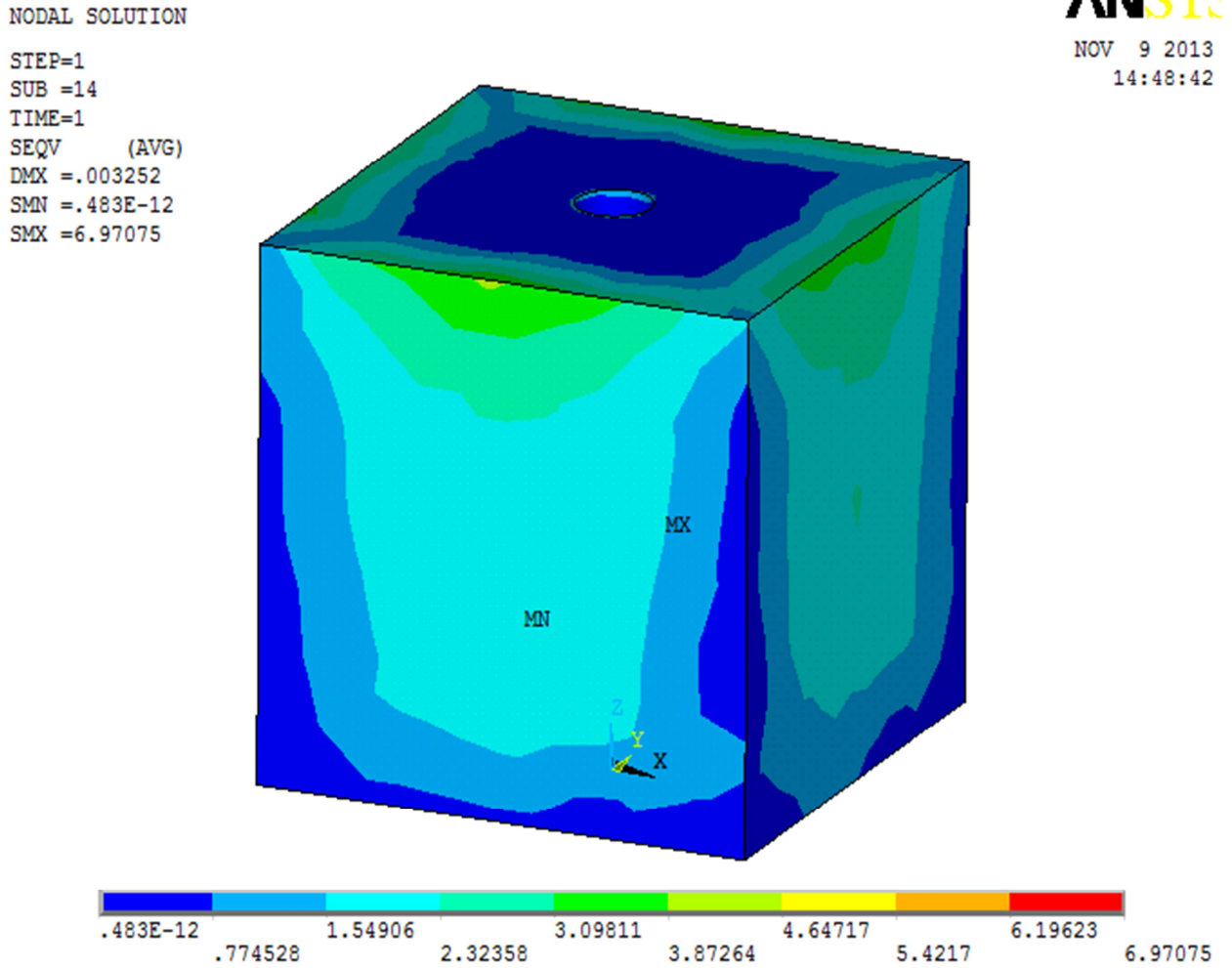
Table 5.4: Seismic Reliability Analysis Results

S/No	Node	Stress (psi)	Rel. Index $\beta$	$P_f$
1	29	7.2035	2.542819	0.005498
2	30	7.2303	2.542674	0.0055
3	34	7.0705	2.543541	0.005487
4	35	7.0892	2.543439	0.005488
5	36	6.8673	2.544643	0.005469
6	39	6.9778	2.544043	0.005479
7	40	7.3004	2.542294	0.005506
8	43	7.3936	2.541788	0.005514
9	47	7.5163	2.541123	0.005525
10	52	7.0293	2.543764	0.005483

Table 5.4 presents the nodal stress results from the seismic time history analysis carried out in ANSYS. It also gives the results from the reliability analysis carried out using the cracking limit state. From the results, it can be seen that the probability of failure of the selected nodes from cracking is quite low. However, some caution needs to be applied in interpreting these results. The nodes selected for the analysis were not the most stressed nodes from the seismic analysis but those from the fatigue analysis. They were selected to be used in the seismic analysis as well in order to properly assess the effect of the

combined loads on them. Also, the cracking of the footing is not as a major concern during earthquakes as is displacement.

Figures 5.6 and 5.7 show the nodal stress plots of the concrete footing under the earthquake induced ground motions.



NODAL SOLUTION  
STEP=1  
SUB =14  
TIME=1  
SEQV (AVG)  
DMX =.003252  
SMN =.483E-12  
SMX =6.97075

**ANSYS**  
NOV 9 2013  
14:52:01

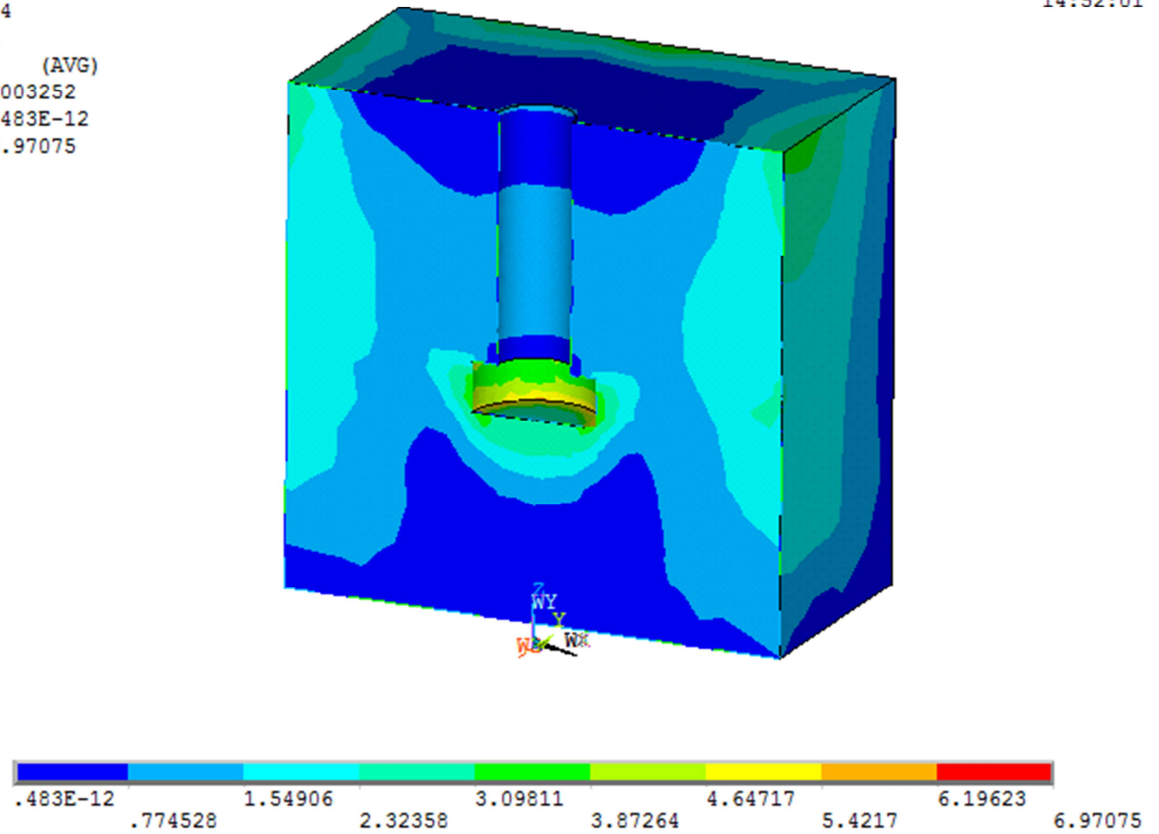


Figure 5.7: Nodal Stresses through a cut section

#### 5.4 ANSYS Multi-hazard Analysis

To replicate a possible multi-hazard scenario, the principal stresses from the fatigue and seismic analyses were combined vectorially in the ANSYS post processor. This is done under the assumption that because the two hazard scenarios act independently, the resulting stresses from each will in no way be influenced by the other. Thus, each node's final stresses will be a vector sum of the different stresses acting on it. This examination provided stress values to be expected in the event of such a scenario playing out. Table 5.5, shows the result of this analysis.

Table 5.5: Stresses of selected nodes under combined loading

S/No	Node	Stress	$\beta$	$P_f$
1	29	129.84	1.825651	0.033951
2	30	130.06	1.824491	0.034039
3	34	127.86	1.836094	0.033172
4	35	130.8	1.820588	0.034335
5	36	127.99	1.835408	0.033223
6	39	128.84	1.830925	0.033556
7	40	133.58	1.805926	0.035465
8	43	130.58	1.821748	0.034247
9	47	130.92	1.819955	0.034383
10	52	129.99	1.82486	0.034011

Figures 5.8 and 5.9 show the nodal stress plots of the concrete footing under the combined stress state.

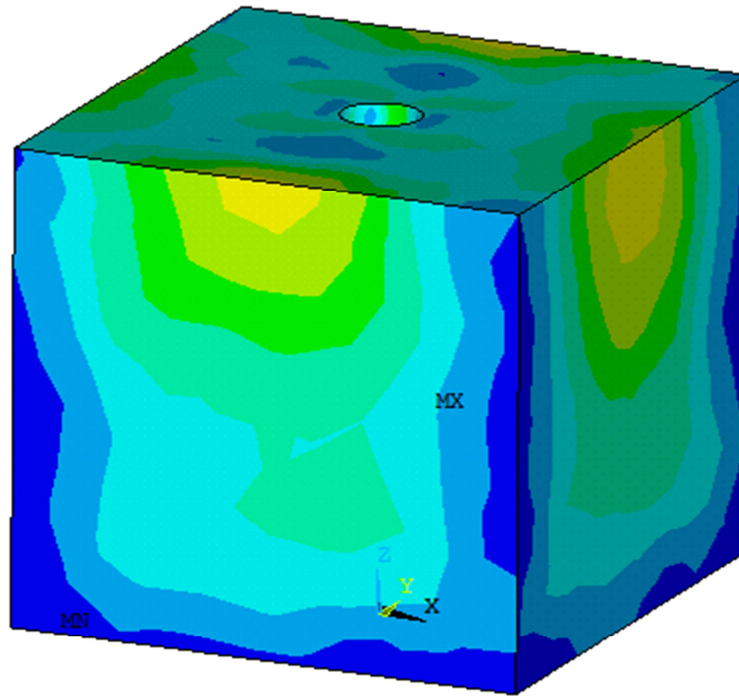


Figure 5.8: Nodal Stress of footing under combined pressure from earthquakes and cyclic winds

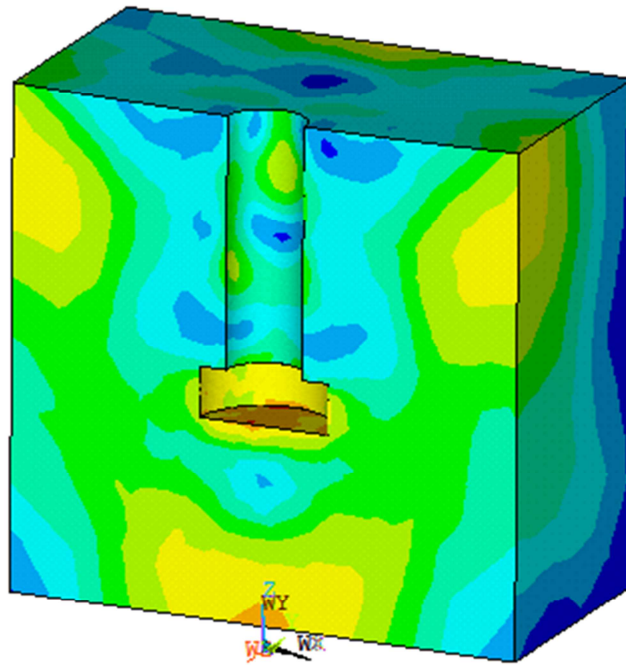


Figure 5.9: Nodal Stresses through a cut section

The results of the multi-hazard analysis as carried out show a definite increase in the stresses of nodes under observation. This expectedly results in a drop in the reliability index and increase in the probabilities of failure of these nodes. Figure 5.8 shows the stress distribution of a section of the model. From this figure, it can be seen that the multi-hazard stress is distributed along the same lines as both the fatigue and seismic stresses albeit with increased values. Figures A-1 to A-3 (appendix A) show the displacement time history for the nodes under observation. These graphs show a sudden spike in the displacement of the nodes at time of 240. This is due to the application of the displacement time history of the earthquake at the end of the fatigue loading. Figures A-4 to A-6, show the stress histories of the selected nodes. From the graph, it can be seen that the resultant stress from the fatigue loading is a triangular wave with maxima and minima values. The seismic stresses induced at the end of the fatigue cycle is less than the fatigue

stresses in both nodes 29 and 34 but is almost equal with that of node 30. This can be explained from the methodology used in the analysis. The nodes selected for observation were not the nodes under the most seismic stress but those under the highest fatigue stress. These were used because of their location in critical areas around the anchor bolts connecting the tower to the footing.

From the results achieved, it can be deduced that changes to the analytical parameters for the multi-hazard analysis would result in similar behavior as a change of the parameter in either the fatigue or seismic analysis. Thus, the sensitivity behavior of the model under multi-hazard loading will be similar too. Therefore, any remedial action proposed to mitigate the effects of these loading scenarios would bring about a similar reaction to the multi-hazard.

## **5.5 CONCLUSIONS**

1. The finite element analysis model developed in ANSYS is a good representation of the conditions under examination.
2. The cyclic wind loads inducing fatigue have divergent resultant stresses on nodes of the model with stress concentrations around the anchor bolts. Although the foundation does not fail under the cyclic action of the winds, the stresses induced in it do cause enough damage that a seismic event occurring afterwards would trigger its failure.
3. The seismic events also show divergent stresses on the model with stress concentrations around the sides and also around the anchor bolts.

4. The multi-hazard analysis show an increase in stresses all around the model with critical areas around the anchor bolts, areas identified as crucial for reliability studies. The reliability studies on these areas show a reduction in the performance indices of the accompanying nodes and an attendant increase in their probability of failure.

## CHAPTER SIX

### 6.1 DISCUSSION OF RESULTS

The preceding chapters present two approaches for evaluating the performance of a wind turbine's foundation, specifically the bond between the anchor bolts and the concrete, under multi-hazard loading.

A MATLAB code is used to evaluate a fatigue limit state as well as a resonance limit state for the concrete foundation. The resulting performance indices are then combined under a series methodology to determine the performance of the system under simultaneous albeit independent loading scenarios. From the analyses, it can be seen that there is a notable drop in the performance of the system when under multi-hazard loading as compared to being under a single type of loading.

A more sophisticated finite element analysis is also carried out in ANSYS. First, a simplified model of the foundation is built with an anchor bolt imbedded in it. This model is validated by performing a pullout analysis of the anchor bolt. The concrete cracking plots showed a conical cracking pattern, in consonance with the theoretical behavior of concrete in a pullout analysis. Also, to further validate the model, a comparison is made of the fatigue stress results obtained with those gotten from hand calculations. This comparison showed good correlation of the two results.

Using historical wind data as well as seismic displacement time histories, dynamic transient analyses are carried out on the model. The ensuing stresses from the individual fatigue and seismic analyses are then evaluated as is the results from the combined loading analysis. The resulting performance indices are consistent with those from the

MATLAB code with a defined drop in the performance of the footing under the multi-hazard compared to the individual loading scenarios. However, for a design lifetime of 20 years as recommended for wind turbine systems, the structural system does show enough resilience against the multi-hazard evaluated. Nevertheless, the results pose critical questions especially to the veracity of current design standards and to the performance of the foundation under more extreme yet probable multi-hazard loading conditions.

The most significant result from this research is the considerable drop in the performance of the foundation when subjected to multi-hazard loading. Wind turbines are considered critical infrastructure and are thus designed to withstand rigorous loading scenarios. However, as shown in the results, there is still a possibility of their failure occurring as a result of a possible combined loading scenario not considered in design but likely to occur in a seismically active region also prone to high winds like Idaho Falls.

## **6.2 CONCLUSIONS**

This thesis investigated a multi-hazard approach towards defining the performance of a structure over time. Some conclusions drawn from the study include:

1. The threat posed by cyclic wind loads to wind turbine foundations is not inconsequential.
2. Also, the menace posed by seismic activities is quite significant especially from larger earthquakes.
3. The threat to structural systems from multi-hazard load combinations is real.
4. The current design standards which are based on Turkstra's rule of load combination completely negate the possibility of load components acting at their

extreme value at the same time, do not adequately cover this growing concern. As such, the design of wind turbine foundations under the current standards could prove inadequate to resist certain load combinations and be prone to failure.

5. Finite element analysis is a viable tool for analyzing multi-hazard effects on structural systems especially for complicated geometry for which hand calculations may be difficult.
6. The foundation showed some vulnerability to multi-hazards. Although, the resultant stresses are within its capacity, the performance indices indicated a significant drop in capacity when loaded under a multi-hazard condition.
7. A multi-hazard approach towards design is advantageous in that it takes into account the several and vastly varying types and magnitudes of loads a structure is likely to come under during its design life and merges them into an integrated approach geared towards appraising the system reliability. Newly developed load combination methods such as the load coincidence method which does consider possible overlapping load case scenarios might help in mitigating the effects of multi-hazard loads.
8. Although somewhat simplified for the case of this study, the basic approach identified is of general applicability for a wide range of engineering design purposes.

Conclusively, it can be seen that multi-hazards pose a greater threat to system reliability than any single hazard does. Thus, it is imperative that more attention is given to this budding field of analysis.

### **6.3 RECOMMENDATIONS**

From the observations made in this study, some recommendations can be made to improve the wind turbine's foundation's reliability. These include:

1. An increase in design compressive strength of concrete used will reduce fatigue damage and consequently improve the multi-hazard reliability.
2. An increase in the number of anchor bolts would reduce fatigue stress critical values and help improve the foundation's reliability.
3. An increase in damping will improve the seismic reliability and reduce the probability of failure.
4. Increasing the footing size will not have any telling impact on the reliability and is thus not recommended.

### **6.4 FUTURE WORK**

From this work, a number of future applications to the study of multi-hazards can be made such as:

1. The approach used in this study to determine the multi-hazard reliability of a wind turbine's foundation can be extended to the entire structure.
2. Other multi-hazard failure scenarios should be explored and a more holistic multi-hazard analysis carried out.
3. Field studies should be carried out on currently established wind turbines to verify the results of this study.

## BIBLIOGRAPHY

- AASHTO, “Standard Specifications for Structural Supports for Highway Signs, Luminaires and Traffic Signals,” Fourth Edition, LTS-4. American Association of State Highway and Transportation Officials. Washington, DC, 2001.
- Ariduru, Seçil. "Fatigue life calculation by rainflow cycle counting method." *MSME thesis, Middle East Technical University, Ankara, Turkey* (2004).
- ASCE, “Minimum design loads for building and other structures,” Standard ASCE/SEI 7-05. American Society of Civil Engineers, Reston, Va., USA, 2005.
- Ayyub, M.B. and McCuen R.H, “Probability, Reliability and Statistics for Engineers and Scientists,” Third Edition, CRC Press, 6000 Broken Sound parkway NW, Suite 300, Boca Raton, Fl., USA,2011.
- Ceren B, “International Wind Turbine Foundation 2012- Exemplified by a 6MW,” *ICCI 2013, International Conference, Istanbul, Turkey*, 2013.
- Cheng, Z, Yang, P, Jiang H, "Anti-overturning reliability analysis of gravity foundation of wind turbine in coral sands," *Electronics, Communications and Control (ICECC), 2011 International Conference on* , vol., no., pp.2554,2557, 9-11 Sept. 2011
- Duthinh, D., & Simiu, E, “Safety of structures in strong winds and earthquakes: Multihazard considerations,” *Journal of structural engineering*, 136(3), 330-333, 2009.
- Deierlein, G. G., Liel, A. B., Haselton, C. B., & Kircher, C. A, “ATC 63 methodology for evaluating seismic collapse safety of archetype buildings,” In *Proceedings of ASCE-SEI Structures Congress, Vancouver, BC*, 2008.

- Dexter, Robert Joseph, and Matthew J. Ricker. *Fatigue-resistant design of cantilevered signal, sign, and light supports*. No. 469. Transportation Research Board, 2002.
- Ebel, John E., and Alan L. Kafka. "A Monte Carlo approach to seismic hazard analysis." *Bulletin of the Seismological Society of America* 89, no. 4 (1999): 854-866.
- Göransson, Frida, and Anna Nordenmark. "Fatigue Assessment of Concrete Foundations for Wind Power Plants." (2011).
- IEC, "Wind turbines – Part 1: Design requirements. 3rd ed. Standard IEC 61400-1:2005-08," International Electrotechnical Commission, Geneva, Switzerland, 2005.
- Kacin, Jennifer Ann. "Fatigue life estimation of a highway sign structure." PhD diss., University of Pittsburgh, 2009.
- Kafali, Cagdas, and Mircea Grigoriu. "Seismic fragility analysis: Application to simple linear and nonlinear systems." *Earthquake Engineering & Structural Dynamics* 36, no. 13 (2007): 1885-1900.
- Kuhn B., Marquis J., Rotatori H, "Wind Turbine Design and Implementation," Senior Design Project, Worcester Polytechnic Institute, Worcester, 2010
- Li, X., Whalen, T. M., & Bowman, M. D, "Fatigue strength and evaluation of double-mast arm cantilevered sign structures," *Transportation Research Record: Journal of the Transportation Research Board*, 1928(-1), 64-72, 2005.

- Lavassas, I., G. Nikolaidis, P. Zervas, E. Efthimiou, I. N. Doudoumis, and C. C. Baniotopoulos. "Analysis and design of the prototype of a steel 1-MW wind turbine tower." *Engineering structures* 25, no. 8 (2003): 1097-1106.
- Logan D.L, "A First Course in the Finite Element Method," Fourth Edition, Wiley and Sons Ltd 2007.
- McCullough, Megan, and Ahsan Kareem. "Performance-based engineering in multi-hazard coastal environments."
- Miner, M. A, Cumulative damage in fatigue. *Journal of applied mechanics*, 12(3), 159-164, 1945
- Nowak, A.S. and Collins, K.R, "Reliability of Structures," McGraw Hill Publishers, Boston, Ma., USA, 2000.
- NWCC Wind Rose Database, National Water and Climatic Center, <http://www.wcc.nrcs.usda.gov/climate/windrose.html>. Accessed January 2013
- Nuta, E. N. E., Christopoulos, C. C. C., & Packer, J. A. P. J, " Methodology for seismic risk assessment for tubular steel wind turbine towers: application to Canadian seismic environment," *Canadian Journal of Civil Engineering*, 38(3), 293-304, 2011.
- PEER Ground Motion Database, Pacific Earthquake Engineering Research Center, [http://peer.berkeley.edu/peer\\_ground\\_motion\\_database](http://peer.berkeley.edu/peer_ground_motion_database). Accessed August 2013.
- Prowell, Ian, and Paul Veers. "Assessment of wind turbine seismic risk: Existing literature and simple study of tower moment demand." *Rep. No. SAND2009-XXXX (to be published)* (2009).

- Ragan, Patrick, and Lance Manuel. "Comparing estimates of wind turbine fatigue loads using time-domain and spectral methods." *Wind engineering* 31, no. 2 (2007): 83-99.
- Rao, S., & Roesler, J. R, "Cumulative Fatigue Damage Analysis of Concrete Pavement Using Accelerated Pavement Testing Results," In *Proc., 2nd International Conference on Accelerated Pavement Testing, Minneapolis, Minnesota, 2004.*
- Rao, S. S, "Mechanical Vibrations," 5th edition. SI, Pearson Education International, 2011.
- Repetto, Maria Pia, and Giovanni Solari. "Dynamic alongwind fatigue of slender vertical structures." *Engineering Structures* 23, no. 12 (2001): 1622-1633.
- SAS, "ANSYS 12.1 Finite Element Analysis System," ANSYS Inc., 2010.
- SAS, "ANSYS Element Reference manual." Release 12, ANSYS Inc., 2009.
- Singh S.P, Mohammadi Y, Kaushik S.K, "Probability of fatigue Failure of Steel Fibrous Concrete containing Mixed Fibers," *Asian Journal of Civil Engineering (Building and Housing), Vol. 7, No. 1, 2006.*
- Sørensen, J. D., Frandsen, S., & Tarp-Johansen, N. J, "Effective turbulence models and fatigue reliability in wind farms," *Probabilistic Engineering Mechanics*, 23(4), 531-538, 2008.
- Spence W, Sipkin A.S, Choy G.L, "Measuring the size of an earthquake," *Earthquake and Volcanoes, Vol. 21, No 1, 1989.*
- Sutherland, Herbert J., and Paul S. Veers. "Effects of cyclic stress distribution models on fatigue life predictions." *Wind Energy* 16 (1995): 83-90.

- Toft, H. S., & Sorensen, J. D., "Reliability-based design of wind turbine blades," *Structural Safety*, 33(6), 333-342, 2011.
- Tarp-Johansen N.J, Madsen P.H, Frandsen S, "Partial Safety Factors for Extreme Load Effects, Proposal for the 3<sup>rd</sup> Ed. Of IEC 61400: Wind Turbine Generator Systems- Part 1: Safety Requirements," Riso National Laboratory, Roskilde, Denmark, March 2002.
- Tso, W. K., and A. S. Moghadam. "Pushover procedure for seismic analysis of buildings." *Progress in Structural Engineering and Materials* 1, no. 3 (1998): 337-344.
- Tsompanakis, Y., Papadopoulos, V., Lagaros, N. D., & Papadrakakis, "Reliability analysis of structures under seismic loading," In *Proc. 5th world congress on computational mechanics WCCM-V, Vienna, Austria, 2002*.
- Weatherill, Graeme A., and Paul W. Burton. "The application of multiple random earthquake simulations to probabilistic seismic hazard assessment in the Aegean region." In *Firs European Conference on Earthquake Engineering and Seismology. Geneva, Switzerland. 2006*.
- Witcher, David. "Seismic analysis of wind turbines in the time domain." *Wind Energy* 8, no. 1 (2005): 81-91.
- Wolanski, A.J, "Flexural Behavior of Reinforced and Prestressed Concrete Beams," Masters thesis, Marquette University, Milwaukee, 2004.
- Zhao, X., and P. Maisser. "Seismic response analysis of wind turbine towers including soil-structure interaction." *Proceedings of the Institution of Mechanical Engineers, Part K: Journal of Multi-body Dynamics* 220, no. 1 (2006): 53-61.

## **Appendix A**

### **Time History Plots of Selected Nodes**

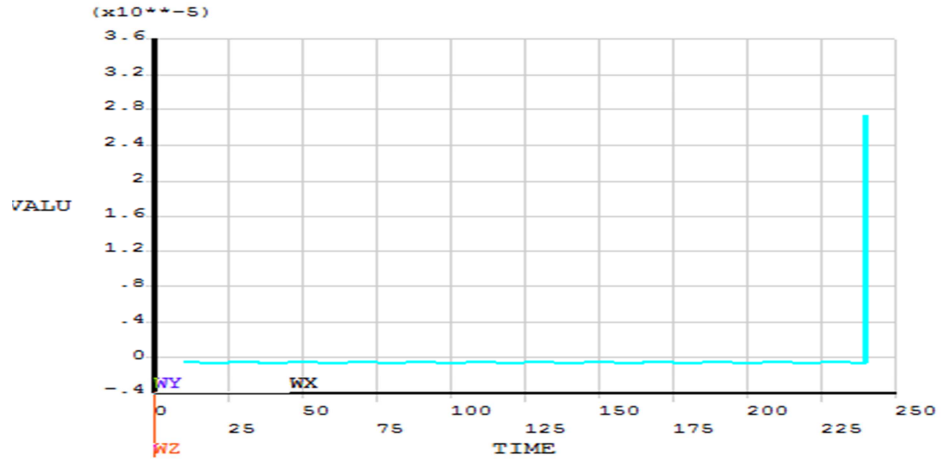


Figure A-1: Displacement Time history for Node 29

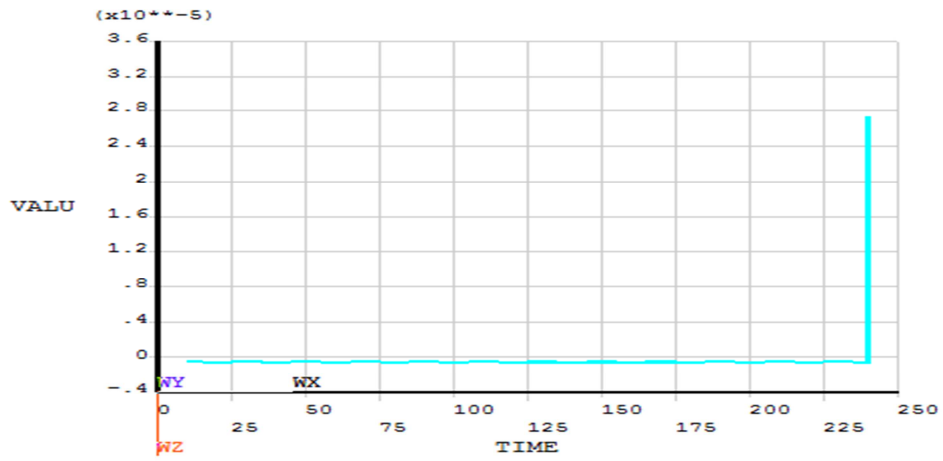


Figure A-2: Displacement Time history for Node 30

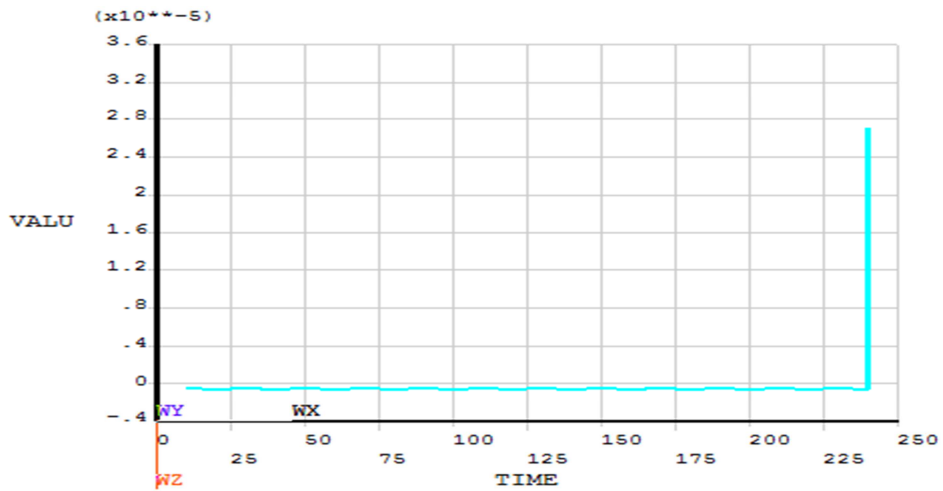


Figure A-3: Displacement Time history for Node 34

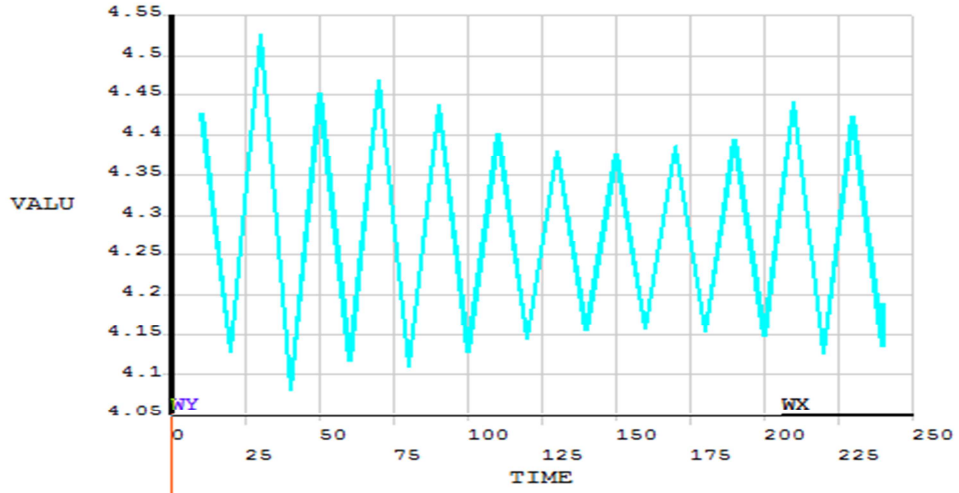


Figure A-4: Stress Time history for Node 29

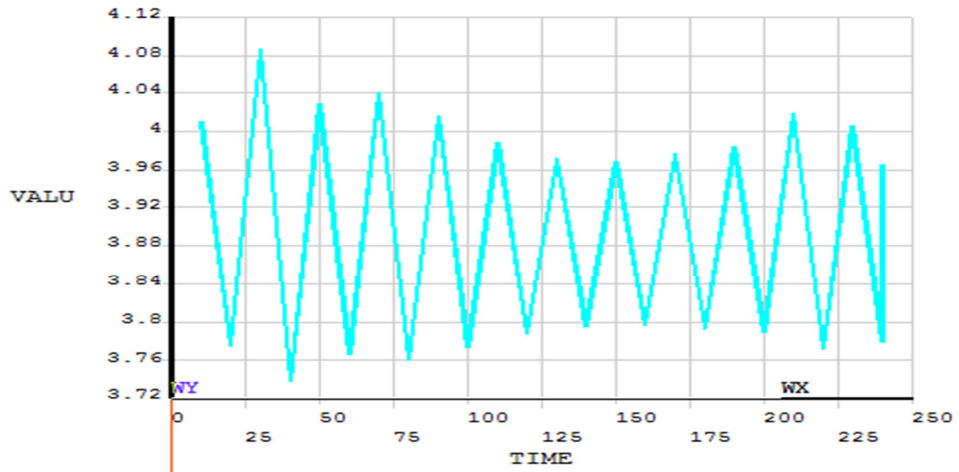


Figure A-5: Stress Time history for Node 30

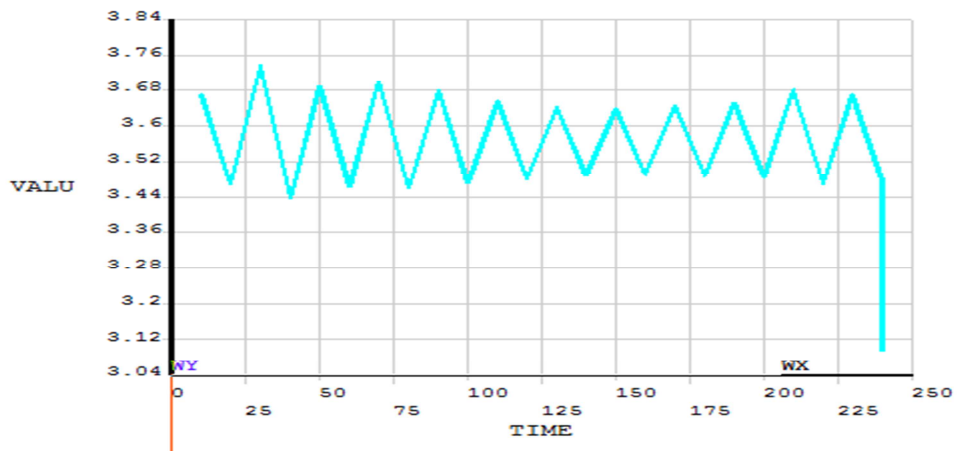


Figure A-6: Stress Time history for Node 34

**Appendix B**  
**Wind Rose Diagram**

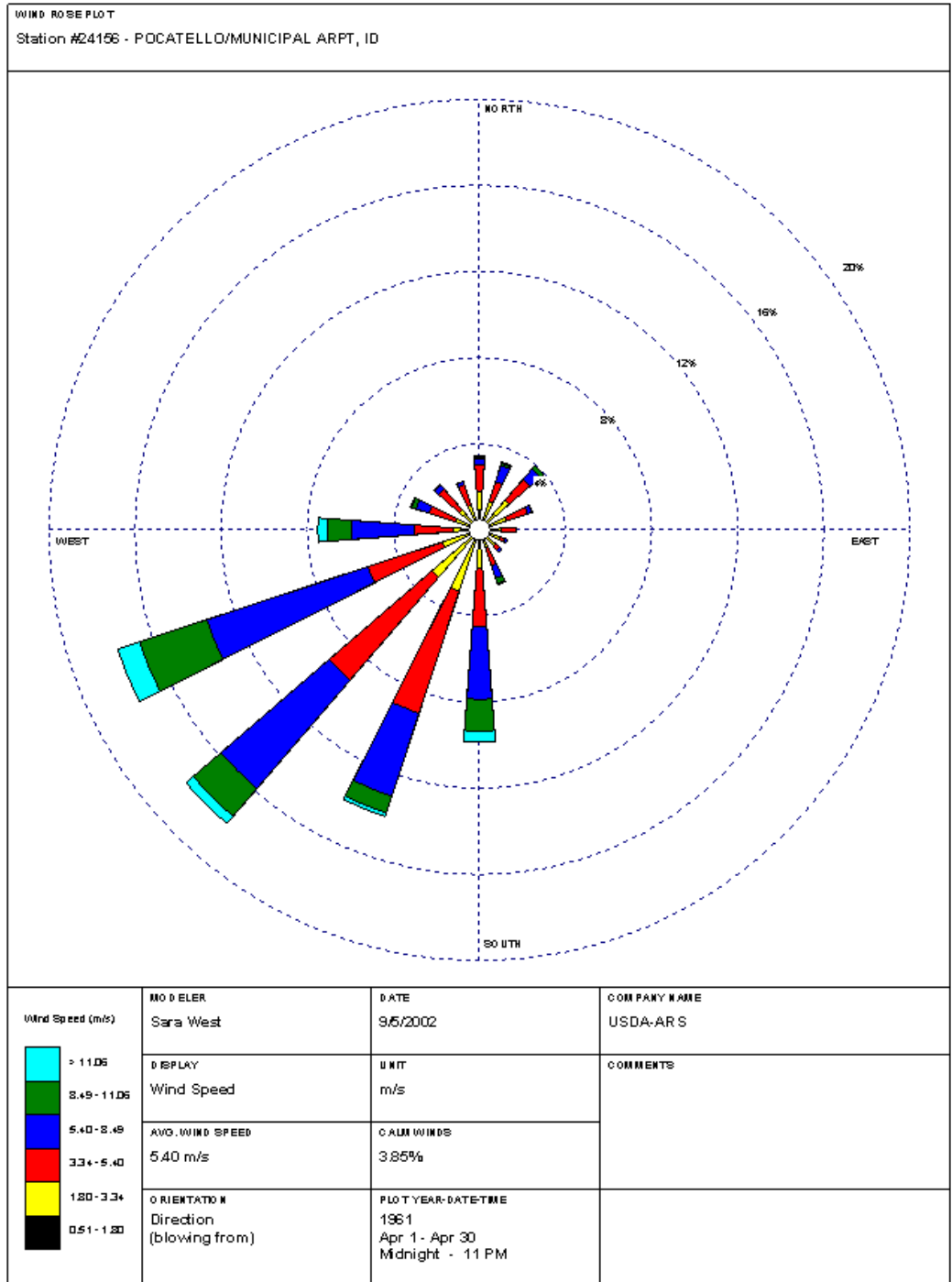


Figure B-1: Wind Rose Diagram (NWCC, 2013)

**Appendix C**  
**MATLAB Source Code**

```

%clc
Seismic Analysis;
syms r
L = 4.88
B = 4.88
H = 0.9188
Dens = 1300
Wf = L*B*H*Dens
Wt = 3444703
F = (Wf + Wt)*9.81
K = 540000*L*B
Y = F/K
Xi = 0.01
%UMs = 7
UT = 10
UD = 1500
SDMs = 0.15
SDT = 0.01
SDD = 0.25
RMs = norminv(rand(1,100));
RT = norminv(rand(1,100));
RD = norminv(rand(1,100));
T = UT + (RT*SDT);
D = UD + (RD*SDD);
t = [6:0.1:8]
for s = 1:length (t)
    UMs = t(s)
    Ms = UMs + (RMs*SDMs);

for x = 1:100
A(x) = ((T(x)) * 10.^(Ms(x) - (1.66*(log10((D(x))*1)))-3.3))* (10.^-0)
m = (((A(x)/Y).^2)*((1-(r.^2)).^2)+((2*Xi*r).^2))-((2*Xi*r).^2)-1
eig(m)
u = vpa(solve(eig(m)))
real = u(find(imag(u)==0))

r1= vpa((real(1)))
r2 = vpa((real(2)))
if r1>0
    rv(x) = r1
else
    rv(x) = r2
end
end
rv'
Ur = mean(rv)
q = (rv - Ur).^2
SDr = sqrt((sum(q))/(x-1))
Ebeta(s) = (Ur - 2.8)/(SDr)
end
Ebeta'
Pfe = normcdf(double(-Ebeta))

```

```

Clc
Fatigue Analysis;
clearvars
syms h db dt c Ix Cd If z R y M SR F P n N D g(x) t Xd Xe Xa Xs Xrfc Xr
a1 a2 a3 a4 a5 a6 a7 Del UD Ue Ua Us Urfc Ur UDel SDD SDe SDa SDs SDrfc
SDr SDdel

h = 250
db = 8
dt = 7
c = 4
fc = 3204.74
t = 0.75/12;
disp t
di1 = db - t
di2 = dt - t
Ix = pi*((db.^4))/64
Cd = 1.0
If = 0.8
y = 365
R = [8,12]
z=rand(y,1)*range(R)+min(R)

P = (5.2*Cd*If*(z.^2))/(125)
F = P*h*((db+dt)/2)
M = (F*h/2)
S = M*c/Ix
SR = S/(640*144)

for i = 1:y

if z(i) >= 11
    n(i)= 15000;
else
    n(i) = 9500;

end

end

disp(n')
N = 10.^(2.13*(SR.^-1.2));
disp(N')
q=n./(N')
D = vpa(sum(q))
Del = 1
Xd = 1
Xe = 1
Xa = 1
Xs = 1
Xrfc = 1
Xr = 1

UD = 1
Ue = 1
Ua = 1

```

```

Us = 1
Urfc = 1
Ur = 1
Udel = 1
SDD = 0.2
SDe = 0.2
SDa = 0.2
SDs = 0.05
SDrfc = 0.02
SDr = 0.05
SDdel = 0.3
for i = 1:20
    D(i)=i*D
a1 = Ur
a2 = Del
a3 = -D(i)*Xe*Xa*Xs*Xrfc
a4 = -D(i)*Xd*Xa*Xs*Xrfc
a5 = -D(i)*Xd*Xe*Xs*Xrfc
a6 = -D(i)*Xd*Xe*Xa*Xrfc
a7 = -D(i)*Xd*Xe*Xa*Xs
Beta = ((Udel*Ur) -
(D(i)*UD*Ue*Ua*Us*Urfc))/(sqrt(((a1*SDdel).^2)+((a2*SDr).^2)+((a3*SDD).
^2)+((a4*SDe).^2)+((a5*SDa).^2)+((a6*SDs).^2)+((a7*SDrfc).^2)))
B = vpa(Beta)
Pff(i) = normcdf(double(-B))
end
disp(Pff')
i = 1:20;
plot(i,Pff)

```

### Multi-Hazard Analysis;

```

Fatigue
Pff = Pff
Seismic_FORM
Pfe = Pfe
hold on
for j = 1:length(Pfe)

    for v = 1:length(Pff)
        Pf(v) = Pfe(j)+Pff(v) - (Pfe(j)*Pff(v));
    end
    tb(:,j)= Pf';
    v = 1:length(Pff);

    plot(v,Pf)

end
Pff
tb ;
table2
table

```